

LZAP AND PPM PHOSPHATASES:
RECIPROCAL REGULATION AND SHARED MECHANISMS
ALTERING TUMOR BEHAVIOR

By

Xinyuan Lu

Dissertation

Submitted to Faculty of the
Graduate School of Vanderbilt University
In partial fulfillment of the requirements
for the degree of

DOCTOR OF PHILOSOPHY

In
Cancer Biology
August, 2013
Nashville, Tennessee

Approved:

Professor Wendell G. Yarbrough

Professor Robert Matusik

Professor John McLean

Professor Ann Richmond

ORIGINAL PUBLICATIONS

1. **Lu X**, An H, Jin R, Zou M, Guo Y, Su P, Liu D, Shyr Y, Yarbrough WG. PPM1A is a RelA phosphatase with tumor suppressor-like activity. *Oncogene*, 2013, accepted.
2. An H, **Lu X**, Liu D, Yarbrough WG. LZAP inhibits p38 MAPK (p38) phosphorylation and activity by facilitating p38 association with the wild-type p53 induced phosphatase 1 (WIP1). *PLoS ONE*, 2011;6:e16427.
3. Godoy JM, Sewell A, Johnston B, Brown BT, **Lu X**, Sinard RJ, Rohde S, Mannion K, Netterville JL, Yarbrough WG. Viable biobanking of primary head and neck squamous cell carcinoma. *Laryngoscope*, 123:641–645, 2013.

To my father, Yixing Lu and my mother, Yan Tang, who made all of this possible

&

To my grandparents, Jigao Tang and Zhihua Zhang, who continue to be enormously

supportive

In memory of Pengchun Lu and Ruixian Zhou

ACKNOWLEDGEMENTS

This dissertation would not have been possible without the greatest efforts and support from numerous people—many more than I can list here. I am deeply thankful to all of them for guiding me through the whole process and for their generous inputs during all stages of my work.

First, I would like to acknowledge my mentor, Dr. Wendell Yarbrough, who provided this great opportunity to me to start and to finish this work. I am obliged for his mentorship during the past seven years. His guidance from the very beginning of my graduate study all the way to the final stage enables me to develop my understanding of cancer biology and translational research. None the less, the research environment Dr. Yarbrough created along with his trust enabled me to progress toward becoming an independent scientist. He also provides opportunities exposing me to various aspects of research as well as career development and is always supportive of my career goal.

I would also like to thank my committee members, Dr. Robert Matusik, Dr. Ann Richmond and Dr. John McLean. They not only gave me insightful suggestions and guidance during my training but also generously provided me access to their lab personnel and resources.

I am grateful to the past and present Yarbrough lab members. They are wonderful people to work with and helped me get through difficulties in research as well as in my life. Specifically, I would like to thank Dr. Jialiang Wang, whose innovative discoveries became the foundation of my work and who constantly gives me advices and listens to me even after his graduation. I would like to thank Dr. Hanbing An, who has taken time to train me hand by hand and directly supervised me throughout my dissertation. She is a great colleague, teacher and friend and is like elder sister to me. I am also indebted to many of mine collaborators and colleagues. They are: Dr. Renjie Jin, Dr. Alissa Weaver, Dr. Christine Chung, Dr. Yan Guo, Dr. Dr. Zhirong Yin, Dr. Yin Cai, Dr. Jinming Yang, Dr. Oriana Hawkins, Dr. Yeemon Thu, Dr. Dan Liu and Brandee Brown. I also appreciate the help and support from our neighbor labs and from students and staffs in Cancer Biology especially Dr. Jin Chen and Tracy Tveit.

I am grateful for my parents and my family who cultivated my interest in science and encouraged me to study overseas since I was a kid and whose love and guidance have supported me during this work. I would like to show my gratitude to my aunt, Yian Lu, a previous researcher in the department of immunology at Vanderbilt, from whom I heard Vanderbilt for the first time in my life and I always receive warm greetings from her and her family in the U.S.

My acknowledgement would not be complete without mentioning my wonderful friends outside the lab. These include Luping Lin, my classmate and close friend; Shan He, Xiaoyan Wu and Jie Zhao, my amazing roommates as well as friends who made my stay in Nashville comfortable and full of memories.

Again I would like to thank all of the contributors with my utmost sincerity. This work was supported by NIH R01 DE013173 to WGY and by funds provided through an endowment from Barry and Amy Baker to the Barry Baker Laboratory for Head & Neck Oncology, from the Vanderbilt Ingram Cancer Center, from the Department of Otolaryngology at Vanderbilt University, and from the Vanderbilt Bill Wilkerson Center.

TABLE OF CONTENTS

| | |
|---|-----|
| ORIGINAL PUBLICATIONS | ii |
| DEDICATIONS..... | iii |
| ACKNOWLEDGEMENTS | iii |
| LIST OF TABLES..... | ix |
| LIST OF FIGURES | x |
| LIST OF ABBREVIATIONS..... | xii |
| Chapter | |
| I. INTRODUCTION | 1 |
| 1. Mechanisms of NF-κB signaling | 1 |
| 1.1 General introduction to NF-κB family | 1 |
| 1.2 Regulation of NF-κB activation and nuclear translocation..... | 3 |
| 1.3 Post-translational modification of RelA | 5 |
| 1.4 Down regulation of canonical NF-κB responses | 8 |
| 1.4.1 Inhibition of canonical NF-κB activity by classical IκB proteins..... | 8 |
| 1.4.2 Termination of canonical NF-κB responses in the nucleus | 9 |
| 1.4.3 Dephosphorylation of RelA and responsible phosphatases | 9 |
| 2. NF-κB signaling in cancer | 11 |
| 3. Serine/threonine protein phosphatase magnesium/manganese-dependent family (PPM/PP2C)..... | 13 |
| 3.1 The PPM family..... | 13 |
| 3.2 PPM1A/PP2C α | 14 |
| 3.3 PPM1B..... | 18 |
| 3.4 Wip1/PPM1D | 18 |
| 4. LZAP | 25 |
| 4.1 General introduction to LZAP | 25 |
| 4.2 Mechanisms of LZAP activity | 26 |
| 4.3 Regulation of LZAP | 29 |
| 5. Summary and Dissertation Goals..... | 31 |

II. PPM1A IS A RELA PHOSPHATASE WITH TUMOR SUPPRESSOR-LIKE ACTIVITY 33

| | |
|--|----|
| Abstract | 33 |
| Introduction | 34 |
| Materials and Methods | 36 |
| Expression Plasmid and small hairpin RNA expression Constructs | 36 |
| Cell lines, cell culture, transfection and virus infection | 36 |
| Antibodies and reagents..... | 36 |
| Immunoprecipitation and immunoblotting | 37 |
| <i>In vitro</i> phosphatase reaction and malachite green phosphatase assay..... | 37 |
| Luciferase reporter gene assay..... | 37 |
| cDNA synthesis and real-time PCR | 37 |
| Chromatin Immunoprecipitation (ChIP) Assays | 38 |
| <i>In vitro</i> cell invasion assay | 38 |
| Cell fractionation | 38 |
| DNA binding assay..... | 38 |
| Obtaining conditioned medium (CM) and ELISA Assay..... | 38 |
| The Gene Expression Omnibus (GEO) analysis..... | 38 |
| <i>In vivo</i> tumor metastasis assay and BLI ex vivo analysis..... | 39 |
| <i>In vivo</i> xenograft tumor growth assay | 39 |
| Statistical analysis..... | 39 |
| Results | 40 |
| PPM1A directly dephosphorylates RelA..... | 40 |
| PPM1A inhibits RelA transcription activity, decreases NF- κ B-dependent cell invasion, sensitizes cell to TNF α , but does not alter RelA nuclear localization or DNA binding ... | 44 |
| PPM1A inhibits NF- κ B activation, MCP-1 expression and cell invasion in prostate cancer cell lines..... | 51 |
| PPM1A expression is lower in metastatic human prostate cancer and PPM1A expression inhibits metastases in a mouse model..... | 53 |
| PPM1A decreases xenograft tumor growth | 56 |
| Discussion | 60 |

III. LZAP REGULATES TARGET PROTEIN PHOSPHORYLATION BY FACILITATING

TARGET PROTEIN ASSOCIATION WITH PHOSPHATASES OF PPM FAMILY 63

| | |
|---------------------------|----|
| Abstract | 63 |
| Introduction | 64 |

| | |
|---|-----|
| Materials and Methods | 67 |
| Plasmid constructs | 67 |
| Antibodies and Reagents | 67 |
| Cell culture and transfection | 67 |
| Immunoprecipitation and immunoblotting | 68 |
| Immunofluorescence assay | 68 |
| Cell fractionation | 68 |
| Luciferase reporter assay | 68 |
| Mass spectrometry | 69 |
| Results | 69 |
| LZAP interacts with p38 MAPK <i>in vivo</i> | 69 |
| LZAP inhibits phosphorylation of p38 | 73 |
| Depletion of endogenous LZAP activates p38 | 75 |
| LZAP regulates p38 phosphorylation through altering Wip1 association with p38 | 78 |
| LZAP interacts with Wip1 <i>in vivo</i> | 81 |
| LZAP partially depends on PPM phosphatases to regulate RelA phosphorylation | 81 |
| Discussion | 85 |
| IV. REGULATION OF LZAP | 87 |
| Abstract | 87 |
| Introduction | 88 |
| Materials and Methods | 91 |
| Plasmid constructs and mutagenesis | 91 |
| Antibodies and reagents | 91 |
| <i>in vivo</i> ^{32}P orthophosphate labeling | 91 |
| Results | 92 |
| LZAP is phosphorylated and ubiquitinated | 92 |
| Identification of LZAP binding partners and LZAP binding domain mapping | 94 |
| Discussion | 100 |
| V. SUMMARY AND FUTURE DIRECTIONS | 103 |
| 1. Summary | 103 |
| 2. Future directions | 104 |
| 2.1. Additional NF- κB target genes regulated by PPM1A | 104 |

| | |
|---|-----|
| 2.2 Mechanisms of decreased PPM1A expression in prostate cancer and the role of PPM1A in other cancer types | 107 |
| 2.3 LZAP as a potential regulator of PPM phosphatase activity toward LZAP-associated proteins | 108 |
| 2.4 Regulation of LZAP expression, post-translational modification and stability..... | 110 |
| 2.4.1 LZAP promoter regulation..... | 110 |
| 2.4.2 Phosphorylation sites in LZAP | 112 |
| 2.4.3 LZAP post-translational modification by ubiquitin or ubiquitin-like conjugating systems | 114 |
| REFERENCES | 116 |

LIST OF TABLES

| | |
|--|----|
| Table 1.0.1 Summary of RelA PTM sites and functions | 6 |
| Table 1.0.2 Overview of PPM phosphatases interaction with proteins regulating cell growth and cellular stress signaling..... | 23 |
| Table 2.0.1 Fold changes of NF- κ B target genes measured by RT ² Profiler™ PCR Array | 50 |
| Table 3.0.1 Summary of LZAP, Wip1 and PPM1A activity and binding for shared target proteins . | 65 |
| Table 3.0.2 LZAP predicted motifs from Scansite | 65 |
| Table 4.0.1 Selective results from LZAP binding partner analysis | 96 |
| Table 4.2 Summary of LZAP truncations interaction with RelA or LZAP | 96 |

LIST OF FIGURES

| | |
|--|----|
| Figure 1.0.1 The NF- κ B/Rel and I κ B families of proteins | 2 |
| Figure 1.0.2 Schema of canonical and non-canonical NF- κ B activation..... | 4 |
| Figure 1.0.3 PPM phosphatases regulate p53 signaling..... | 24 |
| Figure 1.0.4 LZAP Inhibits Checkpoint Kinases..... | 28 |
| Figure 2.0.1 PPM1A is a RelA phosphatase | 42 |
| Figure 2.0.2 PPM1A regulates RelA phosphorylation under TNF α stimulation..... | 43 |
| Figure 2.0.3 PPM1A inhibits NF- κ B transcription activity, NF- κ B-dependent cell invasion and sensitizes cells to TNF α | 46 |
| Figure 2.0.4 PPM1A inhibits RelA transcriptional activity | 47 |
| Figure 2.0.5 PPM1A does not interfere with nuclear translocation or DNA binding of RelA | 50 |
| Figure 2.0.6 PPM1A inhibits NF- κ B and prostate cancer cell invasion | 52 |
| Figure 2.0.7 Bioluminescent imaging of mice after intracardiac injection of PC3-LUC cells | 54 |
| Figure 2.0.8 PPM1A expression is lower in metastatic human prostate cancer and inhibits prostate cancer cell metastasis <i>in vivo</i> | 55 |
| Figure 1.0.9 PPM1A inhibits tumor growth <i>in vivo</i> | 58 |
| Figure 1.0.10 Comparing apoptotic and proliferative index of tumor maintain or not maintain PPM1A depletion..... | 59 |
| Figure 3.0.1 LZAP binds to p38 | 70 |
| Figure 3.0.2 Independent and non-overlapping areas of LZAP are sufficient for association with p38 | 72 |
| Figure 3.0.3 LZAP regulates p38 phosphorylation..... | 74 |
| Figure 3.0.4 Loss of LZAP increases p38 kinase activity, but does not alter MKK activation..... | 77 |
| Figure 3.0.5 LZAP regulation of p38 phosphorylation involves Wip1 | 80 |
| Figure 3.0.6 LZAP binds to Wip1 | 82 |

| | |
|--|-----|
| Figure 3.0.7 LZAP PP2C phosphatases require one another for efficient regulation of RelA phosphorylation | 84 |
| Figure 4.0.1 LZAP phosphorylation and ubiquitination | 93 |
| Figure 4.0.2 Mapping of LZAP domains involved in binding to LZAP-associated proteins | 95 |
| Figure 4.0.3 LZAP motifs and binding of LZAP truncations to known LZAP associated proteins and diagram for LZAP protein motifs | 97 |
| Figure 4.0.4 Mapping of LZAP self-association domains | 99 |
| Figure 5.0.1 Relevant transcription factor binding sites in LZAP gene promoter | 111 |
| Figure 5.2 Potential phosphorylation sites on LZAP | 113 |

LIST OF ABBREVIATIONS

| | |
|-------|--|
| ARF | alternative reading frame |
| ATM | ataxia telangiectasia mutated |
| ATR | ataxia telangiectasia and Rad3-related protein |
| BLI | bioluminescent live imaging |
| BrdU | bromodeoxyuridine |
| CCL2 | chemokine (C-C motif) ligand 2 |
| CDK | cyclin-dependent kinase |
| Chk | checkpoint kinase |
| EMT | epithelial-mesenchymal transition |
| ER | endoplasmic reticulum |
| ERK | extracellular receptor-activated kinase |
| FBS | fetal bovine serum |
| GPCR | G-protein-coupled receptor |
| H&E | hematoxylin and eosin |
| HAT | histone acetylation transferase |
| HBx | Hepatitis B virus X |
| HDAC | histone deacetylase |
| HNSCC | head and neck squamous cell carcinoma |
| IB | immunoblotting |
| IF | immunofluorescent |
| Ig | immunoglobulin |
| IHC | immunohistochemistry |
| IKK | I κ B kinase |
| IL-6 | interleukin 6 |
| IP | immunoprecipitation |
| IR | ionizing radiation |
| IVT | in vitro translation |
| kDa | kilo dalton |
| KO | knock out |
| LAPs | LZAP-associated proteins |

| | |
|--------------|---|
| LC | liquid chromatography |
| LPS | Lipopolysaccharide |
| luc | luciferase |
| LZAP | <u>L</u> XX <u>L</u> /leucine zipper-containing <u>A</u> RF-binding protein |
| MAPK | mitogen-activated protein kinase |
| MAPKK | MAPK kinase |
| MAPKKK | MAPK kinase kinase |
| MCP-1 | monocyte chemotactic protein-1 |
| MDM2 | mouse double minute 2 homolog |
| MS | mass spectrometry |
| NF-κB | nuclear factor-kappa B |
| OA | okadaic acid |
| PD | phosphatase-dead |
| PDZ | postsynaptic density 65–discs large–zonula occludens 1 |
| PKAc | protein kinase A |
| PP1 | protein phosphatase 1 |
| PP2A | protein phosphatase 2A |
| PPM | protein phosphatase Mg/Mn dependent |
| PPP | phospho-protein phosphatase |
| PTM | post-translational modification |
| RHD | rel homologous domain |
| SD | standard deviation |
| Ser/S | serine |
| SUMO | Small Ubiquitin-like Modifier |
| TAD | transcription activation domain |
| Thr/T | threonine |
| TNF α | tumor necrosis factor alpha |
| TSGs | tumor suppressor genes |
| UFM1 | ubiquitin fold-modifier-1 |
| UV | ultraviolet |
| Wip1 | Wild-type p53-induced phosphatase |
| WT | wild type |

CHAPTER I

INTRODUCTION

1. Mechanisms of NF-κB signaling

1.1 General introduction to NF-κB family

Nuclear factor-kappa B (NF-κB) was discovered more than 20 years ago as a nuclear factor that binds a site in the immunoglobulin κ enhancer and regulates expression of the κB light chain in B cells³. There are five NF-κB/REL genes that encode seven proteins—p65 (RelA), c-Rel, RelB, NF-κB1 (p50/p105), NF-κB2 (p52/p100) (reviewed in^{4,2}) (Fig. 1.1 adapted from²). All members of the family share an N-terminal Rel homology domain (RHD) responsible for DNA binding, homo- and hetero-dimerization and interactions with IκB proteins². The transcription activation domain (TAD) necessary for the positive regulation of gene expression is present in 3 family members: p65, c-Rel, and RelB. Two of the proteins, NF-κB1 (p105) and NF-κB2 (p100), contain multiple copies of the so-called ankyrin repeat at their C-termini with inhibitory function. Processing of these proteins leads to the production of the p50 and p52 subunits.

NF-κB is active and binds DNA as a dimer. Classic NF-κB (the dimer of p50 and RelA) has been most intensively studied, although many other homo- and heterodimers have been described with some distinct characteristics attributed to. NF-κB dimers bind to κB sites within the promoters/enhancers of target genes and regulate transcription through the recruitment of co-activators or co-repressors. Different NF-κB dimers prefer slightly different DNA sequences enabling differential and enhanced regulation of target gene expression. Dimers composed of p50/p65, p50/c-rel, p65/p65, and p65/c-rel possess transcriptional potential, whereas homodimers of p50 or p52 uniformly inhibit transcription when bound to DNA. More studies to determine biologically relevant targets for different NF-κB dimers are needed. Additional differences between

NF-κB dimers include: cell type specificity, differential subcellular localization, differential interactions with forms of IκB, and differential activation^{5, 6}.

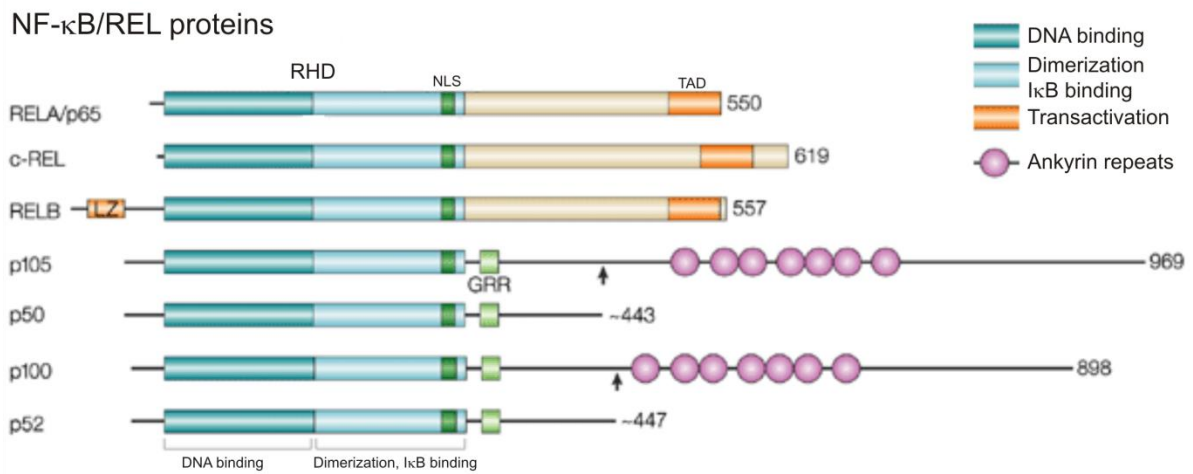


Fig. 1.1 The NF-κB/Rel and IκB families of proteins, adapted from². The NF-κB/Rel family is characterized by the presence of the Rel homology domain.

1.2 Regulation of NF-κB activation and nuclear translocation

NF-κB is a ubiquitous eukaryotic transcription factor that resides in the cytoplasm of most cells in an inactive form bound to the inhibitor, IκB. Diverse signals such as inflammatory cytokines, UV, and LPS, trigger destruction of IκB and release of NF-κB which translocates to the nucleus where it regulates transcription of target genes. It is critical to note that NF-κB's ability to respond to signals makes it an inducible factor, and since activation of NF-κB does not require new protein synthesis, the signal is transmitted rapidly⁷.

Two major NF-κB activating pathways have been characterized, canonical (or classical) and non-canonical (or alternative). These distinct methods for NF-κB activation target different NF-κB homo/heterodimers via distinct kinases and IκB proteins (reviewed in⁸ and⁹). The canonical pathway activates NF-κB dimers consisting of combinations of RelA (p65), c-Rel, RelB and p50 while the non-canonical pathway is responsible for the activation of p100/RelB complexes (Fig. 1.2 adapted from¹⁰).

IκB binds to the RHD domain of NF-κB and sequesters it in the cytoplasm. Inhibitory activity of IκB requires direct binding to NF-κB dimers and is thought to be mediated through masking of the nuclear localization signals also located in the RHD¹¹. Signaling through inflammatory cytokines such as TNFα and IL-1 activates a high molecular weight protein complex known as the signalsome that contains IκB kinases (IKKα/β/γ) responsible for phosphorylation of IκB. The IKK complex also has NF-κB regulatory functions (see below). Phosphorylation of IκB marks it for ubiquitination and subsequent degradation that is dependent on the 26S proteasome (Fig. 1.2). Degradation of IκB results in NF-κB nuclear localization and dependent on post-translational modification of Rel family proteins, transcription or transcriptional inhibition of NF-κB responsive genes. The elaborate system of sequestration of NF-κB in the cytoplasm allows rapid induction of NF-κB activity within cells following appropriate stimulation.

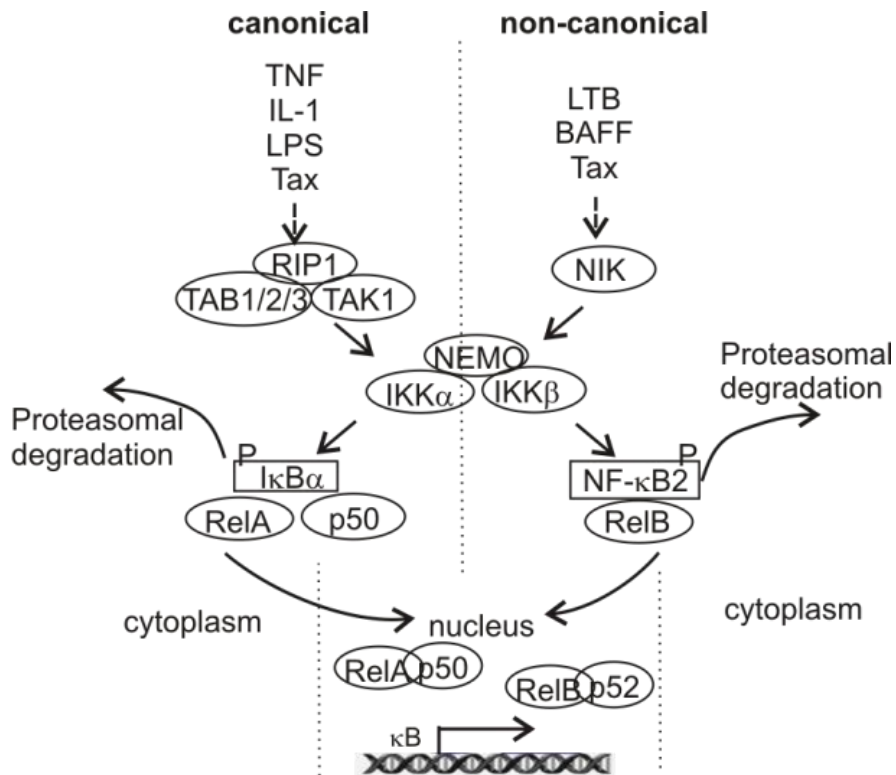


Fig. 1.2 Schema of canonical and non-canonical NF- κ B activation. In the canonical NF-B activation pathway, stimulus-induced phosphorylation of two N-terminal serines in the I κ Bs is mediated by the IKKs. After ubiquitination and degradation of I κ B by the 26S proteasome complex, the liberated NF- κ B heterodimer (p50:p65) translocates to the nucleus and regulates transcription of target genes dependent on post-translational modification. In the alternative (non-canonical) pathway, IKK is activated by different members of the TNF-family (for example, BAFF and CD40). Along with NIK, IKK induces the phosphorylation-dependent processing of p100 and generation of p52:RelB heterodimers. p52:RelB translocates to the nucleus and regulates transcription

1.3 Post-translational modification of RelA

Like many transcription factors (e.g. E2F1 and p53), post-translational modification alters various physiological functions of the NF-κB including DNA binding, interactions with co-activators and co-repressors, as well as, termination of the NF-κB response^{2, 12-14}. To date, most studies have focused on RelA modification, with reports related to modifications of other NF-κB subunits being extremely limited. Even with RelA, the complexity of its nuclear regulation and modification is only beginning to be understood. Basal and signal-induced phosphorylations of RelA are most thoroughly characterized. Site-specific phosphorylation is often a prerequisite for additional modifications (acetylation, ubiquitination, and isomerization of specific amino acid residues¹⁵) regulating RelA activity. As is frequently the case, studies examining NF-κB post-translational modification present different levels of evidence that a specific enzyme is modifying a particular site, and it is recognized that modifications likely differ dependent on cell type and the nature of the NF-κB-inducing stimulus¹⁶.

The RelA subunit of NF-κB is targeted for phosphorylation at many phospho-acceptor sites within both the RHD (S205, S276, S281, S311, T254) and TAD (S468, S529, S535, S536, T435, T505) (Table 1.1, adapted from¹⁰ and¹⁴). Phosphorylation of RelA occurs both within the cytoplasm and nucleus and many responsible kinases that are activated by a variety of stimuli have been identified (reviewed in²). Phosphorylation of individual amino acids has been associated with different consequences, both activation and inactivation. Phosphorylation of S536 increases NF-κB transcriptional activity while phosphorylation of S529 increases NF-κB DNA binding and oligomerization. On the other hand, phosphorylation of T505 inhibits RelA transcription possibly through promoting association of RelA with HDAC¹⁷. A recent study shows that phosphorylation of S468 controls RelA COMMD1-dependent ubiquitination and target gene-specific proteasomal elimination.

Table 1.1 Summary of RelA PTM sites and functions (adapted from ¹⁰ and ¹⁴)

| Modification | Modification amino acid | Enzymes | Function of modification |
|-----------------------|-------------------------|----------------|---|
| phosphorylation | S536 | IKK α | transactivation ▲ |
| | | IKK β | transactivation ▲ |
| | | IKK ϵ | transactivation ▲ |
| | | TBK1 | nuclear export ▼ |
| | | RSK1 | turnover ▲ |
| | S535 | CaMKIV | transactivation ▲ |
| | S529 | CKII | transactivation ▲ |
| | S468 | GSK-3 β | transactivation ▼ |
| | | | turnover ▲ |
| | | IKK β | transactivation ▼ |
| | | IKK ϵ | transactivation ▲ |
| | S311 | PKC ζ | transactivation ▲ |
| | S276 | PKAc | transactivation ▲ |
| | | MSK1 | transactivation ▲ |
| | S205 | unknown | transactivation ▲ |
| | S281 | unknown | transactivation ▲ |
| | T505 | ATR | transactivation ▼ |
| | | Chk1 | transactivation ▼ |
| | T435 | unknown | transactivation ▼ |
| | T254 | unknown | I κ B interaction ▼ stabilization ▲ prolyl isomerization ▲ |
| dephosphorylation | S536 | Wip1 | transactivation ▼ |
| | | PP2Ac PR65 | transactivation ▼ |
| Acetylation | T435 | PP4 | transactivation ▲ |
| | K310 | CBP/p300 | transactivation ▲ |
| | K218/221 | CBP/p300 | DNA binding ▲ I κ B interaction ▼ |
| Oxidation | K122/123 | PCAF, p300 | DNA binding ▼ |
| | C38 | — | inhibition |
| Nitration | Y66 | nitric oxide | inhibition |
| | Y152 | nitric oxide | inhibition |
| Proline isomerization | P255 | Pin-1 | stabilization ▲ nuclear localization ▲ |
| | | | |
| Ubiquitination | aa220-335 | SOCS-1 | degradation ▲ |
| Methylation | K314/315 | Set-9 | inhibition |

The serine 536 residue of RelA is conserved between human, mouse, chicken, and xenopus. Phosphorylation of S536 was first identified by Sakurai *et al.* through an *in vitro* kinase assay using TNF α stimulated whole cell lysate and immunoprecipitated IKK α or IKK β ¹⁸. Further, with inhibition of I κ B α degradation by a proteasome inhibitor, N-acetylleucyl-leucyl-norleucinal (ALLN), this group demonstrated that the activity to phosphorylate Ser-536 could be induced in the cytoplasm¹⁹. Whether phosphorylation at S536 by IKKs is part of the activation mechanism leading to RelA nuclear translocation or a mechanism to prime RelA's transactivation potential before nuclear localization is unknown. However, phosphorylation of Ser-536 can also result in an I κ B-independent mechanism of NF- κ B activation^{20,21}. Specifically, in some cell types, induction of the p53 tumor suppressor results in RSK1 kinase activation²⁰, which phosphorylates RelA at S536. Since activation of RSK1 is associated with its cytoplasmic to nuclear translocation, it is proposed that, in this instance, Ser-536 phosphorylation occurs in the nucleus. This results in RelA nuclear accumulation through disruption of the cytoplasmic/nuclear shuttling of NF- κ B/I κ B α complexes that occurs in unstimulated cells²⁰.

The phosphorylation of highly conserved serine 276 and its critical role for RelA transcription activity was identified by Zhong *et al.* and protein kinase A (PKAc) was the first known kinase targeting this residue²². Ser-276 in RelA is also phosphorylated by the MSK1 kinase, although this is a nuclear event¹². Phosphorylation of S276 promotes RelA interaction with transcriptional co-activator CBP/p300²² altering the balance between transcriptionally repressed RelA bound to HDACs vs. transcriptionally activated RelA bound to p300/CBP²³. The finding that the phosphorylation status of Rel proteins, especially of RelA, is the decisive parameter for their association with either transcriptional activators HATs (e.g. CBP/p300) or suppressors (e.g. HDACs) is important for understanding of NF- κ B regulation. Both S536 and S276 residues of RelA may be important for promoting association with HDACs since phosphorylation of both residues is required for RelA acetylation at K310²⁴.

It is becoming more and more apparent that RelA phosphorylation at different sites serves as an integrator for multiple incoming signals, which likely serve to regulate the kinetics, strength and selectivity of RelA transcriptional activity.

1.4 Down regulation of canonical NF-κB responses

NF-κB is activated by various stimuli including: TNF α and bacterial/viral signal triggered danger-sensing receptors of the innate and adaptive immune systems. Active NF-κB binds to consensus target sequences in various promoters and induces the expression of a plethora of genes encoding molecules that promote proliferation, survival and differentiation of immune cells, as well as driving expression of factors such as proinflammatory cytokines that organize and execute immune and inflammatory responses. Thus, prompt activation of NF-κB is critical for host defense against various classes of pathogens; however, NF-κB activity can be deleterious resulting in tissue damage, uncontrolled immune response, and cancer if they are not appropriately down regulated^{25, 26}. Many distinct negative regulatory mechanisms have evolved that operate at different molecular levels in the NF-κB signaling pathways to maintain homeostasis (review²⁷).

1.4.1 Inhibition of canonical NF-κB activity by classical IκB proteins

Degradation of IκB proteins is a decisive step in canonical NF-κB activation (see section 1.2); however, re-establishment of IκB serves as a critical regulator to limit excessive NF-κB activity²⁸. Restoration of IκB following its proteasomal destruction is accomplished largely through a negative feedback loop, where IκB α genes are directly transcribed by active NF-κB²⁹⁻³¹. Newly synthesized IκB α enters the nucleus and associates with DNA-bound NF-κB dimers³², resulting in cytoplasmic re-localization of NF-κB via the nuclear-export sequence present in IκB α . Acetylation of RelA by lysine acetyltransferase CBP (p300) complexes prevents IκB α binding to RelA and extends the promoter occupancy of functional RelA complexes³³.

1.4.2 Termination of canonical NF-κB responses in the nucleus

Although IκB-mediated cytoplasmic export of nuclear NF-κB is important for deactivation of NF-κB responses, additional negative regulatory mechanism operate in the nucleus. These include IκB-independent displacement of active NF-κB from DNA and proteolytic degradation of active NF-κB dimers. The SUMO E3 ligase PIAS1 can directly interfere with the binding of RelA dimers to DNA and regulates expression of distinct NF-κB target genes, particularly at early time points following NF-κB activation³⁴. IKKα has additional negative regulatory roles in the termination of nuclear canonical NF-κB responses, as it accelerates the turnover of RelA and c-Rel^{35,36}. While activated in the cytoplasm by pro-inflammatory signals, IKKα phosphorylates RelA specifically at Ser536 and thereby enhances its later proteasomal degradation in the nucleus.

At least two E3 ubiquitin ligases control degradation of nuclear RelA³⁷. One of these, PDLIM2, is essential to prevent uncontrolled inflammation *in vivo*³⁸. PDLIM2 has a PDZ (postsynaptic density 65-discs large–zonula occludens 1) domain in addition to its E3 ligase activity. The PDZ domain of PDLIM2 has chaperone function and promotes the transport of RelA to promyelocytic leukemia (PML) nuclear bodies. Thus, PDLIM2 not only targets nuclear RelA for proteasomal degradation but also re-localizes DNA-bound RelA to areas of transcriptional silencing. The other known E3 ligase that terminates the RelA responses in the nucleus is the EC2S complex, which contains SOCS1, Cullin-2 and COMMD1^{39,40}. Functionally, COMMD1 bridges RelA to SOCS1 and Cullin-2 after pro-inflammatory stimulation where the EC2S complex mediates ubiquitin-dependent degradation of RelA. The EC2S complex appears to be particularly important for termination of NF-κB responses at later stages of cell stimulation³⁹. Phosphorylation of p65 at Ser468 controls its COMMD1-dependent ubiquitination and target gene-specific proteasomal elimination⁴¹.

1.4.3 Dephosphorylation of RelA and responsible phosphatases

Phosphorylation of RelA is dynamically regulated with a balance between protein serine/threonine kinases, and protein serine/threonine phosphatases. Time course experiments reveal

that nuclear RelA S536 phosphorylation markedly decreases 10-20 min after TNF- α stimulation. Pre-treatment with calyculin A (CalyA), a phosphatase inhibitor for protein phosphatase PP1 and PP2A partially inhibited dephosphorylation¹⁸, suggesting that CalyA-sensitive phosphatases dephosphorylate RelA after the nuclear translocation. Nelson *et al.* showed that following TNF α stimulation, RelA dynamically oscillates between the nucleus and cytoplasm corresponding to rapid dephosphorylation at Ser-536, suggesting that dephosphorylation at S536 may be intricately involved in regulating the level and duration of NF- κ B activity⁴². Despite these data that dephosphorylation of RelA is critical for RelA regulation; identification of involved phosphatases, as well as mechanisms regulating involved phosphatases is lacking. To date, phosphatases implicated as direct or indirect regulators of NF- κ B include only serine/threonine type 2C protein phosphatase (PPM) family members (Wip1 (PPM1D, PPM δ), PPM1A and PPM1B) and the serine/threonine type 2A protein phosphatase (PP2A).

RelA was found to bind protein phosphatase 2A (PP2A) subunit A (PR65) and was dephosphorylated by a purified PP2A core enzyme, a heterodimer formed by the catalytic subunit of PP2A (PP2Ac) and PR65, in a concentration-dependent manner⁴³. Okadaic acid, an inhibitor of PP2A, increased basal RelA phosphorylation in melanocytes and blocked dephosphorylation of RelA after interleukin-1 stimulation⁴³. The PP2A family contains many different subunits and has been reported to have tumor suppressor-like function or oncogenic functions depending on context and the particular activated PP2A trimeric complex (reviewed in ^{44,45} and⁴⁶). An emerging view suggests that specific PP2A complexes play critical roles in cell transformation by regulating particular substrates.

More recently, a genome-wide search for regulators of NF- κ B using RNAi identified Wip1 as a negative regulator of NF- κ B signaling. Wip1 was found to directly dephosphorylate RelA at S536, a residue critical for full activation of transcriptional activity⁴⁷. Overexpression of Wip1 resulted in decreased RelA phosphorylation and NF- κ B inhibition in a dose-dependent manner. Conversely, Wip1 knockdown resulted in increased NF- κ B function. TNF α mRNA is increased in WIP1^{-/-} mice

where enhanced inflammation in many organs is also observed⁴⁷. PPM1D, which encodes Wip1, is a transcriptional target of NF-κB, suggesting a potential negative feedback loop⁴⁸. Inhibition or activation of NF-κB decreases or increases Wip1 expression, respectively. ChIP analysis showed basal binding of the p65 subunit to the PPM1D promoter region encompassing the κB site, which is enhanced after NF-κB activation by TNFα. Wip1 expression is induced by LPS-stimulation of mouse splenic B-cells and is required for maximum proliferation. Taken together, these data suggest that Wip1 likely regulates RelA activity through a negative feedback loop.

PPM1A and PPM1B are the other members of PPM family and these PPM family members indirectly regulate NF-κB through dephosphorylation and inhibition of IKKβ⁴⁹. Overexpression of PPM1A or PPM1B results in dephosphorylation of IKKβ at Ser177 and Ser181 and termination of IKKβ-induced NF-κB activation. PPM1A and PPM1B associate with the phosphorylated form of IKKβ, and the interaction between PPM1A/PPM1B and IKKβ is transiently induced by TNFα. Functionally, knockdown of PPM1A and PPM1B expression enhances TNFα-induced IKKβ phosphorylation, NF-κB nuclear translocation and NF-κB-dependent gene expression (IL-6).

2. NF-κB signaling in cancer

NF-κB target genes regulate development, inflammation, immune response, proliferation, apoptosis, cellular transformation, angiogenesis and differentiation (reviewed in ⁵⁰). Given its involvement in multiple cellular processes, NF-κB activity is tightly and intricately controlled. Constitutive NF-κB activity is associated with human diseases including asthma, arthritis, Alzheimer's disease, diabetes and inflammatory bowel disease (reviewed in ⁵¹) and aberrant NF-κB activity has been shown to directly contribute to tumorigenesis, neovascularization, tumor growth and metastases²⁵ and reviewed in ⁵⁰.

NF-κB is amplified, overexpressed, or activated in various tumor types including breast, stomach, thyroid and colon cancer and NF-κB activities promotes many aspects of oncogenesis including cellular transformation and proliferation while protecting tumor cells from apoptosis (reviewed in ⁵²

and⁵³). NF-κB activation and increased S276 phosphorylation has been described in head and neck squamous cell carcinoma (HNSCC) and adjacent dysplastic mucosa⁵⁴ and multiple NF-κB responsive genes are overexpressed in these tumors⁵⁵.

Experimental data also supports the role of NF-κB in tumorigenesis. Inhibition of NF-κB through expression of either IκB super repressor⁵⁶ or dominant negative IKK⁵⁷ markedly inhibits foci formation while increasing apoptosis. Many anti-apoptosis genes are NF-κB targets including: TRAF1, TRAF2, c-IAP1, c-IAP2, xIAP, BCL-XL (reviewed in⁵³ and⁵⁸). A genetically modified mouse model expressing c-Rel driven the mouse mammary tumor virus promoter revealed that c-Rel expression associated with development of breast adenocarcinomas in one-third of mice post-partum. Increased NF-κB signaling was associated with increased expression of anti-apoptotic and proliferation promoting genes in tumors⁵⁹. Inhibition of NF-κB activity in HNSCC cells was shown to inhibit xenograft tumor growth and since these tumors had no known activation of oncogenes, these data suggest that NF-κB activation may be important for tumors without known alteration of oncogenes⁶⁰.

Dysregulation of NF-κB in prostate cancer has been identified as a major driver of distant metastasis, which is the primary cause of death in this common male cancer⁶¹⁻⁶³. Comparison of metastatic prostate cancer and localized disease in multiple expression array profiling studies using the integrative microarray analysis of pathways (IMAP) revealed that NF-κB was the third most dysregulated pathway from a list of approximately 100 pathways that were significantly dysregulated in metastatic prostate cancer⁶⁴. Min *et al.* substantiated the importance of NF-κB for prostate metastases using a murine model showing that an oncogene-tumor suppressor cascade drives metastatic prostate cancer by coordinately activating Ras and NF-κB⁶³. One transcriptional target of NF-κB, monocyte chemotactic protein-1 (MCP-1), also known as chemokine (C-C motif) ligand 2 (CCL2), has been implicated in prostate cancer migration, invasion and metastasis altering both tumor cells and the microenvironment⁶⁵. MCP-1 is particularly implicated in bony prostate metastases as well as in other tumor types including renal cancer, bladder cancer, and breast cancer⁶⁶.

Mechanisms governing MCP-1 expression are not fully described; however the suspected importance of this cytokine in tumor progression is affirmed by the recent initiation of clinical trials using a neutralizing antibody targeting MCP-1. IL-6, another transcriptional target of NF-κB and a cytokine is also implicated in metastases, particularly in cancers of the prostate⁶⁷, colon⁶⁸, and breast⁶⁹. Studies reveal that both MCP-1 and IL-6 facilitate the survival of myeloid monocytes within the tumor microenvironment, as well as their differentiation to tumor-promoting M2-type macrophages^{70,71} that are implicated in promotion of prostate and breast tumor metastasis. Inhibition of IL-6 and IL-6 receptor are also therapeutic targets for prevention of inflammation, tumor progression and metastasis and their targeting has shown promise in pre-clinical models and phase II clinical trials (prostate and ovarian cancer)^{72,73}. Additional phase II clinical trials using an anti-IL-6 monoclonal antibody are currently underway or have been recently completed.

3. Serine/threonine protein phosphatase magnesium/manganese-dependent family (PPM/PP2C)

3.1 The PPM family

Ser/Thr protein phosphatases are divided into three super-families based on their unique sequence and structure composition, namely phospho-protein phosphatase (PPP), protein phosphatase magnesium/manganese-dependent (PPM) and transcription factor II F (TFIIF)-interacting carboxyl terminal domain (CTD) phosphatase (FCP)⁷⁴. The PPP family, including PP1, PP2A and PP2B (calcineurin), consists of oligomeric holoenzymes, composed of a highly conserved catalytic subunit and one or two regulatory subunits essential for subcellular localization and substrate specificity. Two of the phosphatases involved in regulation of NF-κB signaling, PPM1A and Wip1/PPM1D, are members of the PPM family (formerly PP2C family). PPM family members (solely represented by PPM) have two structural domains, a conserved N-terminal catalytic domain and a C-terminal region with substantial structural and sequence variance among different isoforms. Unlike their PPP counterparts, which function as homo- and hetero-, di- and trimetric complexes, PPMs are functional as monomeric enzymes. Therefore, their activity is not regulated by inhibitory proteins or by

regulatory subunits. PPM phosphatase requires divalent cations (Mg^{2+} or Mn^{2+}) for catalytic activity. Because intracellular concentrations of Mg^{2+} and Mn^{2+} do not fluctuate substantially under physiological conditions, it is also unlikely that these metal-dependent phosphatases are regulated by the availability of bivalent cations. Based on these two observations, it is expected that activities of type 2C protein phosphatases are controlled predominantly by: 1) tissue- or cell type-specific expression, 2) post-translational modification, 3) subcellular compartmentalization, or 4) protein stability or degradation. PPM phosphatases are insensitive to the potent inhibitor of the PP1 and PP2A phosphatases, okadaic acid. Sanguinarine was identified as a potent and specific PPM inhibitor with selectivity for PPM as compared with PP1, PP2A and PP3B *in vitro*⁷⁵.

PPM family members are evolutionarily conserved in prokaryotes and eukaryotes and in multicellular organisms ranging from plants to mammals, (reviewed in⁷⁶⁻⁷⁸). Following functional diversification via gene duplication in metazoa, PPM isoforms have gained specificity for various signaling pathways and tissue expression patterns. Recent studies in mammalian cells have revealed at least 18 PPM family members, namely PP2Ca/PPM1A, PP2C β /PPM1B, PP2C γ , PP2C ϵ , PP2C η , PP2Cm, T-cell activation-PPM (TA-PPM), integrin-linked kinase-associated serine/threonine phosphatase 2C (ILKAP), NERRP-2C, Wild-type p53-induced phosphatase (Wip1)/PPM1D, partner of Pix 1 and 2 (POPX1 and POPX2, respectively), PH domain and leucine-rich repeat protein phosphatase 1 and 2 (PHLPP1 and PHLPP2, respectively), pyruvate dehydrogenase phosphatase isoenzyme 1 and 2 (PDP1 and PDP2, respectively), PPM1H and PPM1J. These proteins are largely implicated in the regulation of stress signaling cascades, phosphatidylinositol 3-kinase (PI3-K)/Akt signaling, pre-mRNA splicing, protein ubiquitination and degradation and cell metabolism, as well as cell death/survival signaling⁷⁴.

3.2 PPM1A/PP2C α

PPM1A is the best characterized member of the type 2C family of protein phosphatases. It was first identified in 1992, using a rat liver library and a human teratocarcinoma library⁷⁹. A few years

later, the structure of human PPM1A⁸⁰ revealed a novel protein fold that consists of two domains; an N-terminal catalytic domain, that is composed of a central β-sandwich surrounded by α-helices and that is common to all PPMs, and a 90-residue C-terminal domain, that merely contains α-helices and that is characteristic for mammalian PPMs. This latter domain is remote from the catalytic site, suggesting that it has a role in defining substrate specificity. PPM1A is expressed in virtually all tissues with both cytoplasmic and nuclear and localization⁸¹.

As an enzyme with broad substrate specificity, PPM1A participates in the regulation of several important signaling pathways including TGFβ/Smad⁸², MAPK (JNK/p38), AMPK, p53/MDM2, Wnt/Axin, Cdk2 and Cdk6 (reviewed in¹) and the nerve growth factor activated Akt/ERK pathway⁸³.

MAPK: The modular mitogen-activated protein kinase (MAPK) cascades contain a core of three protein kinases (MAPK kinase kinase (MAPKKK), MAPK kinase (MAPKK) and MAPK that are evolutionarily conserved from yeast to mammals. In mammals, MAPK cascades regulate various cellular activities, including gene expression, proliferation, survival/apoptosis, differentiation and embryogenesis. These functions mediated by MAPK signaling that transduces signals from G-protein-coupled receptors (GPCR), tyrosine receptor kinases and oxidative stress sensors in response to diverse intracellular and extracellular cues. The activation of MAPKs is mediated through a phosphorylation relay mechanism from MAPKKK, MAPKK to MAPK. Activity of MAPKKK and MAPKK can be inhibited through phosphorylation suggesting that protein dephosphorylation by phosphatases can modulate MAPK pathways both positively and negatively⁷⁴. In mammalian cells, three distinct MAPK cascades are found. The prototypic MAP kinases ERK1 and ERK2 are activated by mitogenic signaling through the MAPKKKs A-RAF, B-RAF, and C-RAF, and the MAPKKs MEK1 and MEK2⁸⁴. The two other MAPKs, JNK and p38, are activated by stress such as UV radiation, heat shock, osmotic shock, or wound stress⁸⁵.

Upon such environmental stresses, PPM1A inhibits activation of both the JNK and the p38 pathway. Down regulation of JNK signaling has been attributed to PPM1A inhibition of MAPKKs as both MKK4 and MKK7, two major upstream regulators of JNK, are dephosphorylated by PPM1A

under physiological as well as under stress conditions. Regulation of p38 activity, by PPM1A was also attributed to dephosphorylation and inhibition of p38 specific MAPKKs, f MKK3b and MKK6b. In addition, PPM1A and p38 co-immunoprecipitate in a single complex, indicating that they also interact directly. Interestingly, p38 and PPM1A could only be co-immunoprecipitated when following stress, suggesting that PPM1A may only complex with p38 when the latter is present in its phosphorylated (i.e., stress-activated) form.

Recently, PPM1A has been shown to directly dephosphorylate the extracellular receptor-activated kinase (Erk). Using biochemistry techniques, Li *et al.* found that PPM1A negatively regulated ERK by directly dephosphorylating its Thr202 position after EGF stimulation. Additional kinetic studies revealed key residues involved in phospho-ERK recognition by PPM1A. Importantly, PPM1A preferred the phospho-ERK peptide sequence over a panel of other phosphopeptides through the interactions of basic residues in the active site of PPM1A with the pThr-Glu-pTyr motif of ERK. Whereas Lys165 and Arg33 were required for efficient catalysis or phospho-substrate binding of PPM1A, Gln185 and Arg186 determined of PPM1A substrate specificity. The interaction between Arg186 of PPM1A and Glu203 and pTyr204 of phospho-ERK was identified as a hot-spot for phospho-ERK-PPM1A interaction⁸⁶.

p53/MDM2: PPM1A increases the transcriptional activity of p53, in a p53 dose-dependent manner⁸⁷. Using cells that stably express the human papilloma virus E6 protein, inhibition of colony formation by PPM1A was mediated (at least in part) by p53. These findings indicated, for the first time, that PPM1A is an important physiological regulator of p53 signaling. While a phosphatase deficient mutant of PPM1A did not alter MDM2, PPM1A down regulates MDM2 expression and activity to inhibit of p53. The mechanism of PPM1A increasing the proteasomal degradation of MDM2 has yet to be elucidated. It is not clear if MDM2 is directly dephosphorylated by PPM1A or if MDM2 is regulated indirectly by PPM1A.

IKK β /NF- κ B: Recently, PPM1A has been identified as an indirect regulator of NF- κ B by dephosphorylating and inactivating IKK β ⁴⁹. PPM1A and PPM1B were first identified as IKK β

phosphatases through a functional genomic approach by screening a library of serine/threonine phosphatases and identifying those whose overexpression inhibits IKK β -mediated NF- κ B activation with dephosphorylation of IKK β at the conserved residues Ser177 and Ser181 within the kinase activation loop. *In vitro* phosphatase assays confirmed that bacterially synthesized GST-PPM1A and GST-PPM1B dephosphorylated immunoprecipitated IKK β while the phosphatase-dead mutants did not. Functionally PPM1A was shown to inhibit NF- κ B transcription though inhibition of IKK β . Expression of IL-6, a pleiotropic cytokine as well as target of NF- κ B was inhibited by PPM1A following TNF α stimulation⁴⁹ or the hepatitis B virus X protein (HBx) perturbation⁸⁸.

Regulation of these pathways has been attributed to PPM1A phosphatase activity toward key components of the pathway in some cases (Smad2/3, MKK6, MKK4, p38 and Axin), but has not been fully characterized in others (Akt/ERK, p53/MDM2 and Cdk2 and Cdk6). In addition, PPM1A has been implicated in regulation of proliferation¹, cell invasion and migration⁸⁹, but PPM1A targets regulating these activities have not been identified.

Little is known about the regulation of PPM1A expression and/or activity. Recently, protein N-myristoylation, the irreversible covalent linkage of 14-carbon saturated fatty acid, myristic acid, to the N-terminal glycines was reported to be essential for PPM1A and PPM1B to dephosphorylate a physiological substrate, a subunit of AMPK (AMPKa)⁹⁰. An additional study revealed that hepatitis B virus X protein binds to endogenous PPM1A and that recombinant HBx dose-dependently reduced phosphatase activity of recombinant PPM1A *in vitro*⁸⁸.

3.3 PPM1B

As was the case for PPM1A, PPM1B was first identified using a rat liver library and a human teratocarcinoma library⁷⁹. Investigation of the transcripts of the PPM1B gene revealed that there are at least five different isoforms. As these isoforms differed only in their C-terminal domains, it has been suggested that the C-terminus is responsible for substrate specificity⁹¹. Several studies provided evidence showing that PPM1B is an important negative regulator of cellular signaling with similar physiological functions as PPM1A. PPM1B participates in the regulation of MAPK (p38/JNK), IKK β /NF- κ B, TAK1, p53/MDM2 and BAD (reviewed in¹). In regulation of pathways PPM1B shares with PPM1A, it is not clear if the two phosphatases have redundant roles or have different substrate specificities that may make their function complementary.

3.4 Wip1/PPM1D

The Wip1/PPM1D (wild- type p53-induced phosphatase 1) gene was originally identified by screening for p53 activated genes in WMN Burkitt lymphoma cells⁹². Tumor cell lines with wild-type p53 consistently showed that IR increases Wip1 mRNA while p53-deficient cell lines showed little or no induction of Wip1 expression. Like other 2C family members, Wip1 is insensitive to Okadaic acid-mediated inhibition. Cellular fractionation and indirect immunofluorescence indicated that the 61kDa Wip1 protein localizes to the nucleus⁹². In independent studies, Tong and colleagues⁹³ identified human Wip1 as a ubiquitously expressed protein up regulated in response to different types of stress, e.g., UV radiation or ethanol incubation. Overexpression of Wip1 in HEK293 cells blocks cell cycle progression, induces cell cycle arrest in early S phase, inhibits DNA synthesis, and induces cell death. Because of these findings, and because of the fact that it was a p53-induced gene, Wip1 was initially assumed to be a protein with growth inhibitory functions. Later experiments, however, convincingly demonstrated that it possesses growth-promoting, rather than growth suppressing properties, and that it contributes substantially to the development of several different types of malignancy. As outlined below, over the past few years, a significant amount of evidence

suggests that Wip1 functions as an oncogene, and that it exerts its effects through a variety of downstream mechanisms, e.g. inhibiting p38, p53, and ATM, interfering with cell cycle checkpoints (Chk1 and Chk2), and negatively affecting base-excision repair.

MAPK: The first report describing Wip1 as a regulator of cell growth and cellular stress signaling was provided by Imai and colleagues⁹⁴. Besides being activated by IR- or UV-induced stress, they observed up regulation of Wip1 expression in response to oxidative (H₂O₂) and ribotoxic stress (anisomycin). In addition, Wip1 dephosphorylates and inactivates the MAPK, p38 and attenuates the stress-induced p38-mediated phosphorylation of p53 on Serine 38 and Serine 46, resulting in a reduced transcriptional activity of p53 and in an inhibition of p53-mediated apoptosis⁹⁴. Taking into account that p53 induces the expression of Wip1, that Wip1 dephosphorylates and inactivates p38, and that this reduced activity of p38 results in a reduced transcriptional activity of p53, these three proteins seem to promote and negative feedback loop that is of substantial importance for regulating both cell growth and cellular stress signaling.

ERK activation by HER2/neu is also Wip1 dependent and crossing of MMTV-*neu* mice with Wip1 KO mice revealed that in the absence of Wip1, ERK activation by HER2/neu in cells responsive to hormone signaling was significantly reduced⁹⁵. However, to date, it remains unclear if Wip1 functions as a direct ERK phosphatase.

p53: In addition to inactivating p53 through a p38-dependent mechanism, Wip1 also directly dephosphorylates p53⁹⁶. In an *in vitro* phosphatase assay, purified Wip1 robustly dephosphorylates p53 Serine 15 phospho-peptide as well as full-length Serine 15-phosphorylated p53 in a magnesium-dependent and okadaic acid-independent fashion. Phosphorylation of p53 on Serine 15 is mediated by the kinases ATM and ATR in response to IR and UV irradiation, and it has been shown to be important for the apoptotic activity of p53⁹⁷, as well as for p53 stability, as pS15 inhibits the interaction of p53 with MDM2⁹⁸. Analyses of effects of IR and UV irradiation on protein levels and phosphorylation of p53 in mouse embryonic fibroblasts (MEFs) provided additional evidence for involvement of Wip1 in regulating p53 signaling⁹⁶. Transfection of the cells with wild-type Wip1

attenuated Serine 15 phosphorylation, and reduced the overall level of p53 (by promoting its interaction with MDM2). Transfection with phosphatase-dead mutant Wip1, or co-expression of Wip1 siRNA did not inhibit p53 activity⁹⁶. Taken together, these observations convincingly demonstrate that Wip1 plays an important role in regulating the activity and the stability of p53.

MDM2: In addition to promoting MDM2 interaction with p53 by dephosphorylating p53 at S15, Wip1 also directly stabilizes Mdm2⁹⁹. Wip1 interacts with and dephosphorylates Mdm2 at serine 395, a site phosphorylated by the ATM kinase. Dephosphorylated Mdm2 has increased stability and affinity for p53, facilitating p53 ubiquitination and degradation.

ATM: Wip1 dephosphorylates the ataxia-telangiectasia muted kinase (ATM) at Ser1981, a site critical for ATM monomerization and activation; moreover Wip1 is critical for resetting ATM phosphorylation as cells repair damaged DNA¹⁰⁰. Wip1 physically interacts with ATM even in unstressed cells, which seems to point towards a mechanism by which Wip1 assists in setting a threshold for the initial activation of ATM. The tumor suppressor protein ATM is known to be a master regulator of cell cycle checkpoints after DNA damage, specifically after IR-induced DNA double-strand breaks. ATM (co-)controls the activities of several different signaling pathways involved in cell cycle regulation and in the cellular stress response (e.g. p53), and its net effects include cell cycle arrest, activation of DNA repair and induction of apoptosis¹⁰¹. Taking the abovementioned observations into account, it seems reasonable to assume that by dephosphorylating and inactivating ATM, Wip1 functions as a positive regulator of cell growth and as an inhibitor of cellular stress signaling.

Chk1: Co-immunoprecipitation analyses, revealed that Wip1 also interacts with checkpoint kinase 1 (Chk1), yet another important regulator of cell cycle progression and cellular stress signaling⁹⁶. Wip1 directly dephosphorylates Chk1 on Serine 345 and Serine 317, and as a result, overexpression of Wip1 significantly reduced the kinase activity of Chk1 following UV-induced stress. Several breast cancer cell lines that endogenously express high amounts of Wip1 exhibited an attenuated UV-induced Chk1 Ser-345 phosphorylation as compared to cells expressing low amounts

of the phosphatase, confirming that Wip1 plays a physiological role in regulating Chk1 signaling. Again Wip1 abrogates both the intra-S and the G2/M checkpoint after IR and UV radiation in U2OS cells. These findings suggest that one of the primary functions of Wip1 is to reverse the p53- and the Chk1-induced cell cycle arrest, and to return the cells to a homeostatic state following the completion of DNA repair⁹⁶.

Chk2: Not long after Wip1 was identified as a Chk phosphatase, two groups showed that Wip1 also dephosphorylates Checkpoint kinase 2 (Chk2)^{102, 103}. Chk2 and Wip1 physically interact in a yeast two-hybrid screen and co-immunoprecipitated. After IR-induced Chk2 phosphorylation, Wip1 dephosphorylates two Serines (S19 and S33/35) and two Threonine (T68 and T432) residues in Chk2. siRNA-mediated knockdown of Wip1 resulted in an abnormally sustained Threonine 68 phosphorylation of Chk2 with increased susceptibility of several cell types to IR. As a result, overexpression of Wip1 suppressed the contribution of Chk2 to the IR-mediated induction of the G2/M checkpoint. Based on these studies, Wip1 can be considered not only a regulator of Chk1, but also an important physiological inhibitor of Chk2 signaling in response to DNA damage.

RelA/NF-κB: Wip1 was recently identified as a negative regulator of NF-κB signaling pathway⁴⁷ in both a p38-dependent and independent manner. Wip1 inhibits expression of NF-κB target genes IL-6, IRF-1 and ICAM expression through p38 while Wip's effect on expression of TNFα, IκBα and MCP-1 is p38-independent. In a dose dependent manner, overexpression of WIP1 decreases NF-κB activation, whereas WIP1 knockdown increases NF-κB function. *In vitro* phosphatase assays using full-length RelA or S536 phospho-peptide as substrates confirmed that WIP1 is a direct phosphatase targeting Ser536 of RelA. Phosphorylation of Ser536 is required for recruitment of the transcriptional co-activator p300 and is essential for the transactivation function of RelA. Wip1 regulates binding of NF-κB to p300 with downstream effects on chromatin remodeling. Consistent with the function of Wip1 to inhibit NF-κB activity, mice lacking WIP1 have phenotypic characteristics of enhanced inflammation providing the first genetic evidence that a phosphatase

directly regulates NF- κ B signaling *in vivo*. Wip1 activity to inhibit NF- κ B including NF- κ B oncogenic activities, suggest that in addition to the accepted role of Wip1 as an oncogene, it may also have tumor suppressor activities. Although untested, the balance between Wip1's oncogenic and tumor suppressive activities may depend on tissue, cellular or molecular context.

Collectively, the findings outlined above demonstrate that PPM phosphatases (Wip1, PPM1A, and PPM1B) are widely regulate proteins critical for cell growth and cellular stress signaling. Table 1.2 (adapted from¹) summarizes the pathways and the proteins impacted by PPM-mediated dephosphorylation. The number of proteins with known activity as tumor suppressors or oncogenes regulated by PPM family members is remarkable. PPM1A and PPM1B share many targets, suggesting either a collaborative or redundant regulation of these signaling pathways. A smaller number of targets are shared between Wip1 and the other 2 PPM family members (PPM1A and PPM1B) possibly attributable to the high amino acid sequence homology of PPM1A and PPM1B, compared to Wip1. There are several cases where PPM1A and Wip1 target distinct proteins within the same pathway with the same effect to increase or decrease activity (e.g. p38, NF- κ B). The major difference between PPM1A and Wip1 relates to their opposite roles in p53 regulation. Wip1 activates MDM2 and directly inhibits p53, whereas PPM1A destabilizes and inhibits MDM2 (Fig. 1.3, adapted from¹). Given the direct and indirect targets of Wip1 (p53, ATM, Chk1, Chk2, MDM2, ARF, and p16), Wip1 has been implicated as an oncogene. Expression data from human cancers also revealed that the Wip1 gene is amplified in many tumor types including pancreas, lung, liver, bladder and breast cancers¹⁰⁴⁻¹⁰⁶. It is not clear whether if PPM1A and Wip1 compete for substrates in these pathways or if they are selectively regulated by different upstream signals. Also the biological functions within the different pathways regulated by each of the PPM phosphatases suggest both oncogenic and tumor suppressor capacities. Regulation of PPM phosphatase activities toward specific targets with the ability to increase preference for one set of targets over others is

likely critical for determining cellular consequences. Given activities that have opposing tumor outcomes, it is likely that the biological consequences associated with PPM phosphatase activity reflect an orchestra of all regulated pathways.

Table. 1.2 Overview of PPM phosphatases interaction with proteins regulating cell growth and cellular stress signaling (adapted from ¹). ↓Indicates that the (over-)expression of the respective phosphatase results in an inactivation of the indicated pathway, ↑ indicates an

| PPM phosphatase | Signaling pathway | Target protein(s) in this pathway | Effect on cell growth | Effect on stress signaling |
|-----------------|-------------------|-----------------------------------|-----------------------|----------------------------|
| PPM1A | AMPK | AMPK | — | ↓ |
| | JNK | MKK4, MKK7 | — | ↓ |
| | p38 | p38, MKK3b, MKK6b | — | ↓ |
| | CDK | Cdk2, Cdk6 | ↓ | — |
| | p53 | MDM2 | ↓ | ↑ |
| | TGFβ | Smad2/3 | ↓ | — |
| | NF-κB | IKKα, IKKβ | ↓ | ↓ |
| PPM1B | JNK | mkk4, MKK7, TAK1 | — | ↓ |
| | p38 | MKK3b, MKK6b | — | ↓ |
| | NF-κB | IKKα, IKKβ | ↓ | ↓ |
| | CDK | Cdk2, Cdk6 | ↓ | — |
| | p53 | MDM2 | ↓ | ↑ |
| | Bcl-xL | BAD | ↓ | — |
| Wip1/PPM1D | p38 | p38 | — | ↓ |
| | p53 | p53, p38, ATM, MDM2 | ↑ | ↓ |
| | ATM | ATM | ↑ | ↓ |
| | Chk | Chk1, Chk2 | ↑ | — |
| | ARF | p38 | ↑ | — |
| | INK4A | p38 | ↑ | — |
| | NF-κB | RelA | ↓ | ↓ |

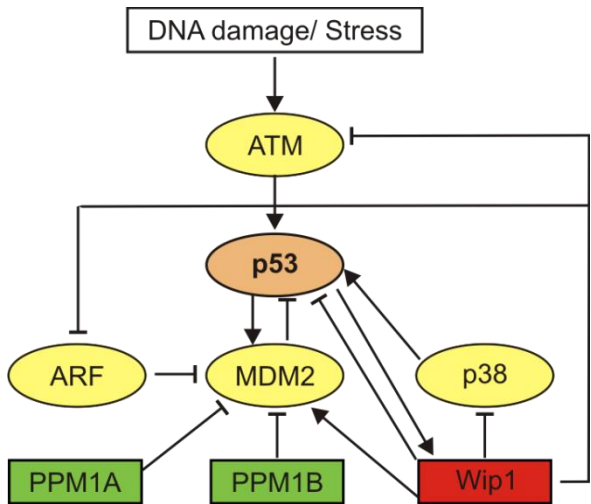


Fig. 1.3 PPM phosphatases regulate p53 signaling (adapted from¹). \perp indicates inhibition of the respective protein, \uparrow indicates activation.

4. LZAP

4.1 General introduction to LZAP

LZAP (also called CDK5rap3 or C53) was first described as a binding partner of the 35kDa CDK5 activator binding protein p35Nck5a in 2000¹⁰⁷. Activity of CDK5rap3 related to p35Nck5a has not been further characterized and is unlikely to represent its major activity since expression of CDK5 and p35Nck5a is restricted to neurons while LZAP is ubiquitously but variably expressed in all tissues tested^{82, 107}. Consistent with alternative roles for CDK5rap3, we have identified this protein as a novel binding partner for the tumor suppressor ARF (alternative reading frame) through an unbiased yeast two-hybrid screen approach in 2006. Based on these data, we renamed this protein LZAP for LXXLL/leucine zipper-containing ARF-binding protein. LZAP is a highly conserved protein in vertebrates, invertebrates and plants, but not in yeast and bacteria. Within the cell LZAP localizes to cytoplasmic and nuclear compartments. Database searches and publications have failed to identify homologs and amino acid or nucleotide alignment of suggest that LZAP shares no significant amino acid homology with any known protein and also lacks conserved functional domains, except for putative leucine zipper (amino acid 357-385) and LXXLL motifs. Human LZAP has two LXXLL motifs and one conserved LXXLL-like LXXFL motif. These motifs are of unknown significance for LZAP activity, but are important for nuclear hormone receptor co-regulator binding to steroid receptors and transcriptional co-activators^{108, 109}. We previously demonstrated that loss of LZAP promotes tumor growth *in vivo* and that LZAP is lost in ~30% of human HNSCC¹¹⁰. We have targeted LZAP in mice and our preliminary findings suggest that homozygous knockout of LZAP is embryonic lethal in early stage of development with inability to identify LZAP-/- embryo as early as embryonic day 4.5 (unpublished data). Interestingly, heterozygous mice with targeted LZAP are susceptible to lung tumor formation (unpublished data). We further explored developmental roles of the LZAP gene during zebrafish morphogenesis¹¹¹. LZAP is maternally deposited in the zebrafish embryo. Expression is initially ubiquitous during gastrulation, and later becomes more prominent in the pharyngeal arches, digestive tract, and brain. Morpholino-mediated depletion of LZAP delays

cell divisions and induces apoptosis during blastomere formation, resulting in fewer and larger cells before epiboly. Cell cycle analyses suggested that LZAP loss in early embryonic cells precipitates a G2/M arrest. Furthermore, the LZAP-deficient embryos failed to initiate epiboly--the earliest morphogenetic movement in animal development--which has few described requirements, but has been shown to depend on cell adhesion and migration of epithelial sheets. These functions provide further insight into LZAP activity and suggest that LZAP is required during early development and inhibits tumor formation. Molecular mechanisms of LZAP activities continue to emerge. We and others have described LZAP functions to regulate activities of ARF, p53, p38 MAPK, NF- κ B, Wip1, Chk1 and Chk2.

4.2 Mechanisms of LZAP activity

RelA and NF- κ B pathway: Our lab reported that LZAP directly binds to RelA and that amino acids 195-313 of RelA are required for the interaction¹¹⁰. LZAP inhibits RelA phosphorylation at S536 and decreases RelA transcriptional activity toward selective gene targets, as well as increases RelA association with HDAC1, HDAC2 and HDAC3. Conversely, loss of LZAP increases both basal and cytokine-induced RelA transcriptional activity. Based on ChIP analyses, LZAP is present on chromatin at select NF- κ B-responsive promoters. These data suggest that LZAP is a potent NF- κ B inhibitor and that endogenous LZAP inhibits both basal and activated NF- κ B, possibly by converting NF- κ B to a transcriptional repressor through interaction with HDACs. Functionally, decreased expression of LZAP increases expression of MMP-9 and increases cellular invasion, both of which are dependent on NF- κ B. Overexpression of LZAP sensitizes cells to TNF α -induced cell death similar to effects of the NF- κ B inhibitor I κ B likely through inhibition of NF- κ B mediated anti-apoptotic signaling. Knockdown LZAP in xenograft tumor cells promotes tumor growth and angiogenesis. In primary HNSCC tumors LZAP protein levels inversely correlated with expression of the NF- κ B regulated genes IL-8 and I κ B α . Collectively, these data suggest that LZAP is a putative

tumor suppressor and that LZAP regulation of NF- κ B activity requires LZAP association with RelA and modification of RelA phosphorylation.

ARF and p53 pathway: Our lab found that LZAP binds ARF in a yeast two-hybrid screen designed to identify ARF-interacting proteins potentially involved in regulation of ARF activity. LZAP binds ARF, co-localizes with ARF, and forms a ternary complex with ARF, HDM2 and p53 in mammalian cells. Expression of LZAP in the presence of ARF further enhances p53-mediated expression of the cyclin-dependent kinase inhibitor p21/Cip1 and enhances the ARF-mediated G1 cell cycle arrest. Upon direct binding to ARF, LZAP reverses ARF inhibition of HDM2's p53 ubiquitination activity, but despite its ability to restore HDM2-mediated p53 ubiquitination, LZAP expression does not decrease p53 stability in the presence of ARF. In fact, when expressed with HDM2 and ARF, LZAP stabilizes p53 protein by inhibiting p53 nuclear export and further augmentations p53 transcriptional activity. Ectopic expression of LZAP in mammalian cells induces a p53-dependent G1 cell cycle arrest. Remarkably, a similar pattern of p53 activation and a p53-dependent G1 cell-cycle arrest were observed in ARF null cells. Because LZAP does not inhibit proliferation in cells lacking p53 activity, LZAP mediated cell cycle arrest is dependent on p53¹¹². These findings suggest that LZAP regulates p53 through ARF-dependent and -independent mechanism(s), the later could be attributable to activity of novel LZAP-binding partners.

Chk1/2: To date, there is a single publication describing LZAP activity towards the checkpoint kinases Chk1 and Chk2 (hereafter called Chk1/2)¹¹³. Passage through the G2/M checkpoint depends on activation of the CDK1/cyclin B complex and is tightly regulated by Chk1/2 through CDC25. Recent evidence indicates that in response to DNA damage, p38 MAPK also triggers the G2/M checkpoint through regulation of CDC25¹¹⁴. Endogenous and exogenous stresses, such as replication fork collapse or IR, result in DNA damage and activation of the apical serine/threonine protein kinases belonging to the PI3K family, including ATM, ATR and DNA-PK. Activated PI3Ks in turn phosphorylate and activate the downstream checkpoint kinases Chk1/2. Although both Chk1 and Chk2 can phosphorylate and inhibit CDC25, Chk1 seems to be the primary kinase responsible for the

G2/M checkpoint¹¹⁵. Chk1/2-mediated phosphorylation of CDC25C at S216 is required for its recruitment of 14-3-3. Binding of 14-3-3 to CDC25C, either directly or through cytoplasmic sequestration, inhibits CDC25C binding to the CDK1/cyclin B complexes¹¹⁴. Jiang *et al.* reported that during DNA damage response, LZAP inhibits Chk1/2 phosphorylation and activation. By counteracting Chk1, LZAP activates CDC25C resulting in downstream CDK1 activation¹¹³ (Fig. 1.4). It is well known that Chk1/2 are phosphorylated and activated after DNA damage by ATM and ATR. Expression of LZAP is associated with decreased phosphorylation and inhibition of Chk1/2, but this effect is not mediated through decreasing the activities of their upstream kinases. Since checkpoint kinases are inhibited by LZAP, their activity toward CDC25C is similarly inhibited, resulting in activation of CDK1 and inappropriate or early progression into mitosis¹¹³. Jiang *et al.* have shown that knockdown of LZAP inhibits CDK1 and delays mitotic entry¹¹³. These results are consistent with an earlier report by the same group that LZAP increases sensitivity to genotoxins related to inappropriate progression through the G2/M checkpoint¹¹⁶. These data show that LZAP binds and inhibits Chk1 resulting in dysregulation of cell cycle progression; however, Chk1 and Chk2 kinases phosphorylate and regulate targets in addition to CDK1, including p53. Mechanisms explaining how LZAP alters Chk1/2 phosphorylation and activity remain unclear.

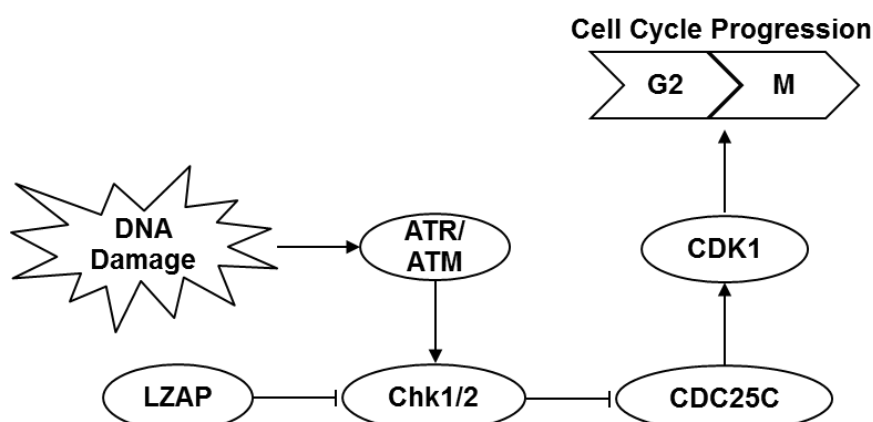


Fig. 1.4 LZAP Inhibits Checkpoint Kinases. LZAP inhibits Chk1 and Chk2 causing activation of CDC25C and CDK1. Simplified, LZAP is an activator of CDK1 through inhibition of checkpoint kinases. Arrows indicate activation and T shapes indicate inhibition.

p38: To better understand LZAP biological activities and to gain mechanistic insight, additional LZAP binding partners have been sought. Through a Scan Site Search (<http://scansite.mit.edu/>) using LZAP sequence, we found that LZAP contains sites predicted to bind to the common MAPK docking domain (D domain). LZAP binding to p38 α MAPK was confirmed by *in vivo* binding assays and immunofluorescent staining of expressed proteins shows nuclear co-localization of p38 α with LZAP¹¹⁷. LZAP expression is associated with a dose dependent decrease in p38 phosphorylation and activity, both at basal level and following cytokine stimulation while siRNA-mediated loss of LZAP increases p38 phosphorylation and activity after cytokine treatment indicating that LZAP regulates p38 phosphorylation at both basal and stimulated levels. LZAP's activity to inhibit p38 phosphorylation does not depend on upstream p38 activating MAPK kinases, MKK3 or MKK6.

4.3 Regulation of LZAP

To date, little is understood regarding regulation of LZAP in normal or tumor tissues. We and others have shown that LZAP is ubiquitously expressed in all human, rat and mouse tissues tested, including pancreas, brain, liver, heart, intestine, spleen, thymus, muscle and lung (^{118, 119} and unpublished data). Expression of LZAP is markedly decreased or undetectable in 30% of HNSCC, but mechanisms of LZAP loss are currently unknown¹¹⁰. LZAP can be phosphorylated in *in vitro* kinase assay by Cdk5¹⁰⁷; however, it is not clear if LZAP is phosphorylated *in vivo* or what sites of LZAP are phospho-acceptor sites. LZAP homodimerization has been suggested by one publication that used LC/MALDI mass spectrometry of bands separated by polyacrylamide gel electrophoresis after Flag-LZAP immunoprecipitation¹¹⁹.

Recently, a novel protein, KIAA0776 (also RCAD/NLBP/UFL1) was reported as a novel LZAP binding partner by four independent groups. KIAA0776 was first reported by Kwon *et al.* using tandem affinity purification of LZAP followed by mass spectrometry¹²⁰. Binding domain mapping determined that amino acids 301-400 in LZAP and 121-250 in KIAA0776 is required for the interaction the two proteins. Loss of KIAA0776 by siRNA knockdown decreases LZAP stability

which could be mediated by binding between LZAP and KIAA0776, since co-expression of LZAP with a KIAA0776 deletion mutant lacking binding activity to LZAP did not influence ubiquitination levels of LZAP and vice versa. On the other hand, expression of wild-type KIAA0776 decreases LZAP ubiquitination¹²⁰. Wu *et al.* reported the identification of two LZAP binding partners, KIAA0776 /RCAD and C20orf116 /DDRGK1¹¹⁹. LZAP forms a large protein complex with these two proteins as demonstrated by size exclusion chromatography. Loss of KIAA0776 decreases LZAP and C20orf116 protein half-life. LZAP and C20orf116 are fairly stable in control cells and are not very robustly subjected to proteasome-mediated degradation; however, after siRNA knockdown of KIAA0776, they observed significant elevation of LZAP and C20orf116 proteins even by 2 hours after MG132 treatment. This is different from the result of the Kwon group where they showed that in control cells, the LZAP level is increased after treatment with MG132. Both of the groups showed that KIAA0776 inhibits cell invasion and negatively regulates the NF-κB signaling pathway thought to be through interaction with LZAP. Wu *et al.* also determined C20orf116, the second LZAP binding protein localizes to the endoplasmic reticulum (ER) and is anchored there by its amino (N)-terminal signal peptide. A third group¹²¹ using Bergmann glia cells further showed that KIAA0776/Mixer is also a novel ER-associated protein and KIAA0776 anchors LZAP to the ER and inhibits LZAP function in the nucleus, e.g. Cyclin D1 transcription repression though NF-κB. KIAA0776 shRNA knockdown shifted LZAP from the cytoplasm to nucleus. This is the first report demonstrating regulation of LZAP subcellular localization. Loss of KIAA0776 eventually induces cell accumulation at G1 phase and suppresses proliferation of C6 glioma cells which are rescued by simultaneous knockdown of LZAP¹²¹. These data are consistent with our finding that LZAP regulates cell cycle arrest in G1 phase¹¹². The fourth paper by Lemaire *et al*, 2011¹¹⁸ identified another LZAP binding protein, UFM1 (ubiquitin fold modifier 1) which belongs to ubiquitin-like proteins family, a novel protein-conjugating system displaying a similar tertiary structure to ubiquitin¹²². Similar to ubiquitin, UFM1 also requires a three enzyme system to complete conjugation to targeted proteins. UFM1 is activated via the E1 enzyme, UBA5, and then conjugated

by the E2 enzyme, UFC1. UFC1 has very recently been identified as the E3 conjugating enzyme¹²³. Interestingly, UFC1 is KIAA0776, one of the LZAP binding proteins; moreover, C20orf116/UFBP1, the other LZAP binding protein, is a substrate of UFM1¹²³. *In vitro* pull down assays confirmed binding between LZAP and UFM1 and again LZAP and KIAA0776¹¹⁸. Co-immunoprecipitation data suggests UFM1, LZAP, KIAA0776 and C20orf116 do not directly interact with each other but rather are part of the complex. It is unclear whether LZAP is a substrate of UFM1 or the interaction between KIAA0776 and LZAP is dependent on KIAA0776 E3 ligase activity. Also there are no reports identifying lysine residue(s) in LZAP targeted for ubiquitination. Due to the consistent results that KIAA0776 decreases LZAP ubiquitination, it is possible that there is competition between KIAA0776 and E3 ubiquitin ligases for the same lysine residue(s) in LZAP. In addition to ubiquitination-mediated proteasome degradation, Jiang *et al.* mentioned as unpublished data in their recent paper that LZAP is cleaved by caspase-3 at three sites (D268, D282 and D311)¹¹³.

5. Summary and Dissertation Goals

NF-κB, a family of transcription factors, mediates effector function of almost all innate and adaptive immune responses and regulates cell proliferation, differentiation and apoptosis. Activated NF-κB also functions as an oncogene in tumorigenesis, progression and metastasis. Because of the role of NF-κB in important biological processes, NF-κB activity is intricately controlled at multiple levels with post-translational modification, in particular phosphorylation, serving a critical role. RelA is the most well studied transactivation-domain containing family member of NF-κB. Our interest in RelA phosphorylation was peaked when we found that LZAP tumor suppressor activity was in part mediated by inhibition of RelA phosphorylation at serine 536¹¹⁰. Since LZAP has no known enzymatic activity and LZAP has no activity to inhibit RelA specific kinases (IKKα/β/ε, TBK1 and RSK, data not shown), the role of LZAP as a regulator of phosphatases was explored. Though dozens kinases have been identified that modify specific serine or threonine residues in

RelA, less is known about RelA specific phosphatases. Given the number of RelA kinases, it is reasonable to expect that more than two phosphatases (PP2A and Wip1) target RelA for dephosphorylation as a mechanism to restore basal steady state RelA activity. I hypothesized that PPM1A, the PPM family member may function as a RelA phosphatase and that the tumor suppressor activity of PPM1A is at least partially dependent on its negative regulation of NF- κ B. We noticed an overlap of LZAP regulated proteins and substrates of PPM1A, PPM1B and Wip1 (e.g. RelA, p53, Chk1/2 and p38) and developed preliminary data suggesting that PPM family members bound to LZAP. Based on these findings, I further hypothesized that LZAP regulated protein phosphorylation and activity through facilitating interaction of PPM phosphatases and target proteins. In this dissertation, RelA and p38 were chosen from the pool of LZAP targets and used as models to study the mechanism(s) of LZAP-mediated dephosphorylation and activity. Since a growing body of literature demonstrates pleiotropic roles of LZAP, including that of a putative tumor suppressor, it is important to understand the regulation of LZAP. Given that LZAP binds to phosphatases, I further hypothesized that post-translational phosphorylation and ubiquitination may regulate LZAP activity and protein stability. The primary objective of my work is to test these hypotheses and more importantly, contribute to the understanding of NF- κ B and LZAP activities and regulation.

CHAPTER II

PPM1A IS A RELA PHOSPHATASE WITH TUMOR SUPPRESSOR-LIKE ACTIVITY

Part of the work presented in this chapter is published under the identical title in *Oncogene*, 2013.

Abstract

NF- κ B signaling contributes to human disease processes, notably inflammatory diseases and cancer. NF- κ B plays a role in tumorigenesis and tumor growth, as well as promotion of metastases. Mechanisms responsible for abnormal NF- κ B activation are not fully elucidated; however, RelA phosphorylation, particularly at residues S536 and S276, is critical for RelA function. Kinases that phosphorylate RelA promote oncogenic behaviors suggesting that phosphatases targeting RelA could have tumor inhibiting activities; however, few RelA phosphatases have been identified. Here, we identified tumor inhibitory and RelA phosphatase activities of the PPM phosphatase family member, PPM1A. We show that PPM1A directly dephosphorylated RelA at residues S536 and S276 and selectively inhibited NF- κ B transcriptional activity resulting in decreased expression of MCP-1/CCL2 and IL-6, cytokines implicated in cancer metastasis. PPM1A depletion enhanced NF- κ B-dependent cell invasion while PPM1A expression inhibited invasion. Analyses of human expression data revealed that metastatic prostate cancer deposits had lower PPM1A expression compared to primary tumors without distant metastases. A hematogenous metastasis mouse model revealed that PPM1A expression inhibited bony metastases of prostate cancer cells after vascular injection. In another xenograft model, PPM1A depletion facilitated tumor growth and cellular proliferation while inhibiting apoptosis. In summary, our findings suggest that PPM1A is a RelA phosphatase with NF- κ B regulatory activity, and that PPM1A has tumor suppressor-like activity. Our analyses also suggest that PPM1A inhibits prostate cancer metastases and since neither gene

deletions nor inactivating mutations of PPM1A have been described, increasing PPM1A activity in tumors represents a potential therapeutic strategy to inhibit NF- κ B signaling or bony metastases in human cancer.

Introduction

NF- κ B, comprised of a family of pluripotent transcription factors, plays a fundamental role in inflammatory and immune responses and aberrant NF- κ B activity can directly contribute to tumorigenesis, neovascularization, tumor growth and metastases^{25, 50}. NF- κ B activation has been described in many tumors including: HNSCC^{54, 110} and breast cancer^{124, 125}. Dysregulation of NF- κ B in prostate cancer has been identified as a major driver of distant metastasis, which is the primary cause of death in this common male cancer⁶¹⁻⁶³. One transcriptional target of NF- κ B, monocyte chemotactic protein-1 (MCP-1), also known as chemokine (C-C motif) ligand 2 (CCL2), has been implicated in prostate cancer migration, invasion and metastasis through effects on both tumor cells and the microenvironment⁶⁵. MCP-1 seems to be particularly implicated in bony metastases for prostate cancer and in other tumor types including renal cancer, bladder cancer and breast cancer⁶⁶. Although mechanisms governing MCP-1 expression are not fully described, the suspected importance of this cytokine in tumor progression is affirmed by the recent initiation of clinical trials using neutralizing antibody targeting MCP-1.

Because of the role of NF- κ B in varied biological processes, NF- κ B activity is intricately controlled at multiple levels. Inhibition of NF- κ B through binding to I κ B α with prevention of nuclear translocation has been well characterized; however, full activation of nuclear NF- κ B transcriptional activity requires phosphorylation of RelA¹²⁶. Phosphor-acceptor sites of RelA have been characterized^{126, 15} particularly implicating serine 536 and serine 276 as critical for NF- κ B activation^{19,23}. Although not as extensively studied, dephosphorylation of RelA is needed to prevent harmful effects of prolonged RelA signaling⁴². To date, only two phosphatases, PP2A and

Wip1/PPM1D, have been shown to directly dephosphorylate RelA, both having activity toward S536^{43, 47}. Deficiency of PP2A contributes to the constitutive activation of RelA in melanoma cells⁴³ and mice lacking Wip1 have an inflammatory phenotype⁴⁷ suggesting that loss of RelA-targeting phosphatases can impact pathological processes including cancer.

PPM1A belongs to the protein phosphatase magnesium/manganese-dependent family (PPM) family together with Wip1 and PPM1B. PPM1A has been implicated in regulation of several signaling pathways including TGFβ/Smad⁸², MAPK (JNK/p38), Cdk2 and Cdk6¹ and the nerve growth factor activated Akt/ERK pathway⁸³. Regulation of these pathways has been attributed to PPM1A phosphatase activity toward key pathway components in some cases (e.g. Smad2/3 and p38), but has not been fully characterized in others (e.g. Akt/ERK, Cdk2 and Cdk6). In addition, PPM1A has been implicated in regulation of proliferation¹, cell invasion and migration⁸⁹, but targets of PPM1A activity that regulate these activities have not been identified. Recently, PPM1A has been described as an indirect regulator of NF-κB through dephosphorylation and inactivation of IKKβ⁴⁹. Here we show that PPM1A directly dephosphorylated RelA at Ser-536 and Ser-276 with resultant inhibition of NF-κB transactivation and decreased expression of target genes, notably including MCP-1/CCL2. We report that PPM1A expression was down-regulated in human metastatic prostate cancer, and that restoration of PPM1A decreased seeding and bony growth of prostate cancer cells in an animal vascular injection model. In addition, loss of PPM1A increased NF-κB dependent invasion and accelerated xenograft tumor growth. These data suggest that PPM1A has tumor suppressor-like qualities that are, at least partially, dependent on regulation of RelA.

Materials and Methods

Expression Plasmid and small hairpin RNA expression Constructs

Myc-PPM1A, Myc-PPM1A (R174G) mutant, GST-PPM1A and GST-PPM1A (R174G) were gifts from Dr. Sun⁴⁹. His-Wip1 was a gift from Dr. Donehower⁹⁹. PPM1A was PCR amplified and subcloned into the pHIT-dell2-puro retroviral expression vector. Other constructs were described previously¹¹⁰. A pSuper-retro vector (provided by Dr. Reuven Agami) was used to generate shRNA plasmids for PPM1A with the following target sequence 5'-AAGTACCTGGAATGCAGAGTA-3' (ref.⁴⁹). Lentiviral vector pGIPZ and plasmid coding for PPM1A-targeting shRNA (Clone ID V2LHS_35113) were from Open Biosystems, Waltham, MA. PPM1A-1 (catalog# SI02659258, Hs_PPM1A_5) and PPM1A-2 (catalog # SI02659265, Hs_PPM1A_6) siRNA were purchased from QIAGEN, Germantown, MD. Control siRNA (nontargeting#1) was from Dharmacon, Waltham, MA.

Cell lines, cell culture, transfection and virus infection

IKKalpha^{-/-}, *IKKbeta*^{-/-} (*IKK1*^{-/-}, *IKK2*^{-/-}) double null MEFs were a gift from Dr. Verma (the Salk Institute for Biological Studies, Laboratory of Genetics, San Diego, CA). PC3 and LNCaP cell lines were provided by Dr. Renjie Jin (Vanderbilt University, Nashville, TN). Cell lines were maintained according to ATCC protocol. TransIT-2020 (Mirus, Madison, WI) was used for MEFs transfection. SiRNA was transfected at 20nM using Lipofectamine RNAiMAX (Invitrogen, Carlsbad, CA). All transfection reagents were used according to the manufacturers' instructions. Cells expressing PPM1A or shRNA targeting PPM1A were infected with indicated virus-containing medium with 4mg/ml polybrene (Sigma-Aldrich, St. Louis, MO). For transient expression, cells were used after 24 h of infection. Stable cell lines were selected for 10 days in puromycin (1ug/ml).

Antibodies and reagents

Rabbit anti-RelA (C20), anti-phospho-S276 RelA (sc101749), anti-GAPDH, anti-I κ B α (C21), anti-I κ K α / β (sc7607) and HRP-conjugated secondary donkey anti-mouse and anti-rabbit antibodies were from Santa Cruz Biotechnology, Santa Cruz, CA. Mouse and rabbit anti-PPM1A were from Abcam, Cambridge, MA (p6c7) and GeneTex, Irvine, CA (GTX109744), respectively. Rabbit anti-

phospho-S468 RelA (Ab31473) was from Abcam. Mouse anti-Flag M2, anti-Flag M2 affinity gel and 3XFlag peptide were from Sigma-Aldrich. Anti-phospho-S536 RelA (Cell Signaling, Boston, MA). TNF α and IL-1 β were from PeproTech, Rocky Hill, NJ.

Immunoprecipitation and immunoblotting

Cells were lysed in 0.5% (v/v) Nonidet P-40 lysis buffer supplemented with protease inhibitor cocktail (Roche, Indianapolis, IN) and phosphatase inhibitor III (Sigma-Aldrich). Total cell lysate was incubated with anti-Flag M2 affinity gel (Sigma-Aldrich) and immunoprecipitation was performed according to manufacturer's instruction. Immunoblotting was performed as previously described¹¹⁷.

***In vitro* phosphatase reaction and malachite green phosphatase assay**

The experiment was performed as described⁴⁹ with modified phosphatase 2C buffer (50mM Tris-HCl pH7.5, 0.1mM EGTA, 0.02% 2-mercaptoethanol \pm 25mM MgCl₂). Flag-RelA protein was used as substrate after elution with using 3 \times Flag peptide (Sigma-Aldrich). Phospho-peptide analysis was performed as described⁴⁷ with modified PPM buffer and malachite green assay kit (#POMG-25H, BioAssay Systems, Hayward, CA). Phospho-peptides synthesized by LifeTein: RelAS536 (GDEDFSpSIADMD), RelAS276 (QLRRPpSDRELS)⁴⁷. His-Wip1 was purified using Ni-beads as described⁹⁹.

Luciferase reporter gene assay

Dual-Luciferase Reporter Assay (Promega, Madison, WI) was performed as previously described¹¹⁰.

cDNA synthesis and real-time PCR

mRNA was extracted using RNeasy mini (QIAGEN). cDNA synthesis was performed using iScript cDNA synthesis kit (BIO-RAD, Hercules, CA). Real-time PCR was performed using iQ SYBR green supermix (BIO-RAD). RT-PCR Array (PAHS-025A, SABiosciences) was used according to manufacturer's instructions. MCP-1 primer sequences: forward 5'ctgctcatagcagccaccc3', reverse 5'gcactgagatcttctattgggt3'. GAPDH was used as control.

Chromatin Immunoprecipitation (ChIP) Assays

ChIP assays were performed using Magna ChIP A/G (#17-10085, EMD Millipore, Billerica, MA) following manufacturer's instructions. 3×10^6 HeLa cells were used for each assay. Anti-RelA antibody (SC-109 X) and normal rabbit IgG (Santa Cruz) were used for immunoprecipitation. Purified DNA was analyzed by real time PCR. Primers ((NM_002982.3 (-) 03Kb) for the kB binding site on MCP-1 promoter were from SA Bioscience/Qiagen.

***In vitro* cell invasion assay**

Transwell invasion assay was performed as described¹¹⁰. 2×10^4 HeLa cells, 5×10^4 PC3-LUC cells or 1×10^5 LNCaP cells were seeded into the upper chamber and analyzed after 21 h, 42 h and 46 h respectively. Membranes mounted to slides were scanned at $1.25 \times$, $10 \times$ and $20 \times$ using the Ariol SL-50 platform at Vanderbilt Epithelial Biology Center or under microscope with $200 \times$ magnifications.

Cell fractionation

Cell fractionation was performed as described¹²⁷ with modified hypotonic buffer (10mM HEPES pH 7.1, 50mM NaCl, 0.3M sucrose, 0.1mM EDTA, 0.5% TritonX100, 1mM DTT) and washing buffer (10mM HEPES pH 7.1, 0.1mM EDTA, 1mM DTT).

DNA binding assay

Assay was performed as described¹¹⁰ using TransAM NF-κB p65 assay kit (cat# 40096, Active Motif, Carlsbad, CA).

Obtaining conditioned medium (CM) and ELISA Assay

Conditioned media were obtained from PC3 cell cultures as described¹²⁸. Cell number from each well was counted to normalize data for differences. MCP-1 concentration was measured by MCP-1 ELISA kit (R&D system, Minneapolis, MN) following manufacturer's protocol.

The Gene Expression Omnibus (GEO) analysis

Normalized PPM1A expression data were downloaded from GEO (<http://www.ncbi.nlm.nih.gov/projects/geo/>) with citations for individual studies. Gene expression were analyzed and plotted with average \pm SD in Prism 5.0 (GraphPad, La Jolla, CA).

***In vivo* tumor metastasis assay and BLI ex vivo analysis**

1×10^5 PC3-LUC cells infected with control or PPM1A-expressing retrovirus suspended in 0.1 ml of PBS were inoculated into the left cardiac ventricle of male nude mice. Metastases were monitored by bioluminescent imaging weekly (Xenogen IVIS 200 imaging system, Alameda, CA). Mice with bioluminescent signal in the chest cavity 1 h post-injection were excluded from the study since this indicated leakage of tumor cells during injection ¹²⁹. Four weeks after injection mice were radiographed (Faxitron X-ray system, Tucson, Arizona), and long bones and spines were decalcified and paraffin embedded. Sections were stained with hematoxylin and eosin.

***In vivo* xenograft tumor growth assay**

Animal protocols were approved by the Vanderbilt University Institutional Animal Care and Use Committee. Female nude mice (Harlan, Indianapolis, IN) were inoculated subcutaneously at 4 spots at age 6 to 10 weeks using 1×10^6 HeLa cells infected with control retrovirus or retrovirus driving expression of PPM1A-specific shRNA. Tumor length (L) and width (W) was recorded weekly using calipers until the largest tumors approached 20 mm in length. Tumor volume was calculated using the formula: volume = $\frac{1}{2} \times L \times W^2$. Each mouse received 100ul (10mg/ml) BrdU i.p. injection 2 hrs before sacrifice. Excised tumors were weighed, and portions frozen or fixed in 4% paraformaldehyde before embedding in paraffin. PPM1A expression was determined in tumors by immunoblotting (10 of 17 control tumors and 12 of 18 PPM1A knockdown tumors were large enough and with sufficient growth record) and tumor growth analyses stratified based on PPM1A expression (maintenance of knockdown). Hematoxylin and eosin staining and immunostaining of BrdU and cleaved Caspase3 were performed by the Vanderbilt Immunohistochemistry Core Laboratory. At least five high-powered fields were counted for each tumor.

Statistical analysis

Statistical analyses were performed using R version 2.14.1 for Windows, and data plotted and analyzed using student t-test, fisher exact test, Wilcoxon rank sum test or Kruskal-Wallis chi-square test. To take into account the correlation among repeated measurements from the same tumor, linear

mixed-effect models were fit to the tumor volume over time. *, **, *** represents p values less than 0.05, 0.01 and 0.001, respectively, unless otherwise noted.

Results

PPM1A directly dephosphorylates RelA

To better understand drivers of cancer progression and metastases, we sought to identify phosphatase inhibitors of NF-κB that work directly to dephosphorylate of RelA. Because the PPM family member Wip1 is one of the two described RelA phosphatases, we considered a PPM family member, PPM1A, as a candidate RelA phosphatase. To begin exploring this possibility, the effect of endogenous PPM1A on RelA phosphorylation was determined in U2OS and HeLa cells. Following PPM1A depletion using two independent siRNAs, RelA phosphorylation at S536 was increased in both cell lines while total RelA levels were not altered (Fig. 2.1A). Depletion of PPM1A further increased RelA phosphorylation following stimulation with TNF α (Fig. 2.2A). siRNA-mediated depletion of PPM1A did not alter total RelA levels (Fig. S1A) and did not affect PPM1B or Wip1 protein expression (Fig. 2.2B). Expression of wild-type PPM1A decreased S536 phosphorylation of ectopically expressed RelA both with and without TNF α stimulation, whereas phosphatase-dead (R174G) PPM1A had no effect (Fig. 2.1B). Interestingly, RelA S276 phosphorylation was similarly decreased by expression of PPM1A (Fig. 1B) and siRNA-mediated depletion of PPM1A increased S276 phosphorylation after TNF α treatment (Fig. 2.2C). Phosphorylation of S468, a known transcriptional inhibition phosphorylation site of RelA^{41, 111} was unaffected by expression of PPM1A (Fig. 2.1B, 0.9 normalized to vector control as 1).

We confirmed reports that PPM1A decreases IKK α and IKK β phosphorylation⁴⁹ (Fig. 2.2D); therefore, decreased RelA phosphorylation observed following expression of PPM1A could be a result of direct activity to dephosphorylate RelA or be mediated by IKKs. To begin exploring these possibilities, PPM1A was expressed in *IKKalpha*-/-, *IKKbeta*-/- double-null mouse embryonic fibroblasts. Notably, PPM1A expression resulted in decreased RelA S536 phosphorylation in the

absence of IKK α or IKK β (Fig. 2.1C lanes 4, 5) indicating that PPM1A regulates RelA independent of IKKs. In these cells, decreased RelA phosphorylation was also dependent on PPM1A phosphatase activity and did not alter in RelA protein levels (Fig. 2.1C).

Although PPM1A activity toward RelA was independent of IKKs, PPM1A regulation of RelA phosphorylation could be mediated through unknown indirect activities or through direct dephosphorylation of RelA. To begin distinguishing these possibilities, *in vitro* phosphatase assays using full-length RelA or RelA-specific phospho-peptides as substrates were performed. To determine PPM1A activity toward the full-length protein, expressed Flag-RelA was immunoprecipitated from 293T cells then incubated with bacterially synthesized GST-PPM1A proteins. Incubation with wild-type (Fig. 2.1D lanes 1-5) but not phosphatase-dead PPM1A (Fig. 2.1D lane 6), decreased RelA phosphorylation at S536 in a dose-dependent fashion. As with all PPM family members, PPM1A phosphatase activity was magnesium dependent (Fig. 2.1D, compare lanes 5 and 7). Because reliable phospho-specific antibodies are available only for S536 and to confirm findings of the full-length phosphatase assay, a peptide-based phosphatase assay was performed. Synthesized RelA phospho-peptides corresponding to phospho-serine 536 and 276 (pS536, pS276) (LifeTein, South Plainfield, NJ) were used as substrates and dephosphorylation was quantified using malachite green assay⁴⁷. Wild-type, but not phosphatase-dead PPM1A dephosphorylated the pS536 peptide with equivalent efficacy as the known RelA S536 phosphatase, Wip1 (Fig. 2.1E, compare lanes 4 and 7). As opposed to Wip1, PPM1A also dephosphorylated the pS276 peptide (Fig. 2.1F, compare lanes 4 and 7). As expected, magnesium was required for activity of both PPM1A and Wip1 (Figs. 2.1E and F, lane 6) and the phosphatase-dead mutant of PPM1A had no activity toward either pS536 or pS276 peptides (Figs. 2.1E and F lane 5). Together, these data suggest that PPM1A is a direct RelA phosphatase and the first phosphatase with potential activity toward pS276 of RelA.

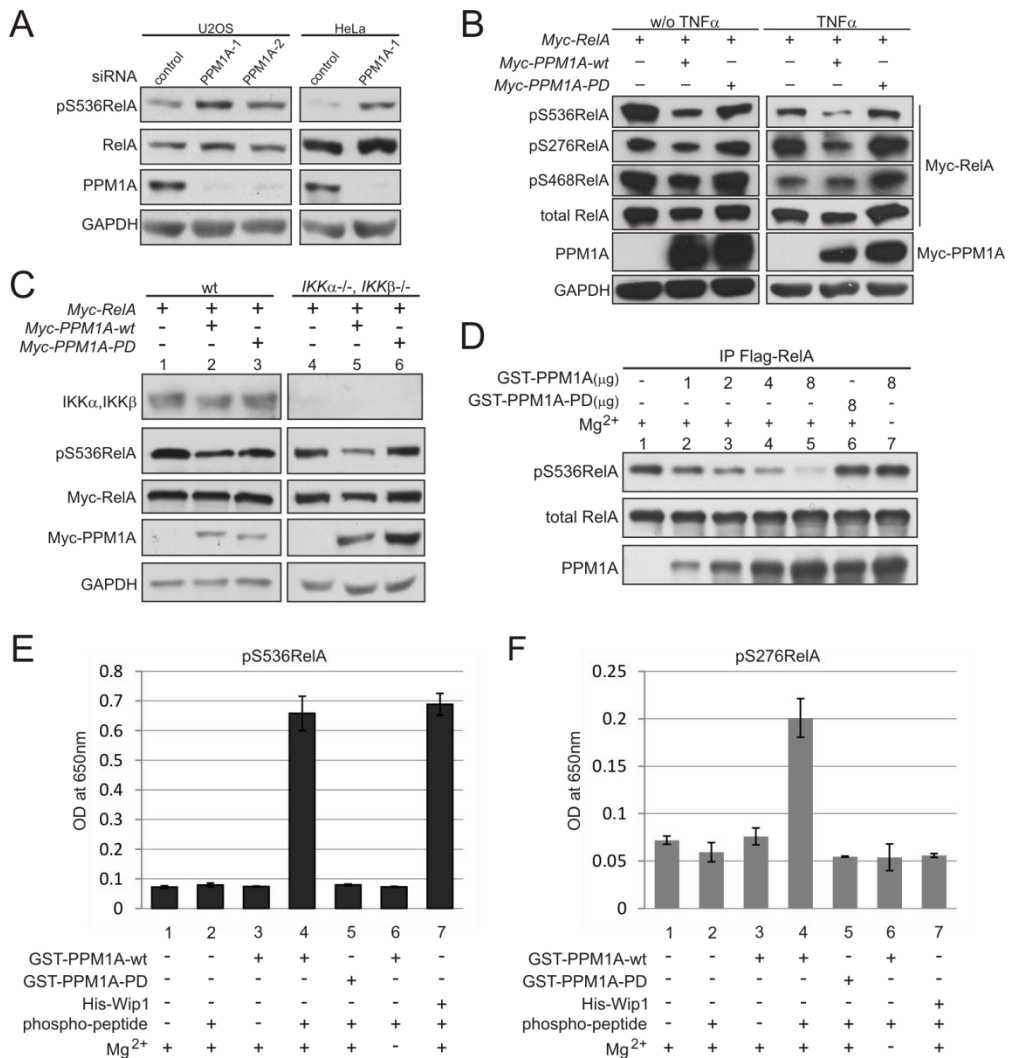


Fig. 2.1 PPM1A is a RelA phosphatase. **(A)** U2OS and HeLa cells were transfected with indicated siRNAs. PPM1A as well as endogenous phospho- and total RelA were visualized by immunoblotting. GAPDH served as loading control. **(B)** U2OS cells were transfected with indicated plasmids and proteins visualized by immunoblotting with GAPDH serving as loading control. PPM1A-wt, wild type PPM1A; PPM1A-PD, phosphatase dead PPM1A **(C)** Wild-type mouse embryonic fibroblasts (MEFs) and $IKK\alpha^{-/-}, IKK\beta^{-/-}$ double null MEFs were transfected with indicated plasmids. Endogenous Ikk α and Ikk β and transfected phospho- and total RelA, as well as PPM1A were visualized by immunoblotting. **(D)** Immunoprecipitated full-length Flag-RelA was used as substrate for *in vitro* phosphatase assay. Phospho- and total RelA were visualized by immunoblotting. Exclusion of PPM1A or magnesium in the phosphatase buffer served as negative controls. **(E and F)** S536 and S276 specific-phosphorylated RelA peptides were incubated with equal amounts of GST-PPM1A or His-Wip1 and free phosphate measured by malachite green assay.

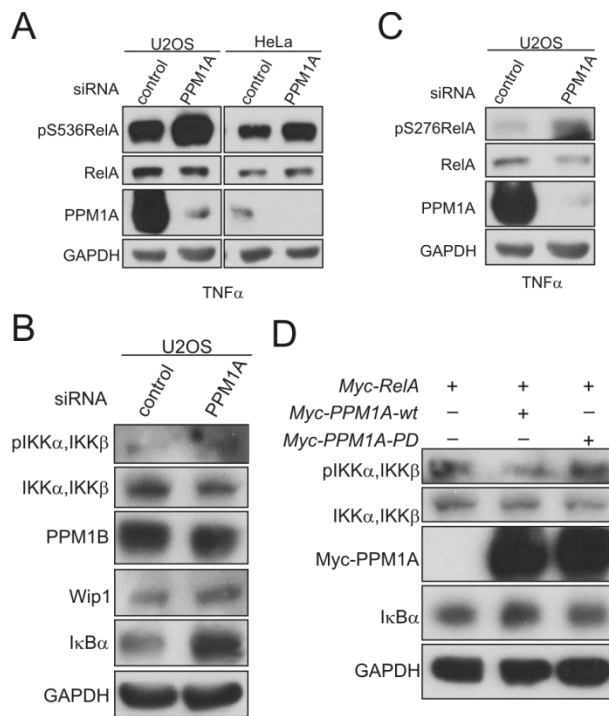


Fig. 2.2 (A) U2OS and HeLa cells were transfected with indicated siRNA and stimulated with 10ng/ml TNF α for 10 min. Endogenous RelA phosphorylation at S536 was visualized by immunoblotting cell lysates. Total RelA was immunoblotted after stripping the membrane. PPM1A and GAPDH were also immunoblotted. (B) U2OS cells were transfected with indicated siRNA. PPM1A, PPM1B and Wip1 were visualized by immunoblotting. (C) U2OS cells were transfected with indicated siRNA and stimulated with 10ng/ml TNF α for 10 min. Endogenous RelA phosphorylation at S276 was visualized by immunoblotting cell lysates. (D) U2OS cells were transfected with plasmids encoding Myc3-tagged RelA with empty vector, Myc3-tagged wild type PPM1A or phosphatase-dead (PD) mutant of PPM1A. Endogenous proteins of NF- κ B pathway including phospho-IKK α and IKK β , total IKK α and IKK β and I κ B α were visualized by immunoblotting.

PPM1A inhibits RelA transcription activity, decreases NF-κB-dependent cell invasion, sensitizes cell to TNF α , but does not alter RelA nuclear localization or DNA binding

Phosphorylation at serine residues S536 and S276 is critical for RelA transactivation activity¹⁴. To determine if dephosphorylation by PPM1A inhibits RelA transcriptional activity, a dual-luciferase reporter assay was performed¹¹⁰. In U2OS cells, endogenous NF-κB transcriptional activity was decreased following ectopic co-expression of wild-type PPM1A and NF-κB responsive reporter (Fig. 2.3A). Likewise, PPM1A also inhibited endogenous NF-κB transcriptional activity after stimulation by TNF α or IL-1 β and reversed luciferase transcription increased by ectopic expression of RelA (Fig. 2.3B) while PPM1A did not inhibit transcription of control reporter without NF-κB responsive element (Fig. 2.4A). Consistent with our observations that phosphatase activity was required for PPM1A to alter RelA phosphorylation, phosphatase-dead PPM1A had no effect on RelA transcriptional activity (Fig. 2.3A and B). S536 and S276 contribute to RelA transcriptional activity and both residues were dephosphorylated by PPM1A *in vitro*. To explore the relative contribution of these two residues to PPM1A-mediated RelA inhibition, RelA mutants mimicking phosphorylation at these sites (RelAS536D and RelAS276D) were expressed with or without PPM1A. S536D and S276D mutants displayed increased transcriptional activity compared to wild-type RelA (Fig. 2.3C). Ectopically expressed PPM1A inhibited transcription by RelAS276D ($p<0.001$), but not by RelA S536D ($p=0.86$). Of note, PPM1A inhibited slightly less efficiently the transcription by the S276D mutant than wild-type RelA (inhibition rate 56% vs. 64%, $p<0.01$). Taken together, these data suggest that dephosphorylation of S276 by PPM1A may contribute to inhibit RelA transcriptional activity, but the majority of PPM1A activity to inhibit RelA transcription relies on dephosphorylation of S536 of RelA.

Given that PPM1A robustly inhibited RelA transcription (Fig. 2.3A-C), we explored NF-κB target genes regulated by endogenous PPM1A by comparing expression between HeLa cells with and without lentivirus-driven PPM1A knockdown. Of tested genes (RT² ProfilerTM PCR Array,

SABiosciences, Valencia, CA), expression of selective RelA responsive genes (Table. 2.1) including MCP-1 and IL6 were increased at least 1.5-fold following PPM1A depletion. These data are consistent with earlier reports^{49,88} that PPM1A regulates IL-6 expression as we confirmed in PC3 (human prostate cancer) cells (Fig. 2.4B). Ability of PPM1A manipulation to alter expression of MCP-1, a chemokine that is linked to tumor progression and metastases, was confirmed by real time PCR (Fig. 2.3D). To determine if PPM1A directly alters ability of NF-κB to bind the promoter region of the MCP-1 gene^{86, 130} RelA chromatin immunoprecipitation was performed following PPM1A depletion in HeLa cells. Following PPM1A depletion, endogenous RelA association with the MCP-1 promoter was observed (Fig. 2.4C). Compared to control cells, cells with PPM1A knock down showed a moderate but significant increase (48 % increase, 20.8 % vs. 30.8 %, p<0.05) of endogenous RelA binding to the MCP-1 proximal promoter region (Fig. 2.3E). These data suggest that PPM1A selectively regulates NF-κB transcription activity.

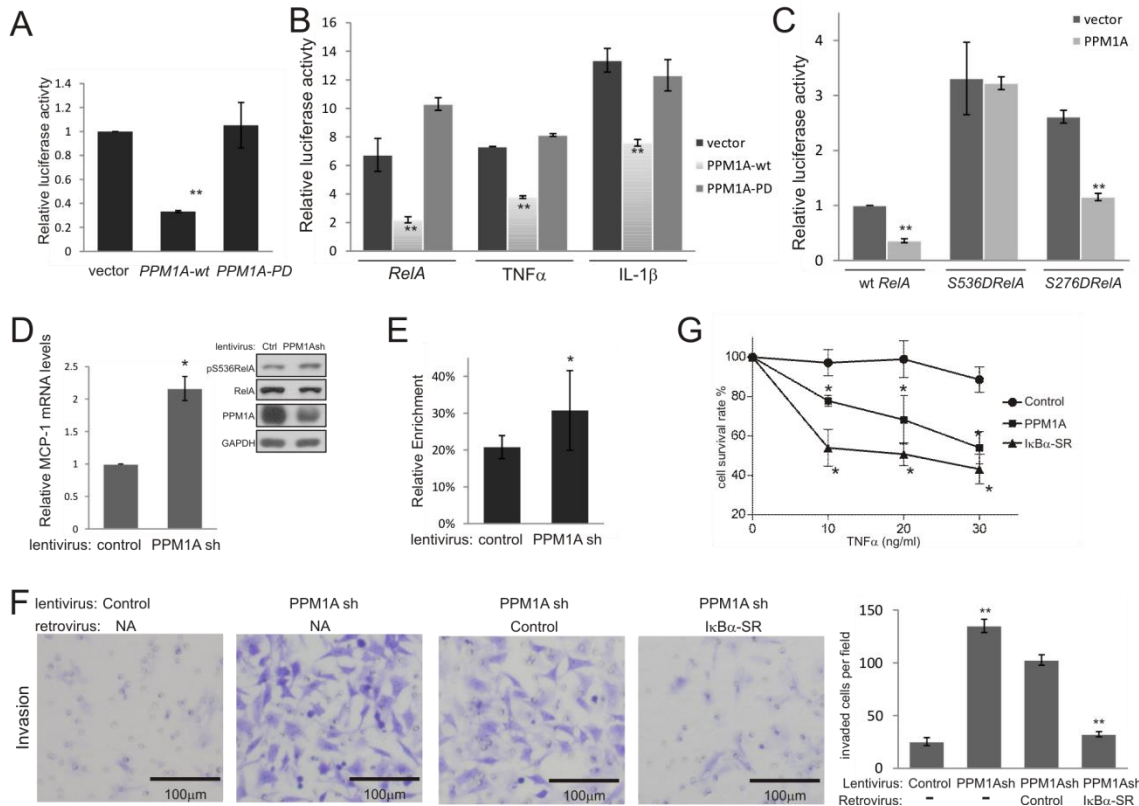


Fig. 2.3 PPM1A inhibits NF-κB transcription activity, NF-κB-dependent cell invasion and sensitizes cells to TNF α . **(A)** U2OS cells were co-transfected with indicated plasmids and *renilla* luciferase and the NF-κB responsive reporter 3κB-ConA-luc firefly luciferase. In this and subsequent luciferase assays, firefly luciferase activity was normalized to *renilla* luciferase and normalized firefly luciferase activity from cells transfected with control plasmids was assigned a value of 1. Error bars, SD derived from 3 analyses. ** p<0.01 **(B)** NF-κB-dependent luciferase activity was determined as described in **(A)** in cells expressing wild-type or phosphatase dead PPM1A and either ectopic expression of RelA or 4 hr treatment with TNF α or IL-1 β . ** p<0.01 **(C)** Luciferase activity was determined following transfection of U2OS with plasmids encoding wild-type or mutant *Flag-RelA* (S536D or S276D) with or without PPM1A as indicated. ** p<0.01 **(D)** q-RT-PCR analyses of MCP-1 expression in HeLa cells selected after infection with PPM1A shRNA encoding lentivirus. Error bars = SD. * p<0.05 PPM1A, pS536RelA, and RelA levels were confirmed by immunoblotting. **(E)** ChIP assays of the binding of RelA to MCP-1 proximal promoter. Samples from HeLa cells as described in **(D)** were prepared and analyzed using antibodies specific for RelA or IgG as control. Immunoprecipitated DNA fragments and input DNA were analyzed by real-time PCR. Values were normalized to input DNA in each group. Error bars = SD. * p<0.05 **(F)** HeLa cells infected with indicated viruses were plated on matrigel coated transwells and invasion measured by direct counting of trespassing cells. Representative photomicrographs are shown (scale bars, 100 μm). Quantification of cell invasion in results represents cell counts from ten randomly selected low-power fields (200×) ** p<0.01. PPM1A and I κ B α -SR expression levels were confirmed by immunoblotting (Fig. S2D). **(G)** HT1080 cells were infected as indicated and treated with indicated doses of TNF α for 24 hr. Cells were stained with trypan blue and live cells were counted. Error bars = SD. *p<0.05

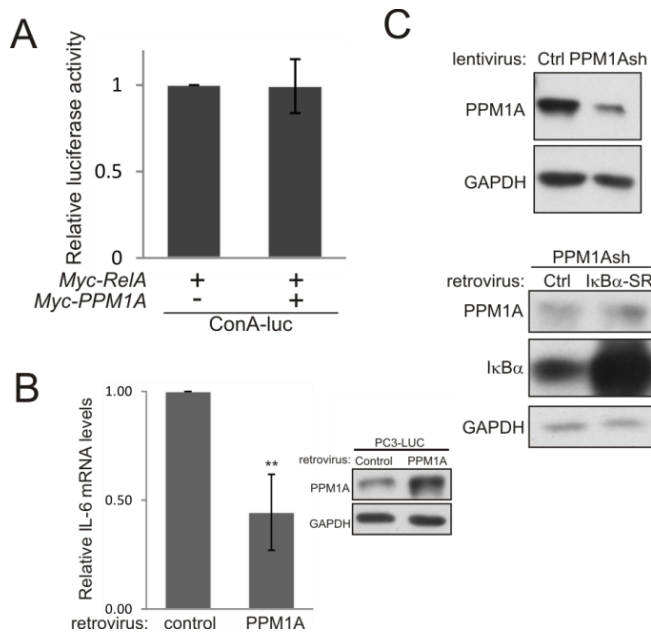


Fig. 2.4 (A) U2OS cells were co-transfected with plasmids encoding wild type *PPM1A* and control vector or *Myc*-tagged *RelA* in addition to *renilla* luciferase and the control reporter conA-luc firefly luciferase as indicated. Luciferase activities were determined by the dual-luciferase assay system 2 days after transfection. In this and subsequent luciferase assays, firefly luciferase activity was normalized to *renilla* luciferase from the CMV promoter as the internal control, and normalized firefly luciferase activity from cells transfected with control plasmids was assigned a value of 1. Error bars, SD over 3 analyses. (B) *PPM1A* decreased IL-6 expression in mRNA level. PC3-LUC infected with *PPM1A* expression or control retrovirus and selected by 1ng/ml puromycin for 10 days. mRNA was extracted for q-RT-PCR analyses of IL-6 mRNA level (primer sequences: forward 5'gcccgactatgaactcccttct3', reverse 5'gaaggcagcaggcaacac3'). GAPDH was used as control. *PPM1A* expression was confirmed by immunoblotting. Error bars, SD over 3 analyses. ** p<0.001 (C) *PPM1A* and *IκBα-SR* expression levels from cells described in (Fig. 2F) were confirmed by immunoblotting.

We previously reported that the tumor suppressor LZAP inhibits NF- κ B activity and diminishes HeLa cell invasion¹¹⁰. To determine if PPM1A inhibition of RelA similarly decreased HeLa invasion, matrigel invasion was measured after PPM1A depletion. Knockdown of PPM1A increased HeLa cell invasion by approximately 5-fold (Fig. 2.3F). I κ B α degradation leads to release and nuclear localization of NF- κ B dimers with the RelA/p50 heterodimer representing the most abundant and the primary target of I κ B α ^{131,132}. To determine if increased invasion associated with PPM1A depletion was dependent on NF- κ B and especially RelA, a non-degradable I κ B α , termed I κ B α -super repressor (I κ B α -SR), was expressed in PPM1A depleted cells. Inhibition of NF- κ B abrogated the increased invasion observed following PPM1A knockdown (Fig. 2.3E). These data suggest that depletion of PPM1A enhances NF- κ B-dependent cell invasion.

TNF α activates apoptotic pathways but rarely results in massive cell death due to simultaneous induction of NF- κ B transcription¹³³. To determine if PPM1A-mediated inhibition of NF- κ B would sensitize cells to TNF α , PPM1A was expressed in HT1080 cells before treatment with increasing doses of TNF α . Remarkably, PPM1A sensitized HT1080 cells to TNF α -induced cell death, albeit to a lesser extent than I κ B α -SR (Fig. 2.3F). In the absence of expressed PPM1A or I κ B α -SR, HT1080 cell survival was minimally impacted by TNF α concentrations tested.

Inhibition of RelA nuclear translocation is a well described mechanism for regulation of NF- κ B. Our data suggest that PPM1A is a direct RelA phosphatase, and although phosphorylation of RelA is not required for nuclear translocation, it is possible that PPM1A could inhibit both RelA phosphorylation and nuclear localization. To explore this possibility, subcellular distribution of expressed RelA and phospho-RelA were determined following co-expression of RelA with wild-type or phosphatase-dead PPM1A. Immunoblotting of cell fractions revealed that neither wild-type nor phosphatase-dead PPM1A inhibited nuclear translocation of RelA (Fig. 2.5A, compare lane 4 to lanes 5 and 6). Consistent with our finding that PPM1A decreased RelA phosphorylation (Fig. 2.1A-C), phospho-S536 RelA was markedly decreased in the nuclear fraction following expression of

wild-type, but not phosphatase-dead, PPM1A. PPM1A was primarily localized to the nucleus (data not shown and⁸²), suggesting that PPM1A may act to dephosphorylate RelA after translocation to the nucleus. Next we determined if overall DNA-binding activity of RelA was altered by PPM1A. RelA DNA binding was stimulated by TNF α and DNA-bound RelA identified and quantitated (Active Motif, Carlsbad, CA). PPM1A expression did not alter TNF α -stimulated DNA-binding activity of RelA compared to control cells at any time point tested (Fig. 2.5B). As a positive control, ectopic expression of I κ B α -SR efficiently inhibited DNA binding by RelA at all the time points. Collectively, these data suggest that PPM1A inhibition of RelA does not depend on inhibition of RelA nuclear translocation and that PPM1A regulation of RelA transcription is gene or promoter specific.

| gene | PPM1AshRNA | TNF α |
|------------|------------|--------------|
| PPM1A | 0.57 | 0.97 |
| CCL2/MCP-1 | 1.67 | 2.93 |
| HMOX1 | 3.29 | 0.52 |
| ICAM1 | 1.51 | 4.14 |
| IL1R1 | 2.14 | 0.68 |
| IL6 | 1.87 | 4.14 |
| IL8 | 2.14 | 7.73 |
| TNFAIP3 | 38.80 | 106.01 |
| TNFRSF10A | 36.76 | 35.51 |
| TNFSF10 | 12.13 | 43.71 |

Table 2.1. Fold changes of NF- κ B target genes measured by RT² Profiler™ PCR Array. mRNA extraction and RT-PCR were performed according to manufacturer's instructions. Compared to HeLa cells infected with control lentivirus, genes listed had more than 1.5 fold increased expression in HeLa cells infected with lentivirus delivering PPM1A shRNA. mRNA extracted from TNF α (10ng/ml 4hrs) stimulated HeLa cells was used as positive control and the fold changes were normalized to the gene expression level in untreated cells.

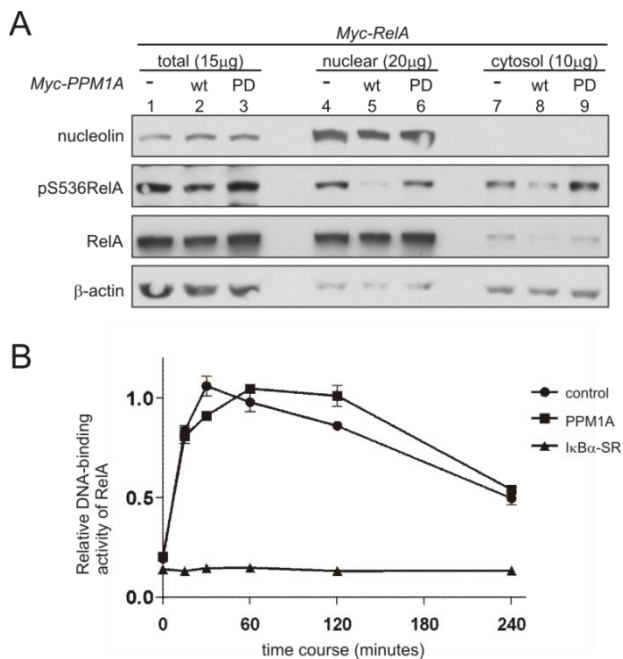


Fig. 2.5 PPM1A does not interfere with nuclear translocation or DNA binding of RelA. **(A)** U2OS cells transfected with indicated plasmids were lysed and total or phospho-RelA visualized by immunoblotting from total lysate or subcellular fractions. Nucleolin and β -actin served as nuclear and cytosol markers, respectively. Amount of protein loaded is indicated. **(B)** Following TNF α stimulation, nuclear extracts were prepared from HeLa cells stably expressing PPM1A, I κ B α -SR or control. RelA DNA-binding activity was measured using TransAM NF- κ B p65transcription factor kit. Error bars = SD.

PPM1A inhibits NF-κB activation, MCP-1 expression and cell invasion in prostate cancer cell lines

We were intrigued that PPM1A regulated expression of MCP-1 (Fig. 2.3D), a chemokine whose expression has been strongly linked to bony metastasis in prostate and advanced breast cancers^{71, 134}. To begin exploring a potential role of PPM1A in regulating bony metastases in prostate cancer, we explored PPM1A expression and the effect of PPM1A manipulation in a pair of prostate cancer cell lines with well-described metastatic and invasive potential, PC3 and LNCaP. LNCaP cells are androgen-dependent with low metastatic potential, whereas, PC3 cells are androgen-independent and highly metastatic. Perhaps related to their aggressive metastatic potential, PC3 express higher levels of MCP-1¹²⁸. We observed that PPM1A protein (Fig. 2.6A) and mRNA (data not shown) expression were approximately 2-fold lower in PC3 cells compared to LNCaP. Although total RelA expression was similar in the two cell lines, RelA S536 phosphorylation was markedly higher in PC3 cells compared to LNCaP (Fig. 2.6A).

Since LNCaP cells expressed higher levels of PPM1A, effects of PPM1A on RelA phosphorylation, MCP-1 expression and cellular invasion were determined by depletion of PPM1A. Consistent with results from other cell lines, PPM1A depletion in LNCaP cells increased RelA S536 phosphorylation (Fig. 2.6B), MCP-1 mRNA expression (Fig. 2.6C) and cell invasion (Fig. 2.6D). To determine the effect of PPM1A in PC3-LUC cells with lower endogenous levels of PPM1A, PPM1A was expressed. Ectopic PPM1A expression did not alter total RelA expression, but markedly decreased RelA S536 phosphorylation (Fig. 2.6E) and resulted in a 50% reduction of MCP-1 mRNA expression and a similar reduction of secreted MCP-1 detected in conditioned media (Fig. 2.6F). Remarkably, expression of PPM1A reduced invasion of otherwise aggressive PC3 cells by more than 50% (Fig. 2.6G).

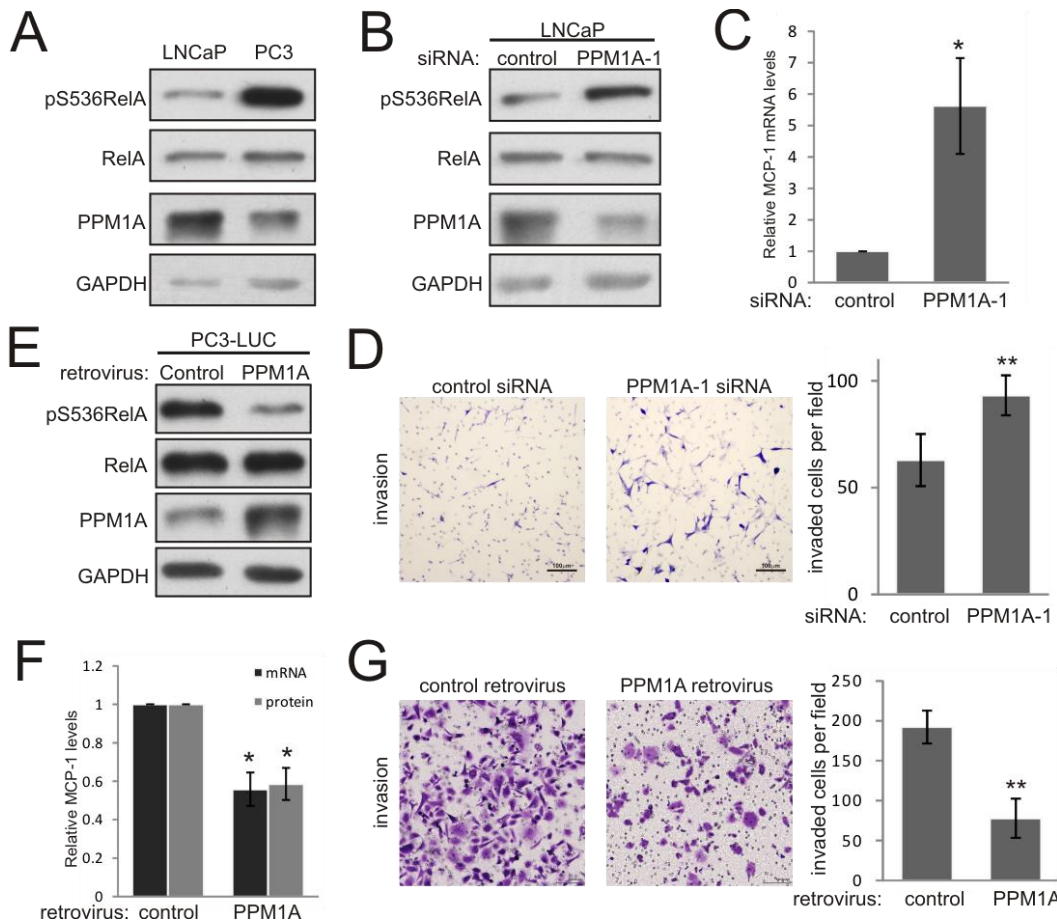


Fig. 2.6 PPM1A inhibits NF-κB and prostate cancer cell invasion **(A)** Endogenous total and phospho-RelA (S536) and PPM1A were visualized in LNCaP and PC3 cells by immunoblotting. GAPDH serves as loading control. **(B)** LNCaP cells were transfected with indicated siRNA and indicated phospho- or total proteins visualized by immunoblotting. **(C)** MCP-1 expression was measured by q-RT-PCR in LNCaP cells transfected as indicated. Error bars = SD. * p<0.05 **(D)** Transwell invasion of LNCaP cells following transfection with indicated constructs were quantified as described in Fig. 2 **(F)**. **p<0.001 **(E)** PC3-LUC cells were infected with indicated retrovirus, selected using puromycin and expression of indicated phospho- or total proteins visualized by immunoblotting. **(F)**, PC3-LUC cells were infected with indicated retroviruses and expression of MCP-1 mRNA or protein, determined by q-RT-PCR or ELISA, Error bars = SD. * p<0.05 **(G)** PC3-LUC cells were infected with indicated retroviruses and transwell invasion determined as in **(D)**. **p<0.001

PPM1A expression is lower in metastatic human prostate cancer and PPM1A expression inhibits metastases in a mouse model

Since PPM1A expression inversely correlated with MCP-1 expression and invasiveness of two prostate cancer cell lines (Fig. 2.6), we examined PPM1A expression in publically available expression data derived from human prostate cancers to determine if PPM1A expression differed in metastatic lesions compared to primary tumors. Indeed PPM1A expression was 2-fold lower in distant prostate cancer metastases compared to primary prostate tumors in patients without distant metastases (Fig. 5A, NCBI GEO, GDS2546^{135, 136}). To begin exploring a potential role of PPM1A in metastasis, an intracardiac injection model was used to study critical behaviors for prostate cancer cell metastases: extravasation and growth in distant sites. Aggressive PC3 cells were chosen since LNCaP cells fail to develop metastasis after intracardiac injection¹³⁷. PC3 cells expressing luciferase (PC3-LUC) with or without stable PPM1A expression (Fig. 2.6E) were injected intracardially into nude mice and bony metastases quantified. Bioluminescent imaging was performed on mice 1 hour after injection and weekly for 4 weeks (example shown Fig. 2.7). Expression of PPM1A in PC3-LUC cells significantly reduced the incidence of metastases in injected mice (38% vs. 93%, Fig. 2.8B), as well as the number of metastases per mouse (Fig. 2.8C). Metastases were confirmed by X-ray imaging (Fig. 2.8D, white arrows indicate osteolytic lesions) and hematoxylin/eosin staining showing metastases of control PC3-LUC cells to the bone marrow cavity (Fig. 2.8E left) and normal bone tissues from mice injected with PPM1A-expressing PC3-LUC cells for comparison (Fig. 2.8E right). Immunostaining of cleaved-caspase-3 revealed that apoptosis (cleaved-caspase-3 positive/total cells) in metastases of PPM1A expression cells increased by roughly 50% compared to control tumors (Fig. 2.8F, 56.7% vs. 77%, p<0.01).

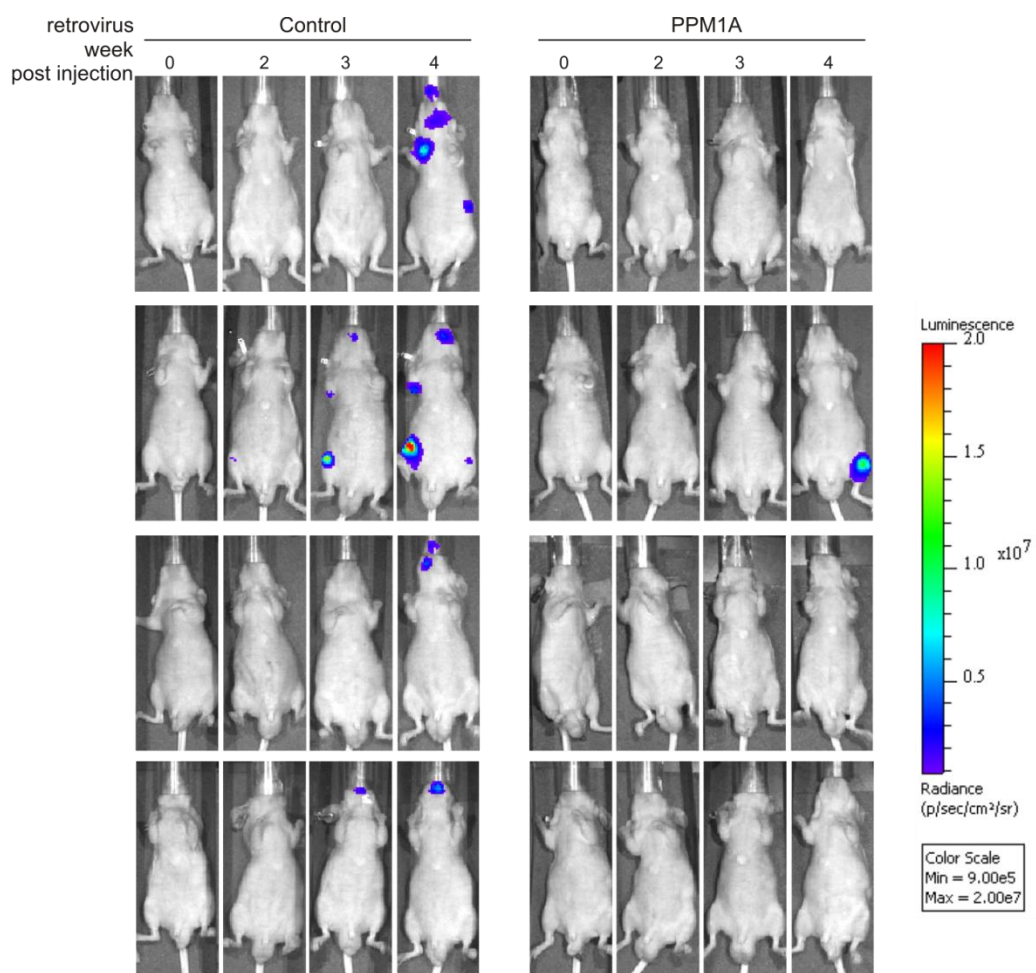


Fig. 2.7 Bioluminescent imaging of mice after intracardiac injection of PC3-LUC cells. Serial Xenogen bioluminescent images from representative mice are shown at indicated time points after intracardiac injection of PC3-LUC with or without expression of PPM1A (Fig. 2.6 E). Color scale of photon radiance is shown on the right.

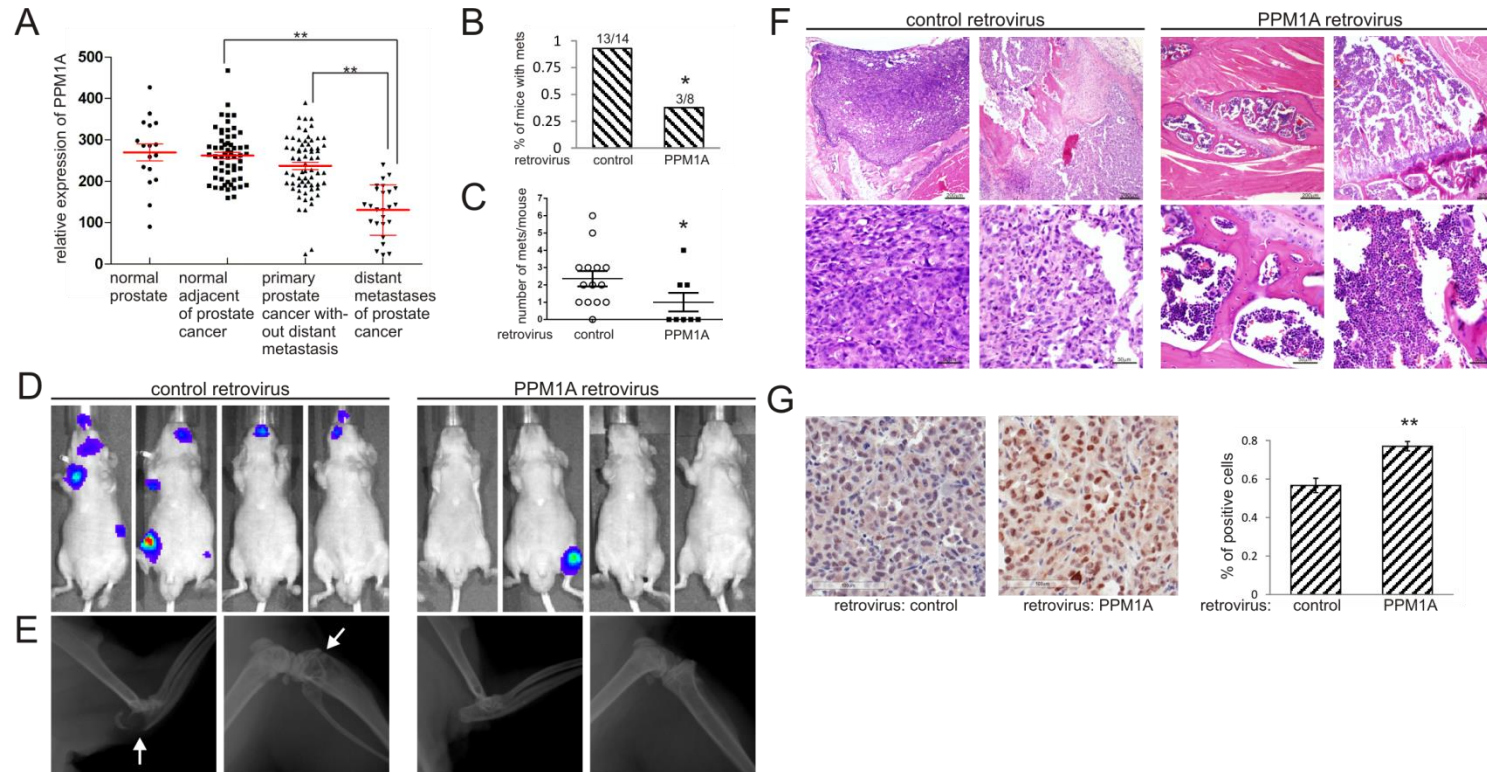


Fig. 2.8. PPM1A expression is lower in metastatic human prostate cancer and inhibits prostate cancer cell metastasis *in vivo*. (A) A GEO search indicated that PPM1A expression is lower in metastatic deposits of prostate cancer compared to: primary prostate cancers without distant metastases ($p=2.43E-9$, fold change 1.82); normal prostate tissue adjacent to cancer ($p=9.77E-14$, fold change 2.00); or normal prostate ($p=2.17E-7$, fold change 2.06). (B) Percentage of mice that developed metastases after intracardiac injection of PC3-LUC cells with or without expression of PPM1A. The number of mice with metastases/injected mice is indicated on top of each bar * $p<0.05$. (C) The number of metastases per mouse at 4 weeks after intracardiac injection of PC3-LUC cells with or without PPM1A expression is indicated * $p<0.05$ (D) Xenogen bioluminescent images of representative mice 4 weeks after intracardiac injection of PC3-LUC cells infected with control retrovirus or retrovirus driving expression of PPM1A. (E) X-ray images of representative mice in (B). Lytic bone lesions are indicated by white arrows. (F) Representative hematoxylin/eosin staining of bone and adjacent tissue samples obtained from mice in (B) are shown. Magnification: top 40×, bottom 200×. (G) Sections of bony metastases described in (B) were immunostained with using anti-cleaved-caspase 3. Percentage of positive staining cells in each group was measured from at least 3 representative tumors and in each tumor at least 5 randomly selected fields (200×). Error bars, SD. ** $p<0.001$.

PPM1A decreases xenograft tumor growth

Given that NF-κB signaling can enhance tumor growth in addition to cellular invasion and metastasis, we further explored the role of PPM1A depletion in primary tumor growth. HeLa cells with and without shRNA-mediated PPM1A-depletion were injected subcutaneously into the flank of nude mice. Immunoblotting confirmed PPM1A loss before injection (Fig. 2.9A). Mice were sacrificed and tumors harvested after 9 weeks. PPM1A knockdown was variably maintained in tumors despite selection of cells before injection. At the endpoint, 7 of 12 tumors derived from PPM1A knockdown cells maintained PPM1A depletion, whereas 5 tumors had regained PPM1A expression to levels equivalent to those observed in control tumors. Tumors that maintained PPM1A knockdown grew faster and were larger compared to control tumors (Fig. 2.9A, $p<0.0001$). Remarkably, tumors that did not maintain PPM1A knockdown were of similar size compared to control tumors (Fig. 2.9A). Analyses of tumor growth maintained statistical significance even if including tumors that failed to maintain PPM1A knockdown in the PPM1A knockdown group comparing to control ones ($P<0.01$, data not shown). Consistent with tumor growth data, the mean wet weight of tumors maintaining PPM1A knockdown was greater than both control tumors and tumors that did not maintain PPM1A knockdown (Fig. 2.9B, $p<0.05$). Before sacrifice, mice were injected with BrdU and harvested tumors were immunostained to determine proliferative index (BrdU-positive cells/total cells). The proliferative index in tumors maintaining PPM1A knockdown was almost twice as high as that of control tumors (Fig. 2.9C, 33% vs. 17%, $p<0.001$) while the proliferative index in tumors not maintaining PPM1A knockdown was similar to that of control tumors (Fig. 2.10 B, 19% vs. 17%, $p=0.62$) and significantly lower than that of the tumors maintaining PPM1A knockdown (Fig. 2.10 B, $p<0.05$). Immunostaining of cleaved-caspase 3 in xenograft tumor sections was used to calculate an apoptotic index (cleaved-caspase 3 positive cells/total cells) revealing that apoptosis in PPM1A knockdown tumors was less than half of that in control tumors (Fig. 2.9D, 5% vs. 12%, $p<0.001$). As observed for the proliferative index, the apoptotic index in tumors not maintaining PPM1A knockdown was similar to control cells (Fig. 2.10

C 15% vs. 12%, p=0.28) and significantly higher than that of the tumors maintaining PPM1A knockdown (Fig. 2.10 C, p<0.0001). Although tumor latency and tumor size were altered by loss of PPM1A expression, tumor incidence was similar in this xenograft model (data not shown). These data suggest that loss of PPM1A increases tumor growth and is associated with increased proliferation and decreased apoptosis. Analyses of tumors that did not maintain PPM1A knockdown further support PPM1A loss as a driver of tumor growth, increased proliferation and decreased apoptosis.

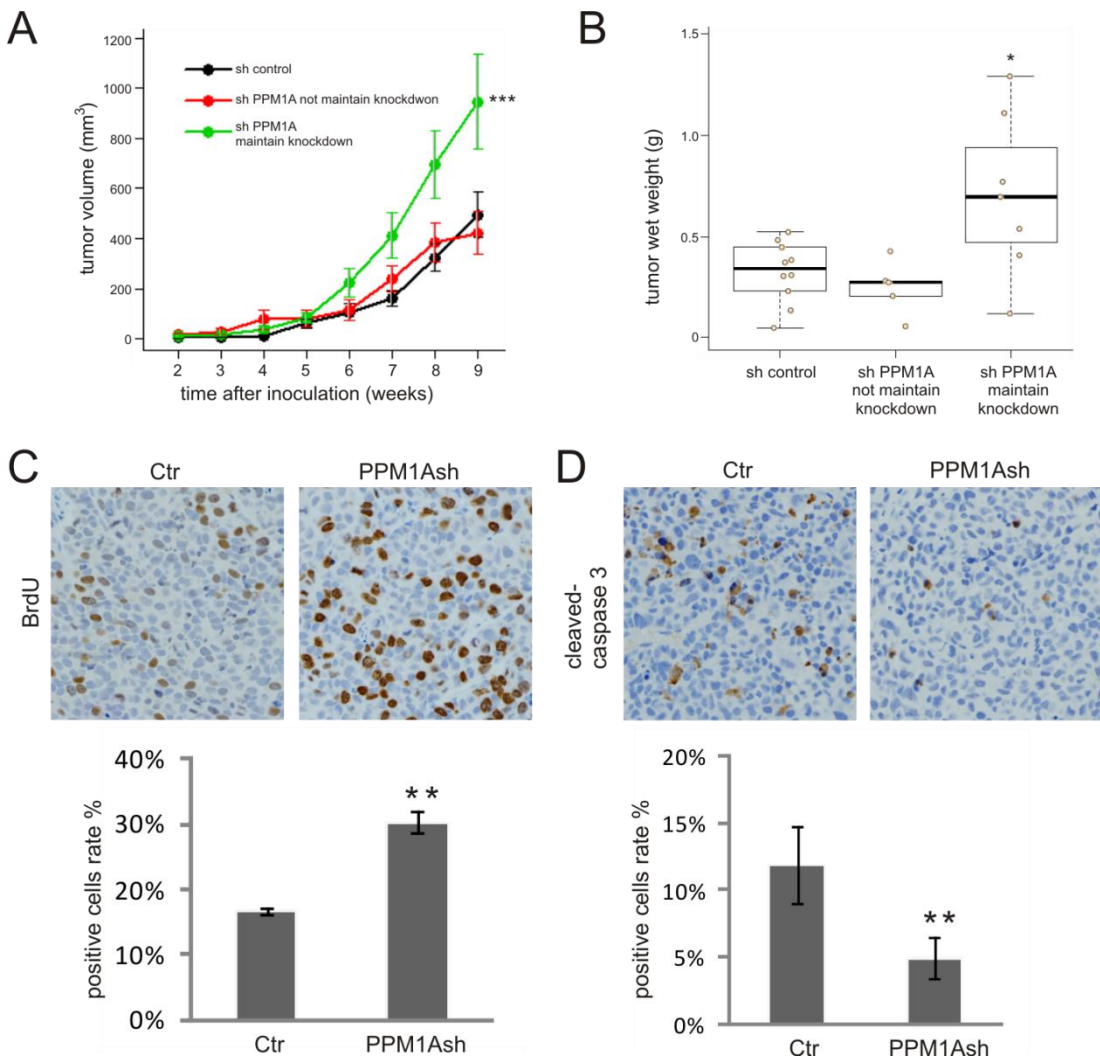


Fig. 2.9 PPM1A inhibits tumor growth *in vivo*. **(A)** HeLa cells were infected with either control retrovirus or retrovirus delivering PPM1A shRNA and selected with 1ng/ml puromycin for 10 days. Five mice (20 injections) in each group were inoculated with 1×10^6 manipulated HeLa cells. Tumor growth was monitored weekly by measurement of length (L) and width (W) using calipers until the largest tumors approached 20 mm in length. Tumor volumes were calculated by using the formula: volume = $\frac{1}{2} \times L \times W^2$. Error bars, mean \pm SD. **p<0.01. ***p<0.0001 **(B)**, tumors from the indicated groups were weighed immediately after removal. Medium xenograft tumor weight is indicated. Error bars, SD. *p<0.05. **C** and **D**, five micrometer sections of xenograft tumor described in **(A)** were immunostained with cleaved Caspase 3 or BrdU-specific antibodies respectively. Mice received 1mg BrdU i.p. injection 2 hr before sacrificing. Percentage of positive staining cells in each group was measured from at least 3 representative tumors and in each tumor at least 5 randomly chose fields (200 \times). Error bars, SD. **p<0.001.

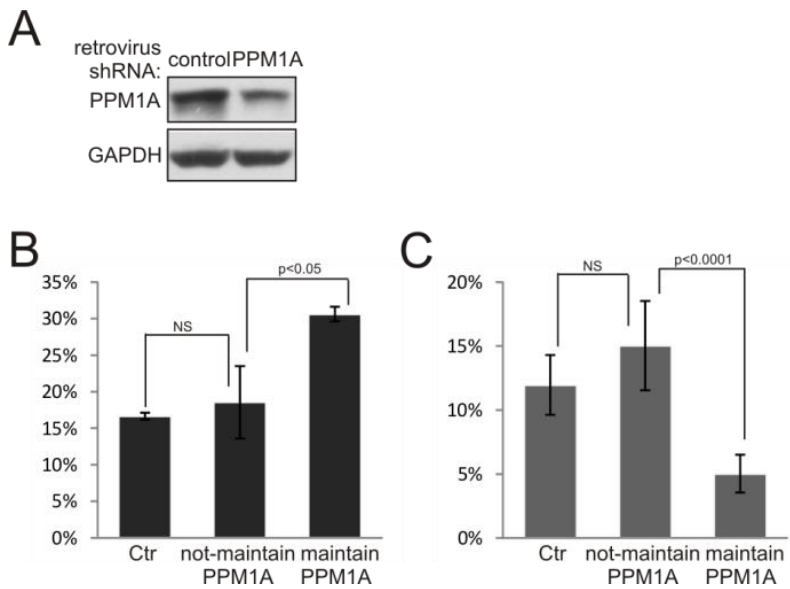


Fig. 2.10 (A) HeLa cells were infected with either control retrovirus or retrovirus delivering PPM1A shRNA and selected with 1ng/ml puromycin for 10 days. Before injection, decreased PPM1A expression was confirmed by immunoblotting. **B and C**, five micrometer sections of xenograft tumor described in (A) were immunostained with cleaved caspase 3 or BrdU-specific antibodies, respectively. Mice received 1mg BrdU i.p. injection 2 hr before sacrifice. The percentage of cells with immunostaining in each group was measured from at least 3 representative tumors and in each tumor at least 5 randomly selected fields (200 \times). Error bars = SD.

Discussion

RelA phosphorylation is necessary for transcriptional competence of nuclear NF- κ B¹³⁸, and dephosphorylation of RelA is an important mechanism for homeostatic down-regulation of NF- κ B activity⁴². In many human tumors NF- κ B activity enhances tumorigenic behavior with upstream kinases largely implicated in triggering or maintaining inappropriate NF- κ B transcription^{139, 140}. Data we present here identify a new RelA phosphatase and suggest that loss of RelA phosphatases may be equally important or an alternative mechanism of NF- κ B activation in human cancer.

We found that PPM1A, a PPM family member, is a direct RelA phosphatase at S536 as indicated by activity of bacterially synthesized PPM1A toward both RelA phospho-peptides and immunoprecipitated full-length RelA. Data presented here also support PPM1A as a phosphatase for the S276 site of RelA. S/TQ and TXY are known consensus target sequences for PPM phosphatases^{141,142}. Since S536 and S276 of RelA are not consensus targets, additional studies with more endogenous PPM targets may reveal additional consensus sequences. Previous reports show that PPM1A targets NF- κ B through dephosphorylation of IKK α and IKK β ⁴⁹. Our data reveal that PPM1A inhibited RelA phosphorylation independent of IKKs (Fig. 2.1C). Inability of PPM1A to inhibit RelA nuclear translocation further suggests that IKKs are not the dominant mechanism of RelA inhibition by PPM1A. Taken together, PPM1A inhibits NF- κ B through at least two mechanisms: 1) inhibition of upstream IKKs, and 2) direct dephosphorylation of RelA. Further studies are required to determine if other kinases responsible for RelA phosphorylation at S536 or S276 (Table 1.1) are regulated by PPM1A. We observed PPM1A-mediated inhibition of RelA with and without stimulation, whereas PPM1A activity to inhibit IKKs was observed only at later time points and after TNF α stimulation⁴⁹, suggesting that PPM1A regulation of RelA directly or through IKKs may depend on timing, as well as cellular and signaling context.

NF- κ B regulation to selectively alter transcription has been widely reported and also varies from cell type to cell type^{110, 143, 144}. For example, the known RelA phosphatase, Wip1, inhibits a subset of

NF-κB targets⁴⁷. We found that among others, PPM1A decreased expression of NF-κB targets IL-6 as previously reported^{49,88} and MCP-1. ChIP assay showed depletion of PPM1A increased RelA associated with the MCP-1 proximal promoter (Fig. 2.3E), but the phosphorylation status of promoter-associated RelA could not be determined due to absence of suitable antibodies. Increased mRNA levels of MCP-1 under similar circumstances suggests that promoter associated NF-κB was transcriptionally active and therefore phosphorylated. These data suggest that PPM1A regulates RelA phosphorylation resulting in altered expression of select NF-κB targets.

IL-6 and MCP-1 are implicated in metastases, particularly in cancers of the prostate⁶⁷, colon^{68,145}, and breast^{71, 69}. Distant metastases in breast and prostate cancer are tightly associated with poor patient outcomes. Targeting MCP-1 is an effective therapeutic approach to prevent metastases in animal models of prostate and breast cancer¹⁴⁶, and a phase II clinical trial using a neutralizing monoclonal antibody against MCP-1 is being conducted in metastatic prostate cancer patients (NCT00992186). IL-6 and IL-6 receptor are also therapeutic targets for prevention of inflammation, tumor progression and metastasis, and their inhibition has shown promise in pre-clinical models⁷². A phase II trial was completed to determine efficacy of anti-IL-6 chimeric monoclonal antibody in patients with metastatic hormone-resistant prostate cancer (NCT00433446) while the results have not been published yet. Given that PPM1A inhibited expression of IL-6 and MCP-1, we explored the role of PPM1A in metastases. Expression data from human prostate cancers revealed that metastatic prostate deposits had significantly lower PPM1A expression when compared to primary tumors in patients without metastases. This exciting finding combined with increased invasion associated with PPM1A depletion (Fig. 2.3E) led us to examine the effect of PPM1A expression in an androgen-independent highly metastatic prostate cancer cell line, PC3. Interestingly, PC3 cells express lower levels of PPM1A when compared to androgen-dependent and less aggressive LNCaP cells. PPM1A expression significantly inhibited PC3 cell invasion (Fig. 2.6G) and abrogated PC3 bony metastases in an intravascular metastases model (Fig. 2.8B-D). Notably, mean PPM1A expression is also decreased in breast cancer and colorectal cancers compared to normal tissue (Oncomine, PPM1A

gene, TCGA breast, TCGA colorectal and colorectal 2 data sets), and a xenograft model of breast cancer MCF7 cells revealed that PPM1A depletion increases tumorigenic potential and tumor growth¹⁴⁷. These data suggest that loss or decreased PPM1A activity may increase aggressive behavior in different tumor types. Although survival data was not included in the prostate cancer dataset to correlate PPM1A expression with prognosis, it will be informative to explore when larger public datasets become available.

Our data suggest that PPM1A is a direct RelA phosphatase with tumor suppressor-like activity that, at least partially, depends on PPM1A ability to inhibit NF-κB. The pathway involves in PPM1A inhibition of xenograft tumor growth is not clear. In addition to NF-κB, PPM1A targets tumor centric proteins including smad2/3, p38 and cdk2 implicating PPM1A in cell cycle regulation, as well as TGFβ and MAPK signaling pathways^{82, 1}. Although data presented here suggest that invasion in HeLa cells was completely dependent on NF-κB, regulation of tumor invasion, progression, and metastasis by PPM1A, likely involves additional PPM1A activities. Decreased expression of PPM1A in distant metastases of human prostate cancer coupled with *in vivo* data suggest that increased PPM1A expression inhibits prostate cancer bony metastases. Neither deletions nor inactivating mutations of PPM1A have been described, suggesting that strategies to increase PPM1A expression or activity in cancer cells could be explored as a therapeutic strategy in human cancers.

CHAPTER III

LZAP REGULATES TARGET PROTEIN PHOSPHORYLATION BY FACILITATING TARGET PROTEIN ASSOCIATION WITH PHOSPHATASES OF PPM FAMILY

Part of the work presented in this chapter is published under the title of “LZAP Inhibits p38 MAPK (p38) Phosphorylation and Activity by Facilitating p38 Association with the Wild-Type p53 Induced Phosphatase 1 (WIP1)” in *PLoS one*, 2011¹¹⁷

Abstract

LZAP (Cdk5rap3, C53) is a putative tumor suppressor that inhibits RelA, Chk1 and Chk2, and activates p53. LZAP is lost in a portion of human head and neck squamous cell carcinoma and experimental loss of LZAP expression is associated with enhanced invasion, xenograft tumor growth and angiogenesis. p38/MAPK can increase or decrease proliferation and cell death depending on cellular context. LZAP has no known enzymatic activity, implying that its biological functions are likely mediated by its protein-protein interactions. To gain further insight into LZAP activities, we searched for LZAP-associated proteins (LAPs). Here we show that the LZAP binds p38, alters p38 cellular localization, and inhibits basal and cytokine-stimulated p38 activity. Expression of LZAP inhibits p38 phosphorylation in a dose-dependent fashion while loss of LZAP enhances phosphorylation and activation with resultant phosphorylation of p38 downstream targets. Mechanistically, the ability of LZAP to alter p38 phosphorylation depends, at least partially, on the p38 phosphatase, Wip1, a PPM family member. LZAP also binds Wip1. Expression of LZAP increased both LZAP and Wip1 binding to p38. *In vitro* phosphatase assay using full-length p38 as substrate revealed that LZAP enhances p38 dephosphorylation by Wip1 in a dose dependent fashion. LC-MS/MS was used to identify LZAP-associated proteins and found that LZAP interaction with

other PPM family members including PPM1A and PPM1B. Our previous study showed both LZAP and PPM1A inhibit RelA phosphorylation and negatively regulates NF- κ B signaling. Here, we show that the ability of LZAP to alter RelA phosphorylation depends, at least partially, on the RelA phosphatase, PPM1A. Taken together, these data suggest that the ability of LZAP to decrease target protein phosphorylation and activity (e.g. p38 and RelA) is at least partially mediated through altering interaction of target proteins and phosphatases.

Introduction

LZAP (Cdk5rap3, C53) was originally identified as a binding partner of the Cdk5 activator p35¹⁰⁷, but insight into LZAP activity was gained when it was found to bind the alternate reading frame protein of the INK4a gene locus, ARF (p14ARF in human and p19ARF in mice). LZAP activates p53 both in the presence and absence of ARF resulting in a G1 cell cycle arrest and inhibition of clonogenic growth¹¹². Further, LZAP inhibits cellular transformation, xenograft tumor growth, and xenograft tumor vascularity at least partially mediated by LZAP's ability to bind and inhibit RelA¹¹⁰. Evidence of a tumor suppressor-like role for LZAP was bolstered when LZAP protein levels were found to be markedly decreased in a subset of head neck squamous cell carcinoma (HNSCC) where its loss inversely correlates with expression of NF- κ B target genes¹¹⁰. LZAP also inhibits the checkpoint kinases (Chk1 and Chk2), promotes mitotic entry and, in the presence of DNA damaging agents, sensitizes to cell death^{113, 116}. Collectively, these data are consistent with a role of LZAP in tumor suppression. Intriguingly, morpholino-directed loss of LZAP expression in zebrafish was lethal during very early embryogenesis resulting in cell death and developmental delay¹¹¹. Combined, these data suggest that either increased or decreased LZAP levels may have detrimental effects on cell survival. LZAP has no known enzymatic activity, implying that its biological functions are likely mediated by its protein-protein interactions. To identify proteins that may contribute to biological activities of LZAP, we screened human LZAP amino acid sequence for motifs recognized by modular signaling domains using the Scansite algorithm¹⁴⁸. Using high stringency criteria,

Scansite analyses suggested that LZAP contained motifs predicted to bind 14-3-3-zeta and the docking domain (D domain) of mitogen activated protein kinases (MAPKs) (Table. 3.1).

Table 3.1 LZAP predicted motifs from Scansite. LZAP protein coding sequence was analyzed using high stringency criteria to identify possible binding motifs.

LZAP predicted motifs from Scansite

| | protein | predicted binding motifs | predicted LZAP binding site |
|-----------------|----------------------|-------------------------------|-----------------------------|
| high stringency | 14-3-3-zeta MAPK1 | 14-3-3 Mode 1 Erk D-domain | T245 V499 |

Table 3.2 Summary of LZAP, Wip1 and PPM1A activity and binding for shared target proteins. + direct binding, - no direct binding; ↑/↓ indicates stimulation or inhibition of activity, * not all Wip1 or PPM1A targets are listed.

| | RelA | Chk1/2 | p38 | p53 | MDM2 |
|--------|------|--------|-----|-----|------|
| LZAP | + ↓ | + ↓ | + ? | - ↑ | - ↓ |
| Wip1* | ↓ | ↓ | ↓ | ↓ | ↑ |
| PPM1A* | ↓ | | ↓ | | ↓ |

p38MAPK belongs to a family of stress-activated MAPKs that respond to cellular stress and cytokines. Expression patterns suggest that p38 α is the primary p38 kinase in most cell types¹⁴⁹. Activity of p38 reflects a balance between the upstream activating kinases (MKK3 and MKK6) and inactivating protein phosphatases, primarily the wild-type p53-induced phosphatase 1 (Wip1/PPM1D/PP2C δ)^{94, 150}. p38 activity results in pleiotropic downstream cellular and tissue effects including: cytokine production, inflammation, cellular differentiation, cell-cycle arrest, apoptosis, and senescence^{149, 151, 152-155}. Given the roles of p38 as an inducer of apoptosis and inhibitor of cellular proliferation, it is ironic that elevated p38 expression has been found in many cancer types, including breast, lung, thyroid and HNSCC, and that p38 has been implicated in promoting cell survival^{152, 156-159}. Given the conflicting cellular effects that can result from p38 activation, the role of p38 in human cancer as a tumor promoter or a tumor suppressor likely depends on tumor and cell specific context¹⁴⁹.

Including p38 as a potential LZAP binding partner, we noticed that LZAP and PPM family members, especially Wip1, shared a pool of target proteins. As summarized in table 3.2, the roles of LZAP, Wip1 and PPM1A in the regulation of RelA, p38, Chk1/2, p53, and MDM2 are detailed. The phosphorylation and activity of RelA is inhibited by LZAP, Wip1 and PPM1A, and similarly, LZAP and Wip1 regulate phosphorylation and activity of Chk1/2 in the same direction. Since p38 is a target of Wip1 and PPM1A and because p38 and LZAP have been shown to activate p53 and to interact physically or functionally with Chk1^{112, 152, 160}, we explored LZAP activity to bind and regulate p38 activity. In addition, we examined if LZAP altered p38 phosphorylation and explored if this activity may be dependent on co-factors such as PPM phosphatases.

Materials and Methods

Plasmid constructs

The full coding sequence and truncation mutants of LZAP were subcloned into pcDNA3-Myc3 and pET-His expression vectors^{112, 110}. Plasmids Flag-p38α and Gal-ATF2 were generous gifts from Dr. Jiahuai Han (The Scripps Research Institute, La Jolla, CA). LZAP that was not a target of siRNA-2(sense strand: 5' -CAAGGTATGTGGACCGAGT)¹¹⁰ was constructed by introducing the silent mutations G294A and G297A in pCI-Neo-LZAP.

Antibodies and Reagents

LZAP polyclonal rabbit antibody has been previously described¹¹², Mouse monoclonal antibody were purchased as follows: Flag (M2), and anti-Flag M2 affinity gel (Sigma); mouse monoclonal antibodies specific to Myc (9E10), p38 (A-12), rabbit GAPDH, normal mouse and Rabbit IgG, and secondary mouse and rabbit antibodies (Santa Cruz Biotechnology); rabbit monoclonal to phospho-T180/Y182 p38 (Cell Signaling); Wip1 rabbit polyclonal antibody (Bethyl); fluorophore-conjugated secondary antibodies (Jackson ImmunoResearch Laboratories); chicken anti-human Myc-tag polyclonal antibody (Thermo Scientific); and all other antibodies (Cell Signaling). TNFα, IL-1β, and LPS were purchased from PeproTech.

Cell culture and transfection

Cell lines were maintained at 37 °C with 5% CO₂, in growth media with 10% fetal bovine serum (FBS) (Invitrogen, Carlsbad, CA). Cell lines were obtained from ATCC or collaborators and have been passed in the Yarbrough lab with biannual authentication of identity based on microsatellite analyses of 3 markers (D7S1482A, Mycl1A and DXS981C). Plasmids were transfected using FuGene6 (Roche, Indianapolis, IN) or TransIT-2020 (Mirus, Madison, WI) for MEFs according to the manufacturer's instructions. The total amount of transfected DNA in any single experiment was kept constant by adding control vector (pcDNA3). Small interfering RNA (siRNA) was transfected at 20 nM using Lipofectamine RNAiMAX (Invitrogen, Carlsbad, CA). Control siRNA duplex (non-

targeting #1) was purchased from Dharmacon (Dharmacon, Chicago, IL). The LZAP siRNA-2 was previously described¹¹² with on-TARGETplus modification, 5' -CAAGGTATGTGGACCGAGT (sense strand); the sequence of Wip1 siRNA is: 5' - GGCUUUCUCGCUUGUCACC dTdT¹⁶¹ purchased from Dharmacon.

Immunoprecipitation and immunoblotting

Cells were lysed in 0.5% (v/v) Nonidet P40 lysis buffer¹⁶² supplemented with protease inhibitor cocktail (Roche). Total cell extracts were incubated with specific antibodies and precipitated with protein A or G sepharose beads (GE Healthcare) before washing and suspension in Laemmli and gel electrophoresis followed by immunoblotting as described¹⁶³.

Immunofluorescence assay

Briefly, cells were fixed with paraformaldehyde permeabilized with Triton X-100, and blocked with BSA. Target proteins were visualized following incubation with primary antibodies followed by fluorophore secondary antibodies and visualization as described¹⁶⁴.

Cell fractionation

Cells were scraped in cytosolic lysis buffer (10 mM Tris-HCl [pH 7.5], 100 mM NaCl, 2.5 mM MgCl₂, and 40 mg/ml digitonin). The lysate was incubated on ice for 5 min and centrifuged (2100 g, 8 min, 4 °C), and the supernatant was designated as soluble cytosolic fraction. The pellet was washed with the same buffer before adding RIPA lysis buffer (10 mM Tris-HCl [pH 7.4], 150 mM NaCl, 1% NP-40, 1 mM EDTA, 0.1% SDS, and 1 mM DTT), incubated on ice for 5 min and centrifuged (14,000 rpm, 10 min, 4 °C), to obtain the nuclear fraction. Whole cell lysates were prepared using RIPA buffer, as described¹²⁷.

Luciferase reporter assay

ATF2 reporter gene assay was performed using the Dual-Luciferase Reporter Assay System (Promega) as described¹¹⁰. Reporter constructs were co-transfected into U2OS cells maintaining equal plasmid amounts. Luciferase activity was measured 24 hours after transfection following the

manufacturer's instructions. Luciferase activity was normalized to *renilla* activity as a control of transfection efficiency.

Mass spectrometry

Flag-tagged LZAP was expressed in HEK293T cells and purified using Flag-conjugated resin as described in Chapter 2. The elution buffer containing LZAP and other potential LZAP-binding proteins were submitted to Vanderbilt Mass Spectrometry Research core lab for LC-MS/MS assay and data analyses.

Results

LZAP interacts with p38 MAPK *in vivo*

To confirm the predicted interaction between LZAP and p38, Myc-tagged LZAP was transiently expressed singly or with Flag-tagged p38 in mammalian U2OS cells before immunoprecipitation. When co-expressed, bands corresponding to Myc-tagged LZAP and untagged LZAP were detected in p38 immunoprecipitates (Fig. 3.1A, lane 2, top panel). Likewise, p38 was readily detected in LZAP immunoprecipitates (Fig. 3.1A, lane 4, top panel). Expressed LZAP was also detected in immunoprecipitates of endogenous p38; however, endogenous p38 could not be detected in LZAP immunoprecipitates following LZAP expression (Fig. 3.1A, lanes 1 and 3, top panels). Expression of proteins was confirmed (bottom panels) and non-immune mouse IgG (middle panels) was used as a control for non-specific immunoprecipitation. To determine if endogenous p38 and LZAP associated in mammalian cells, co-immunoprecipitation of LZAP and p38 was performed using asynchronously growing MCF7 cells, in which LZAP and p38 expression levels are relatively higher compared to U2OS cells (data not shown). p38 was detected in LZAP immunoprecipitates both with and without UV irradiation, but not in precipitates using non-immune rabbit IgG (Fig. 3.1B, compare lanes 3 and 4 to lanes 5 and 6, where the arrow indicates p38). Reciprocal immunoprecipitation using p38-specific antibody did not allow detection of LZAP (data not shown). These data suggest that expressed and endogenous LZAP and p38 exist in a common complex.

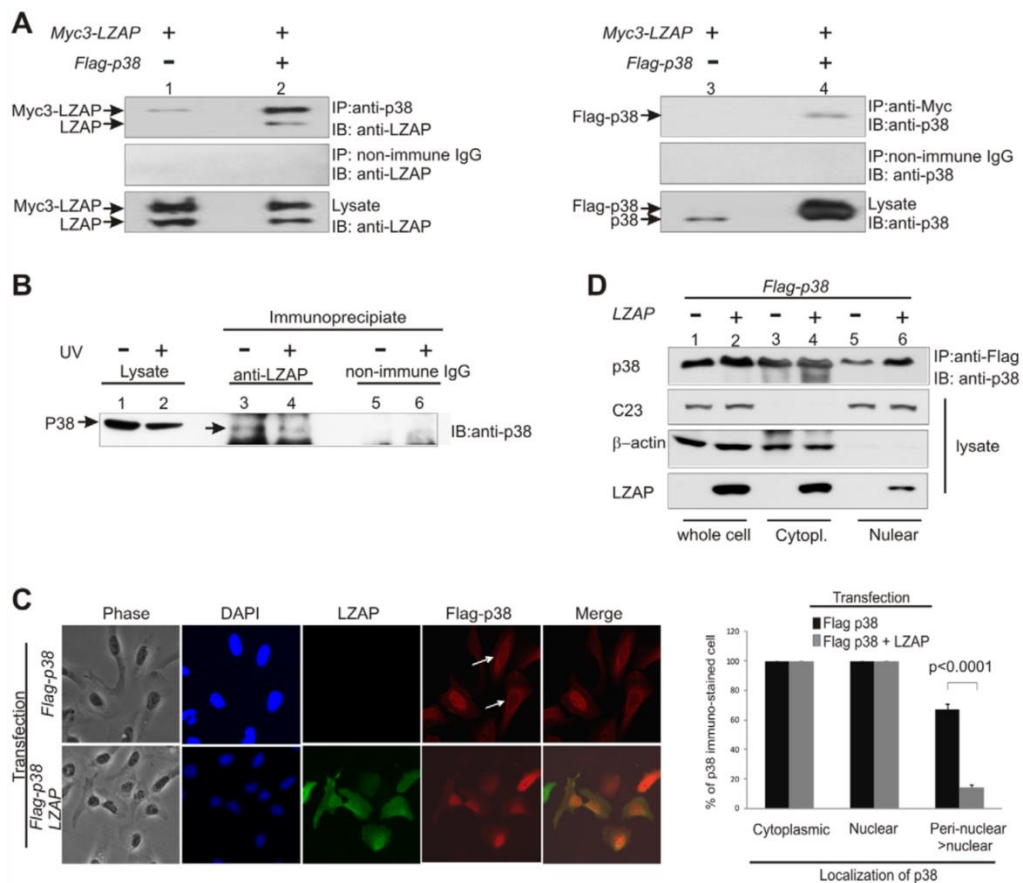


Fig. 3.1 LZAP binds to p38. **(A)** Ectopically expressed LZAP and p38 mutually co-immunoprecipitate. U2OS cells were transfected with indicated plasmids directing expression of tagged LZAP or p38. Immunoprecipitates were prepared using mouse antibodies recognizing Myc (LZAP) or p38, resolved on SDS-PAGE, and immunoblotted using rabbit antibodies recognizing LZAP or p38. Expression of LZAP and p38 was confirmed by immunoblotting (1% of each input lysate was loaded as reference.) Pre-immune IgG was used as control for non-specific immunoprecipitation. **(B)** Endogenous LZAP binds endogenous p38. Lysates from untransfected MCF7 cells without or with UV irradiation (20 J/m²) were immunoprecipitated using LZAP-specific rabbit antiserum or non-immune rabbit IgG, then immunoblotted with antibodies specific to p38 or LZAP as indicated. **(C)** LZAP co-localizes with p38 and alters p38 subcellular localization. U2OS cells were transfected with plasmids directing expression of Flag-p38 with or without LZAP. Cells were fixed and p38 and LZAP expression and localization determined by indirect immunofluorescence using anti-Flag monoclonal antibody and affinity-purified rabbit anti-LZAP antibody. Cytoplasmic, nuclear and peri-nuclear localization of p38 was determined by direct visualization and quantified based on at least 100 cells from at least 3 independent experiments. The shift of p38 localization from perinuclear region to nucleus was statistically significant ($p<0.0001$, using unpaired 2 tailed t test). **(D)** Increased p38 abundance in the nuclear following LZAP co-expression. U2OS cells were transfected with plasmids directing expression of Flag-p38 with or without LZAP. Whole cell, cytoplasmic and nuclear cell lysate were prepared, then immunoprecipitates from each lysate were prepared using anti-Flag M2 affinity gel, resolved on SDS-PAGE, and immunoblotted by rabbit p38 antibody. The levels of C23 (nucleolar protein) and β-actin (cytoplasmic protein) were used to monitor the quality of the fractionation and the even loading of samples (1% of each input lysate was loaded as reference.). Expression of LZAP was confirmed by immunoblotting (1% of each input lysate was loaded as reference). Endogenous LZAP was detected after longer exposure (data not shown).

To determine if LZAP and p38 co-localized or altered one another's subcellular localization, immunofluorescent staining of LZAP and p38 were performed following single or combined transient expression (Fig. 3.1C). When expressed without p38, LZAP localizes to both the nucleus and cytoplasm, but is excluded from nucleoli as previously described (data not shown and ^{112, 110}). In the absence of LZAP, expressed p38 localized to both the cytoplasm and nucleoplasm with more than 60% of cells showing stronger localization to the peri-nuclear region (Fig. 3.1C, top panel arrows). LZAP localization was not altered by co-expression of p38; however, co-expression of LZAP with p38 resulted in a shift of p38 staining from predominantly peri-nuclear to predominantly nuclear (Fig. 3.1C, p38 stained panels and graph, $p<0.0001$).

To confirm the observation that LZAP altered p38 subcellular localization, cellular fractionation was performed on cells expressing p38 with and without LZAP. As expected, both p38 and LZAP localized to both the nuclear and cytoplasmic fractions; however, expression of LZAP increased the amount of p38 detected in the nuclear fraction (Fig. 3.1D). Fidelity of the nuclear and cytoplasmic fractions was confirmed by expression of nucleolin/C23 and β -actin. Combined, immunofluorescence and cellular fractionation data suggest that LZAP and p38 co-localize and that expression of LZAP increases p38 nuclear localization.

To begin defining regions of LZAP required for p38 interaction, LZAP truncation mutants were co-expressed with full length p38 (Fig. 3.2). p38 or LZAP immunoprecipitations revealed that an extended LZAP amino terminus region ($\alpha\alpha 1-303$) was sufficient for binding to p38. Within the amino terminal region of LZAP, $\alpha\alpha 1-111$ was unable to bind p38, suggesting that $\alpha\alpha 112-303$ were required for this binding. A separate and non-overlapping extended carboxyl terminal region of LZAP ($\alpha\alpha 329-506$) was also sufficient for p38 binding. Truncation of the extended carboxyl terminal region abrogated p38 binding suggesting that $\alpha\alpha 329-359$ of LZAP are required for p38 binding; however, amino acids 329-359 of LZAP were not sufficient for binding to p38 because a central LZAP truncation containing this region ($\alpha\alpha 201-358$) failed to bind. Within the central region, an LZAP fragment containing residues 112-358 was capable of binding p38 suggesting that a critical

domain for p38 binding exists between amino acids 112 and 201 of LZAP (Fig. 3.2). Results of these p38 binding experiments using LZAP truncations are summarized (Fig. 3.2).

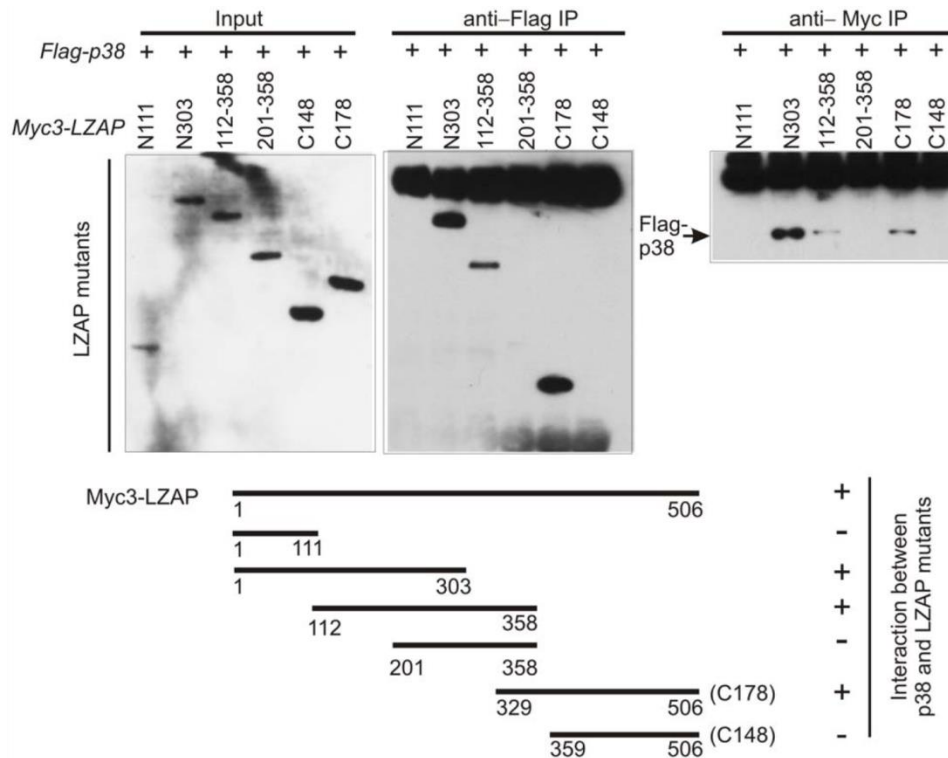


Fig. 3.2 Independent and non-overlapping areas of LZAP are sufficient for association with p38. U2OS cells were transfected with plasmids directing expression of Myc3-tagged truncation mutants of LZAP and full-length Flag-tagged p38. P38 was immunoprecipitated using anti-Flag and LZAP truncation mutants were immunoprecipitated using anti-Myc antibodies before immunoblotting with anti-Myc (to detect LZAP truncations) or anti-p38. Expression of LZAP truncation mutants was confirmed by immunoblotting and binding activity of LZAP truncation mutants is schematically summarized.

LZAP inhibits phosphorylation of p38

MAPK family members are activated by phosphorylation and upon activation are translocated from the cytoplasm to the nucleus¹⁶⁵⁻¹⁶⁷. The dramatic re-localization of p38 from predominantly peri-nuclear to predominantly nuclear in the presence of LZAP (Fig. 3.1C and D) suggests that LZAP may alter p38 activity. To begin exploring effects of LZAP on p38 activity, total and phosphorylated p38 (phospho-T180/Y182) were detected following transient expression of p38 with or without increasing amounts of Myc-LZAP (Fig. 3.3A). Expression of LZAP decreased the amount of phospho-p38 detected in a dose dependent fashion, but did not alter total p38 levels. As expected, the amount of LZAP found in p38 immune-complexes increased as LZAP expression increased (Fig. 3.3A, bottom panel).

Expression of LZAP was associated with increased nuclear p38 levels, but surprisingly, LZAP was also found to decrease total cellular phospho-p38 levels (Fig. 3.1C, D, and 3.3A). To determine if nuclear p38 was phosphorylated in the presence of LZAP, immunofluorescent staining of p38, phospho-p38, and LZAP was performed following transient expression of Flag-p38 with or without Myc-LZAP and activation of p38 using UV irradiation (20 J/m²). Consistent with our previous findings, LZAP expression increased nuclear localization of p38 as indicated by immunofluorescence (Fig. 3.3B, lower panel green). Despite its ability to increase levels of nuclear p38, LZAP strongly inhibited accumulation of nuclear phospho-p38 following UV irradiation (Fig. 3.3B, compare upper and lower red panels). Quantification of phospho-p38 results revealed that 48% of p38 expressing cells were positive for nuclear phospho-p38 in the absence of expressed LZAP, compared to only 11% of p38 expressing cells positive for nuclear phospho-p38 in the presence of expressed LZAP (Fig. 3.3B, p<0.0001). Regardless of LZAP expression, cytoplasmic phospho-p38 was not detected. Data represent examination of more than 100 cells from 3 independent experiments. Combined, these data suggest that LZAP inhibits phosphorylation of nuclear p38.

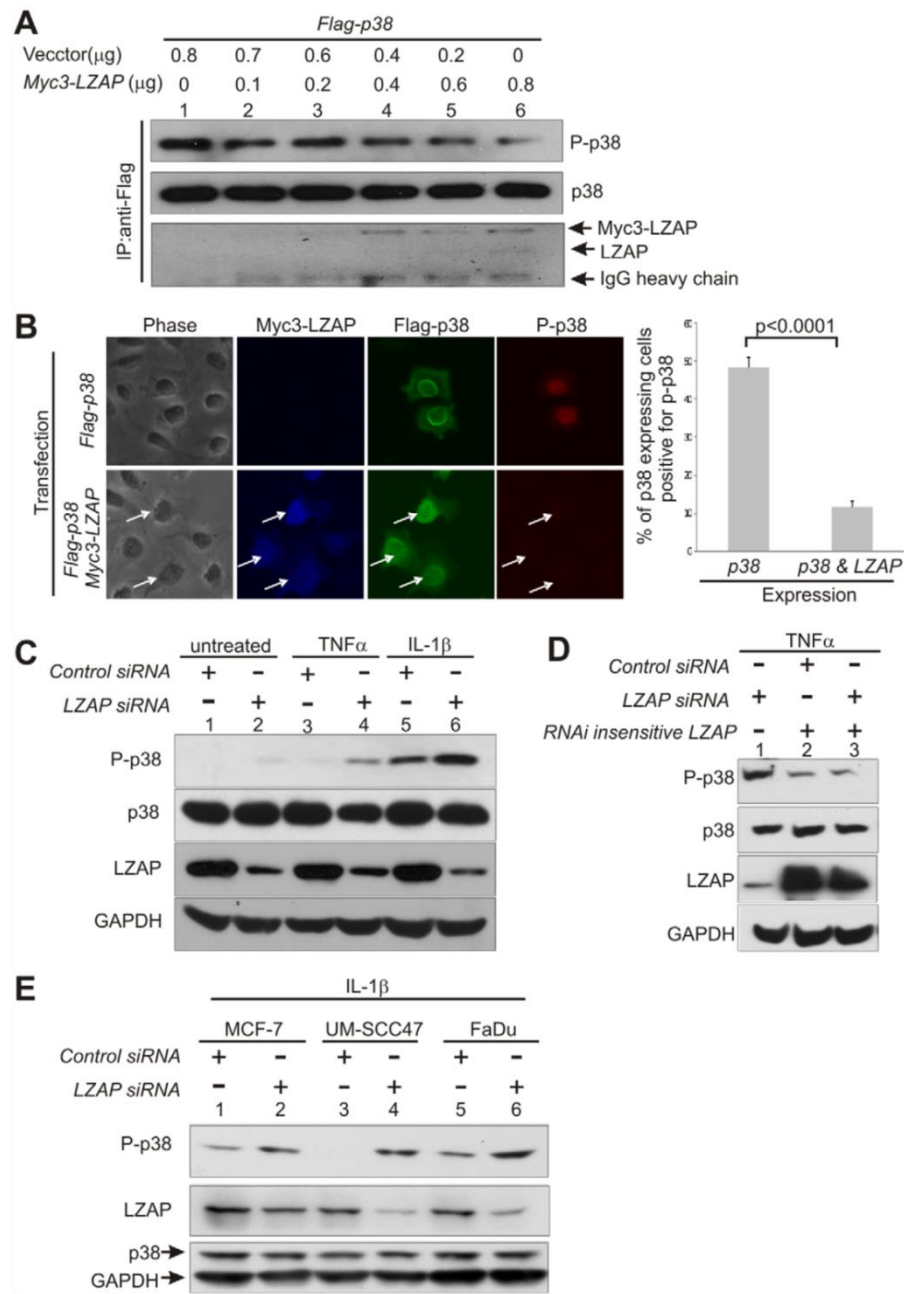


Fig. 3.3 LZAP regulates p38 phosphorylation.

(A) LZAP inhibits phosphorylation of p38 at Thr180/Tyr182. U2OS cells were transfected with plasmids encoding Flag-p38 and with or without increasing amounts of Myc3-LZAP plasmid as indicated. p38 was immunoprecipitated using anti-Flag antibody and p38 phosphorylation at Thr180/Tyr182 determined by immunoblotting. Levels of p38 and LZAP in p38 immunoprecipitates were determined by immunoblotting with antibodies recognizing p38 or LZAP as described [2]). (B) LZAP inhibits accumulation of phosphorylated p38 in the nucleus. U2OS cells were transfected with plasmids directing expression of Flag-p38 with or without Myc3-LZAP. After UV irradiation (20 J/m²), cells were triply immunostained with anti-phospho-p38, anti-Flag, and anti-Myc. The fraction of p38 expressing cells with detectable phosphorylated p38 was determined by direct visualization. Expression of LZAP was associated with a significant decrease in detection of phosphorylated p38 in p38 expressing cells ((p<0.0001, using unpaired 2 tailed t test). Data are derived from examination of at least 200 cells from at least three independent experiments. (C) Depletion of LZAP increases phosphorylation of p38 in U2OS cells. U2OS cells were transiently transfected with control siRNA or siRNA specific to LZAP. Activating phosphorylation of p38 at Thr180/Tyr182 was determined in untreated cells or in cell treated with TNFα or IL-1β by immunoblotting. Expression of LZAP and total p38 was confirmed and GAPDH was used as a loading control. (D) Depletion of the LZAP protein correlates with p38 activation. Twenty-four hours after transfection with control siRNA or siRNA targeting LZAP, U2OS cells were transfected with plasmid encoding RNAi-insensitive LZAP. Transfected cells were selected with G-418 stimulated using TNFα and p38 phosphorylation determined by immunoblotting. Immunoblotting confirmed expression of p38 and si-RNA insensitive LZAP as described [2]. Immunoblotting of GAPDH served as control. (E) Depletion of LZAP increases phosphorylation of p38 in other cell types. MCF7, UM-SCC47 and FaDu cells were transiently transfected with control siRNA or siRNA specific to LZAP. Activating phosphorylation of p38 at Thr180/Tyr182 was determined by immunoblotting in cells treated with IL-1β. Expression of LZAP and total p38 was confirmed and GAPDH was used as a loading control.

Depletion of endogenous LZAP activates p38

To determine if endogenous LZAP regulates p38, LZAP was depleted by siRNA and p38 phosphorylation determined. Knockdown of LZAP in U2OS cells did not alter p38 expression; however, loss of LZAP was associated with increased levels of phospho-p38 levels in either the presence or absence of activating cytokines, TNF α and IL-1 β (Fig. 3.3C). LZAP loss following siRNA treatment was confirmed and GAPDH was used as a loading control (Fig. 3.3C). Off target effects of siRNA were explored by simultaneous siRNA mediated knockdown and expression of LZAP containing silent mutations within the targeting siRNA sequence (RNAi-insensitive LZAP). As described above, cells were treated with TNF α to activate p38 resulting in robust phospho-p38 signal following LZAP knockdown (Fig. 3.3D, lane 1). Regardless of transfection with siRNA targeting LZAP, expression of RNAi-insensitive LZAP resulted in marked inhibition of phospho-p38 levels (Fig. 3.3D, lanes 2 and 3). To determine if LZAP activity was cell type specific, p38 phosphorylation after LZAP knockdown and IL-1 β stimulation was determined in 1 breast cancer cell line (MCF-7) and in 2 head and neck squamous cell carcinoma lines (UM-SCC47, FaDu). As observed in U2OS cells, siRNA-mediated loss of LZAP was associated with increased p38 phosphorylation (Fig. 3.3E). Taken together, these data suggest that endogenous LZAP alters p38 phosphorylation both in the presence or absence of activating cytokines.

Upstream MAPK kinases (MKK3 or MKK6) activate p38 through direct phosphorylation at Thr180 and Tyr182¹⁶⁸. Once activated, p38 phosphorylates downstream target proteins including: MAPKAPK2 and the transcription factor ATF2. To determine if increased p38 phosphorylation observed upon loss of endogenous LZAP correlates with p38 kinase activity, phosphorylation of p38 target proteins was measured in the presence or absence of siRNA targeting LZAP (Fig. 3.4A). After cytokine or LPS stimulation, knockdown of LZAP resulted in increased phosphorylation of p38 targets ATF2 and MAPKAPK2. MAPKAPK2 is itself a kinase that directly phosphorylates HSP27. siRNA-mediated loss of LZAP was associated with increased HSP27 phosphorylation suggesting that a kinase cascade downstream of p38 was activated upon LZAP loss. To begin exploring

potential mechanisms of LZAP activity toward p38, the effect of LZAP loss on MKK3 and MKK6 phosphorylation was determined. LZAP knockdown was not associated with increased phosphorylation of upstream p38 kinases, MKK3 or MKK6 (Fig. 3.4A). Decreased LZAP expression was confirmed by immunoblotting following siRNA treatment (data not shown).

p38-mediated phosphorylation of ATF2 activates ATF2 transcriptional activity¹⁶⁹. In the presence of cytokines, loss of LZAP expression was associated with increased ATF2 phosphorylation (Fig. 3.4A), suggesting that LZAP expression may inhibit ATF2 transcriptional activity. To explore this possibility, a luciferase reporter system relying on a chimeric transcription factor construct containing the GAL4 DNA binding domain fused to ATF2 transcriptional activating domain was used as a surrogate for measurement of ATF2 transcriptional activity¹⁷⁰. In the presence of p38, expression of LZAP resulted in a dose-dependent decrease in ATF2 transcriptional activity (Fig. 3.4B). Data represent 3 independent experiments. Taken together, these data suggest that phosphorylation and activity of p38 and downstream p38 targets are inhibited by endogenous LZAP and upstream MKKs are not mediating LZAP activity toward p38.

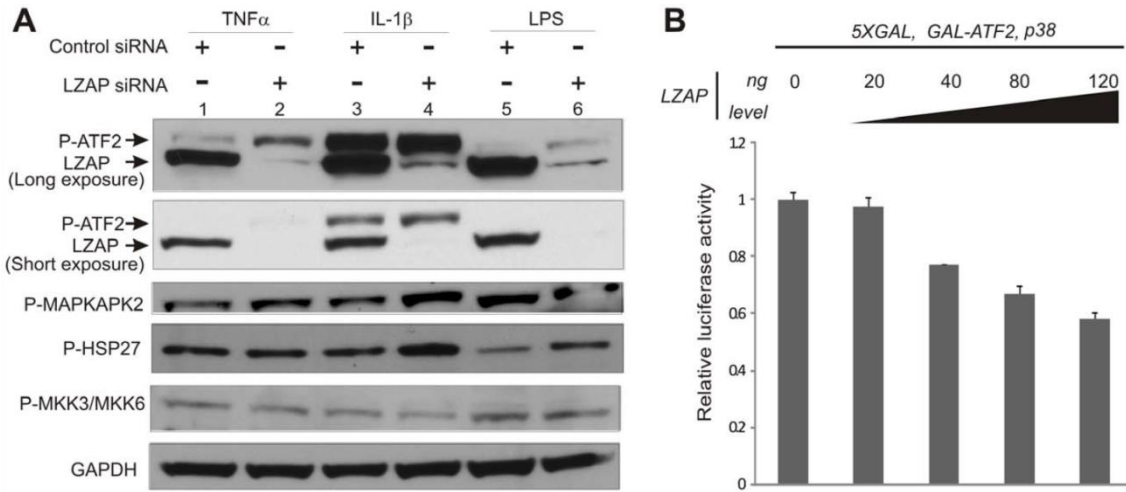


Fig. 3.4 Loss of LZAP increases p38 kinase activity, but does not alter MKK activation. **(A)** Depletion of LZAP increases phosphorylation of p38 targets, but does not alter phosphorylation of MKK3/MKK6. U2OS cells were transfected with control siRNA or siRNA targeting LZAP before stimulation with TNF α , IL-1 β , or LPS. Phosphorylation of direct or indirect p38 targets ATF2, MAPKAPK2, HSP27 and activators of p38, MKK3 and MKK6, was visualized by immunoblotting. LZAP knockdown was confirmed by immunoblotting and expression of GAPDH was used as a loading control. **(B)** LZAP inhibits transcriptional activity of the p38 target ATF2. U2OS cells were transfected with plasmids directing expression of GAL-ATF2 and p38, with or without increasing amounts of LZAP along with a luciferase reporter containing the GAL DNA binding sequence, as indicated. Firefly luciferase activity was normalized based on *renilla* luciferase activity and assigned a value of 1 in cells without transfected LZAP. All normalized luciferase assay data are expressed as the mean with the standard error and are the result of the least three independent experiments.

LZAP regulates p38 phosphorylation through altering Wip1 association with p38

Loss of LZAP did not result in activation of upstream p38-activating kinases MKK3 or MKK6 (Fig. 3.4A), suggesting that LZAP-mediated inhibition of p38 occurred through an alternate mechanisms. Activity and phosphorylation of p38 reflects a balance between upstream activating kinases and inactivating protein phosphatases. Wip1 is a nuclear protein phosphatase that is expressed in response to p53 completing a negative feedback loop through inhibition of p53⁹⁹. In addition to its role in abrogating p53 activity, Wip1 was found to form a physical complex with p38 *in vivo* and to directly dephosphorylate and inactivate p38^{94, 96, 99, 114, 171}.

To determine if the Wip1 phosphatase was involved in LZAP's inhibition of p38, binding of Wip1 to p38 was determined following transient expression of p38 singly or with increasing expression of LZAP. Before p38 immunoprecipitation, cells were UV treated to increase p38 phosphorylation and expression of endogenous Wip1^{92, 94}. Wip1 was not detected in p38 co-immunoprecipitation in the absence of LZAP (Fig. 3.5A, lane 2); however, with increasing LZAP expression, Wip1 association with p38 became detectable and increased concordant with LZAP expression (Fig. 3.5A, lanes 3–5). In agreement with our earlier findings (Fig. 3.1A), LZAP expression had no effect on total p38 level; however, increased expression of LZAP correlated with detection of Wip1 in p38 immunoprecipitates (Fig. 3.5A).

Expression of LZAP resulted in increased association between p38 and its direct phosphatase, Wip1, suggesting that decreased phosphorylation and activity of p38 following LZAP expression may be mediated by Wip1. To explore this possibility, phosphorylation of p38 was compared following transient expression of LZAP with or without siRNA mediated inhibition of Wip1 expression. As expected, expression of LZAP resulted in decreased p38 phosphorylation (Fig. 3.5B, top panel compare lanes 1 and 2). In the presence of LZAP, loss of Wip1 expression restored p38 phosphorylation suggesting that LZAP-mediated inhibition of p38 phosphorylation was at least partially dependent on Wip1 (Fig. 3.5B). Increased p38 phosphorylation following Wip1 loss in the

absence of expressed LZAP has been previously demonstrated^{171,172} and was confirmed in U2OS cells following transfection of siRNA targeting Wip1 (Fig. 3.5B, right panel).

We showed that LZAP binds (Fig. 3.1A, B) and inhibits phosphorylation of p38 (Fig. 3.3) and increases p38 interaction with the Wip1 phosphatase (Fig. 3.5 A). To elucidate mechanisms connecting these observations, an *in vitro* phosphatase assay was performed using bacterially synthesized His-Wip1 and His-LZAP. Expressed full-length Flag-p38 was immunoprecipitated from 293T cells to be used as substrate then incubated with His-Wip1 or LZAP only (Fig. 3.5C lane 1, 2 and 7). p38 was dephosphorylated *in vitro* by Wip1 but not LZAP, which is consistent with the literature and confirms that under these conditions, LZAP has no phosphatase activity. Interestingly, increasing the amount of LZAP incubated with a fixed amount of p38 and Wip1 decreased p38 phosphorylation at lower doses (Fig. 3.5C lane 3,4) which is consistent with our data *in vivo* (Fig. 3.5A). Further increases of LZAP however, reversed this trend resulting in increased levels of phospho-p38 (Fig. 3.5C lane 5, 6). Reactions lacking Mg²⁺ in the buffer served as negative control (Fig. 3.5 lane 8-10). These data suggest LZAP regulates p38 through directly mediating Wip1 binding and/or activity toward p38 and probably in a stoichiometric way. Similarly, *in vitro* phosphatase assays using synthesized pT180 site-specific p38 peptide as substrate (Fig. 3.5D) were performed with bacterially synthesized Wip1 and LZAP⁴⁷. LZAP did not increase p38 peptide dephosphorylation by Wip1 in the peptide assay suggesting that a correct protein structure of p38 is required for LZAP to enhance Wip1 activity. These data suggest that LZAP does not increase Wip1 intrinsic phosphatase activity, but that LZAP may enhance interaction between phosphatase and substrate.

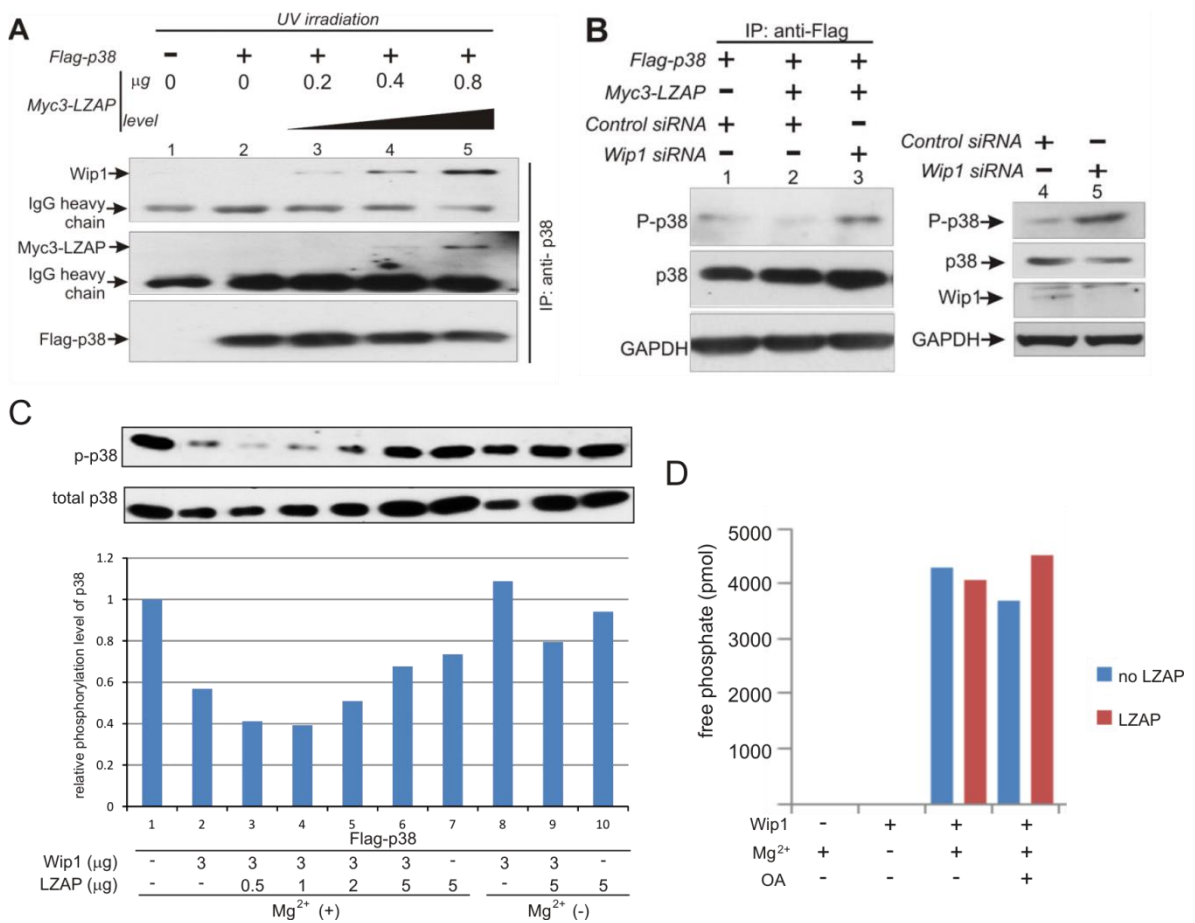


Fig. 3.5 LZAP regulation of p38 phosphorylation involves Wip1. **(A)** LZAP increases Wip1 association with p38 *in vivo*. U2OS cells were transfected with plasmids directing expression of Flag-p38 with or without increasing amounts of Myc3-LZAP as indicated. Immunoprecipitation of Flag-tagged p38 was followed by immunoblotting using antibodies specific to Wip1, or p38. **(B)** Wip1 is required for inhibition of p38 phosphorylation directed by LZAP. U2OS cells were transfected with control siRNA or siRNA targeting Wip1, and after 1 day co-transfected with Flag-p38 with and without Myc3-LZAP, as indicated. Phosphorylation of p38 was visualized by immunoblotting after Flag-p38 immunoprecipitation. Immunoblotting was used to confirm expression of p38 and GAPDH as an indicator of loading. **(C)** Flag-p38 expression vector was transfected into HEK 293T cells, immunoprecipitated with the anti-Flag M2 affinity gel and eluted by 3× Flag peptide, then incubated with indicated amount of recombinant His-Wip1 or His-LZAP in PP2C phosphatase buffer for 30 min before analyzed by immunoblotting as in (A). Magnesium was removed in lane 8-10 as negative control. **(D)** p38MAPK T180 specific-phosphorylated peptides were incubated with recombinant His-Wip1 with or without His-LZAP in PP2C phosphatase buffer for 30 min. Free phosphate was measured by malachite green assay and absorbance at 650nm.

LZAP interacts with Wip1 *in vivo*

To continue explore the mechanism of LZAP-mediated Wip1 and p38 interaction, LZAP and Wip1 interaction was determined. Overexpression of Flag-LZAP and Myc-Wip1 in both U2OS and MCF-7 cells followed by immunoprecipitation with either Flag conjugated beads (Fig. 3.6 A left panel) or Myc antibody (Fig. 3.6 A right panel) showed co-immunoprecipitation of Wip1 or LZAP, respectively. Non-specific IgG was unable to immunoprecipitate either protein. Also immunoprecipitation using LZAP specific antibody for endogenous protein showed co-immunoprecipitation of endogenous Wip1 (Fig. 3.6 B). Following expression of LZAP and Wip1, immunofluorescent staining revealed that Wip1 co-localized with LZAP in the nucleus (Fig. 3.6 C). And interestingly, after co-expression, LZAP nuclear staining changed from a pattern that excluded the nucleolus (98%) to a more evenly distributed pattern including nucleolar staining (17% nucleolar exclusive). Together, these experiments suggest a direct interaction between LZAP and Wip1 *in vivo*. In addition, these data suggest that LZAP regulates p38 phosphorylation and activity by enhancing or stabilizing a protein complex containing both Wip1 and p38.

LZAP partially depends on PPM phosphatases to regulate RelA phosphorylation

Immunoprecipitation and LC-MS/MS identified PPM1A (sequence coverage 33%) and PPM1B (sequence coverage 77%) as potential LZAP binding partners (chapter 4). Since both Wip1 and PPM1A are RelA phosphatases targeting Ser536, which is also a LZAP regulated phosphorylation site, we hypothesize that like p38, LZAP regulation of RelA phosphorylation and activity is may be mediated by phosphatase(s) in a manner similar to what we found for p38. To begin testing this hypothesis, the effect of LZAP on RelA Ser536 phosphorylation was determined in cells with or without siRNA-mediated depletion of PPM1A. As expected, expression of LZAP resulted in decreased RelA phosphorylation in control cells without PPM1A depletion (Fig. 3.7 A, compare lanes 1 and 2). On the other hand, loss of PPM1A expression partially abrogated the ability of LZAP to decrease RelA phosphorylation (Fig. 3.7 A, compare lanes 2 and 4); however, LZAP regulation of PPM1A was not completely dependent on PPM1A (compare lanes 3 and 4). These data suggest that:

1) LZAP-mediated inhibition of RelA phosphorylation was at least partially dependent on PPM1A, 2) there may be additional LZAP-mediated RelA phosphatase(s).

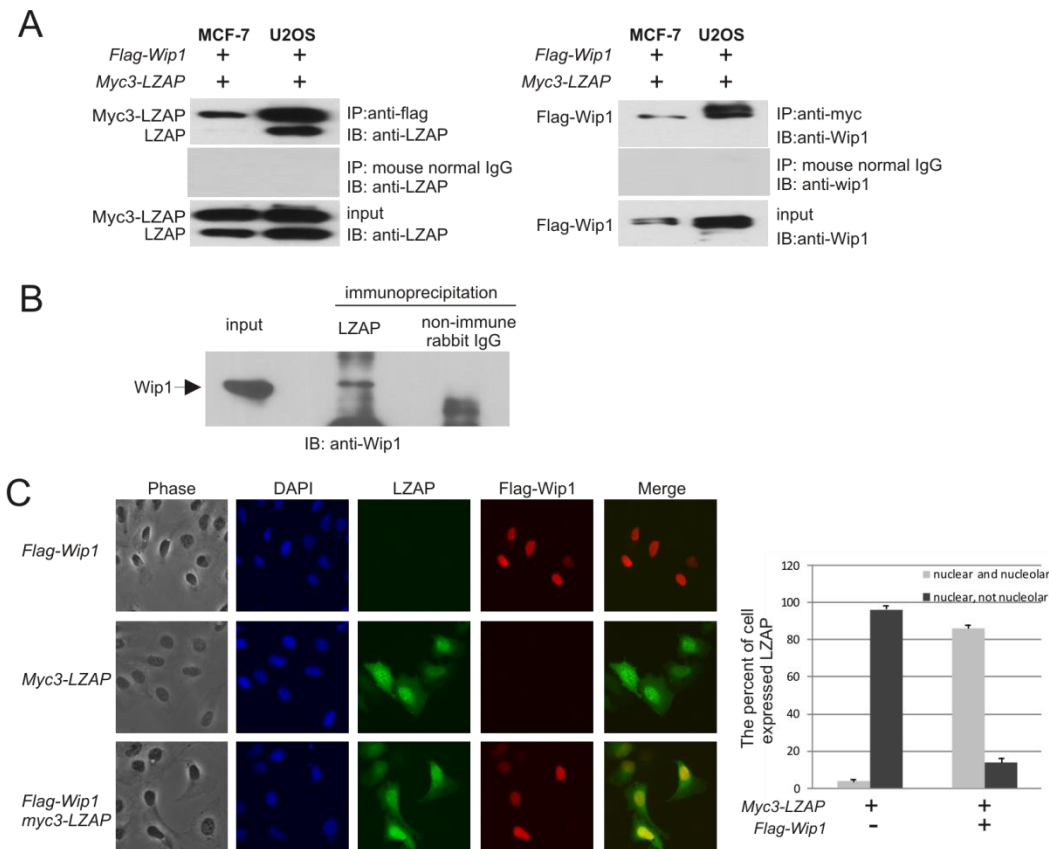


Fig. 3.6 LZAP binds to Wip1. **(A)** Ectopically expressed LZAP and Wip1 mutually co-immunoprecipitate. U2OS and MCF-7 cells were transfected with indicated plasmids directing expression of tagged LZAP or Wip1. Immunoprecipitates were prepared using mouse antibodies recognizing Myc (LZAP) or Flag (Wip1), resolved on SDS-PAGE, and immunoblotted by rabbit antibodies recognizing LZAP or Wip1. Expression of LZAP and Wip1 was confirmed by immunoblotting (1% of each input lysate was loaded as reference.) Pre-immune IgG was used to control for non-specific immunoprecipitation. **(B)** Endogenous LZAP binds endogenous Wip1. Lysates from untransfected MCF7 cells were immunoprecipitated using LZAP-specific rabbit antiserum or non-immune rabbit IgG, then immunoblotted with antibodies specific to Wip1 or LZAP as indicated. **(C)** Wip1 co-localizes with LZAP and alters LZAP nuclear localization. U2OS cells were transfected with plasmids directing expression of Myc3-LZAP with or without Wip1. Cells were fixed and LZAP and Wip1 expression and localization visualized by indirect immunofluorescence using anti-Flag monoclonal antibody and affinity-purified rabbit anti-LZAP antibody. Nucleolar localization of LZAP was determined by direct visualization and quantified based on at least 100 cells from at least 3 independent experiments. The shift of LZAP localization from exclusion of the nucleolus to the whole nucleus (including nucleolus) was statistically significant ($p < 0.0001$, using unpaired 2 tailed t test).

Then to determine if PPM1A dephosphorylation of RelA can be regulated by the presence of endogenous LZAP, phosphorylation of S536 RelA was compared in cells expressing PPM1A, but with or without LZAP depletion by siRNA. As expected, ectopic expression of PPM1A decreased RelA phosphorylation (Fig. 3.7 B, compare lanes 1 and 3) and depletion of LZAP alone increased RelA phosphorylation (Fig. 3.7 B compare lines 1 and 2). Interestingly in the absence of LZAP, expressed PPM1A was not associated with the level of RelA dephosphorylation seen in cells expressing endogenous levels of LZAP (Fig. 3.7 B, compare lanes 3 and 4) though there was still a moderate decrease of RelA phosphorylation compared to LZAP knockdown only (Fig. 3.7 B, compare lanes 2 and 4). *In vitro* PPM1A phosphatase assay using full-length RelA as substrate also revealed that addition of LZAP increases RelA dephosphorylation in a dose dependent manner (Fig. 3.7 C). LZAP alone, even at the highest dose, did not alter RelA phosphorylation (Fig. 3.7 C lane 7). These results indicate that LZAP regulates RelA at least partially through mediating PPM1A dephosphorylation of RelA. Since Wip1 is also reported as a RelA phosphatase⁴⁷ and we showed here that Wip1 binds LZAP (Fig. 3.6), Wip1^{-/-}, p53^{-/-} double null mouse embryonic fibroblasts (MEFs) were used to determine the dependency of LZAP on Wip1 to regulate RelA. As expected, Wip1 knockout was associated with higher basal RelA phosphorylation levels compared to wild-type MEFs (1.64 fold) (Fig. 3.7 D, compare lanes 1 and 3). LZAP decreased RelA phosphorylation in the absence of Wip1, but the amount of decreased phosphorylation was less than in MEFs with endogenous Wip1 (35% vs. 18%, normalized to pS536RelA level in vector control of each group as 100%). These data suggest that part of LZAP's activity toward RelA depends on Wip1. Taking together, these results suggest that the ability of LZAP to regulate RelA phosphorylation largely depends on PPM phosphatases, PPM1A and Wip1.

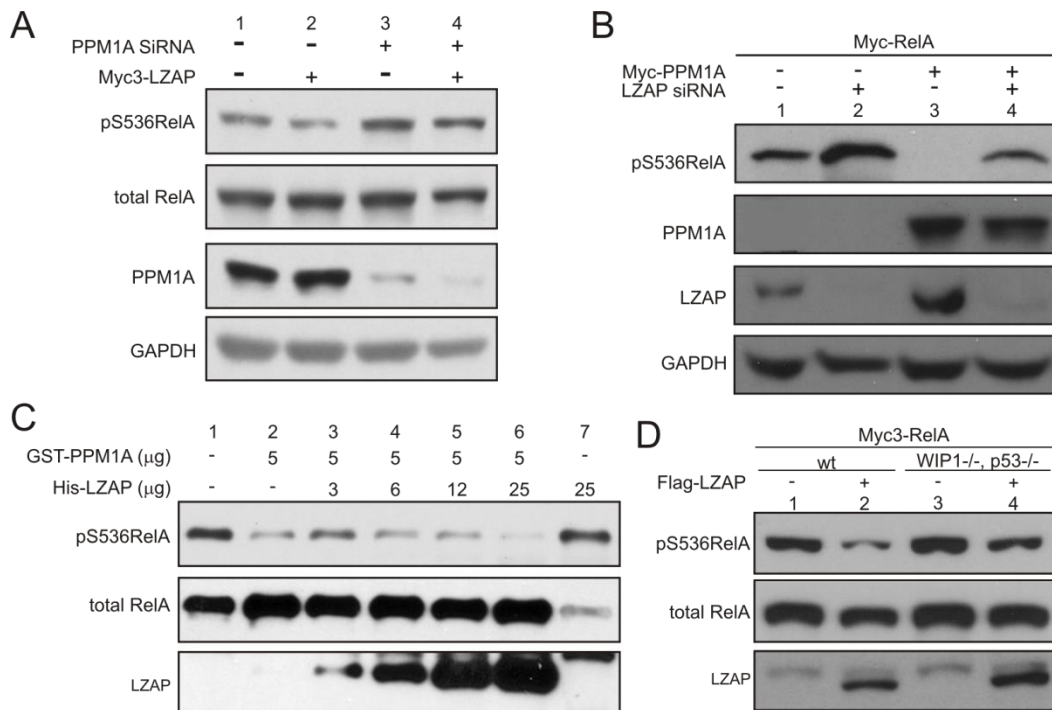


Fig. 3.7 LZAP PP2C phosphatases require one another for efficient regulation of RelA phosphorylation. **(A)** PPM1A is required for inhibition of RelA phosphorylation directed by LZAP. U2OS cells were transfected with control siRNA or siRNA targeting PPM1A, and after 1 day co-transfected with or without Myc3-LZAP, as indicated. Phosphorylation of endogenous RelA at S536 was visualized by immunoblotting. Immunoblotting was used to confirm expression of RelA and GAPDH as an indicator of loading. **(B)** LZAP is required for PPM1A to efficiently dephosphorylate RelA. U2OS cells were transfected with control siRNA or siRNA targeting LZAP, and after 1 day co-transfected with Myc3-RelA with and without Myc3-PPM1A, as indicated. Phosphorylation of RelA, total RelA, LZAP and GAPDH was detected as described in (A). **(C)** Flag-RelA expression vector was transfected into HEK 293T cells, immunoprecipitated with the anti-Flag M2 affinity gel and eluted by 3× Flag peptide, then incubated with indicated amount of recombinant GST-PPM1A with or without His-LZAP in PP2C phosphatase buffer for 30 min before analysis by immunoblotting as described in (A). **(D)** Wild-type or Wip1^{-/-}, p53^{-/-} double null MEFs were co-transfected with Myc3-RelA and control or Flag-LZAP plasmids, as indicated. RelA phosphorylation and LZAP expression level were determined as described in (A).

Discussion

Based on loss of LZAP expression observed in human HNSCC, as well as cellular effects associated with LZAP loss such as enhanced invasion, anchorage independent growth, angiogenesis, and growth of xenograft tumors, LZAP has been identified as a putative tumor suppressor¹¹⁰. LZAP contains no enzymatic motifs suggesting that its activities may be derived through protein-protein interactions. A remarkable number of molecules that are implicated in tumorigenesis (e.g. ARF, RelA, Chk1, Chk2, and p38) bind to LZAP suggesting that LZAP activity may be protean^{110, 112, 113, 116}. Although identification of binding partners has provided insight into LZAP functions, satisfying mechanisms of pleiotropic LZAP activities have been lacking.

Here we report that LZAP bound to the stress activated protein kinase p38, altered p38 subcellular localization and inhibited p38 phosphorylation and activity. Mechanistically, our data suggest that LZAP inhibition of p38 phosphorylation depends on the Wip1 phosphatase, and that in the presence of LZAP, more Wip1 is associated with p38. Conceivably, LZAP may sequester p38 in the nucleus in a complex with Wip1 as a means of p38 inactivation. Alternatively, unphosphorylated nuclear p38 may have unknown activities or may be sequestered in the nucleus so that upon loss of LZAP, rapid activation of p38 could occur through phosphorylation by nuclear kinases.

Depending on cellular context, p38 can mediate opposing cellular responses as an inducer or inhibitor of proliferation and apoptosis¹⁴⁹. To date, most data highlights LZAP as a tumor suppressor, but its role as a p38 regulator implies that LZAP could also have opposing cellular effects or that LZAP inhibition of p38 could be restricted to circumstances where inhibition of p38 suppresses tumor promoting activity.

The mechanism of LZAP activity toward the growing list of LZAP-associated proteins (LAPs) is not well understood. The finding that a portion of LZAP exists in large molecular weight complexes combined with a potential for LZAP to oligomerize (chapter 4) lends credence to this argument and further suggests that LZAP may serve to bring together effector proteins. A large portion of LZAP interacting proteins are phosphorylated, and LZAP expression has been associated with decreased

phosphorylation of these proteins. These observations led us to explore if LZAP had activity to inhibit p38 upstream kinases or to activate p38 phosphatases. We found that LZAP did not alter kinase activity, as measured by phosphorylation, of MKK3 or MKK6; however, LZAP was found to increase association of p38 with its direct phosphatase Wip1 *in vivo* (Fig. 3.5A) and increase Wip1-mediated dephosphorylation of p38 *in vitro* (Fig. 3.5B). Also depletion of Wip1 reversed the decrease of p38 phosphorylation by LZAP, suggesting at least part of the LZAP activity toward p38 depends on Wip1. To explore if this is a mechanism for LZAP regulated RelA phosphorylation, similar experiments were performed with RelA and suggest that LZAP and RelA phosphatases, PPM1A and Wip1, depend on each other to dephosphorylate RelA (Fig. 3.7). Identification of the interaction between LZAP and Wip1 or other PPM phosphatases (Fig. 3.6 and data not shown), which are phosphatases for several LZAP target proteins, further add to the possibility that LZAP form a multi-protein complex with key proteins and their cognate phosphatases to regulate signaling pathways. However, it is still unclear if regulation of phosphatases is a general mechanism of LZAP activity, but it is clear that it is not a universal mechanism since phosphorylation has not been described to play a role in LZAP-mediated ARF activity. It is intriguing that additional described LAPs including Chk1 and Chk2 are also targets of phosphatases, including Wip1^{96,102}. We have previously shown that LZAP activates p53 in the absence of ARF¹¹² raising the possibility that this ARF-independent activity of LZAP may also depend on Wip1, PPM1A or PPM1B.

CHAPTER IV

REGULATION OF LZAP

Abstract

Our studies and those from other groups suggest that LZAP is a putative tumor suppressor with critical activities to regulate key proteins in cancer signaling pathways including: p53, RelA, Chk1 and Chk2 and p38. However little is known about through which LZAP activity is regulated. The activity of many proteins is regulated by post-translational modification (PTM), protein stability, and association with binding partners. Here, we began to explore these mechanisms as well as LZAP self-association as potential means of LZAP regulation. Inorganic ^{32}P isotope labeling revealed that LZAP is phosphorylated *in vivo*, and *in vitro* phosphatase assays using synthesized LZAP phosphopeptides as substrate suggested that Wip1, PPM1A and PPM1B may directly dephosphorylate LZAP. We also observed that manipulation of Wip1 levels resulted in symmetric changes in LZAP protein levels while the ubiquitination of LZAP was decreased upon Wip1 expression. Together with data that PPM phosphatases bind LZAP, these data suggest PPM family phosphatases likely regulate LZAP phosphorylation and stability *in vivo*. The embryonic lethal phenotype of LZAP homozygous knockout mouse model, as well as the impaired zebrafish embryonic development after LZAP knock down indicate that LZAP is an essential protein during vertebrate embryonic development; however functions of LZAP responsible for its requirement for normal development are not clear. To identify potential LZAP regulators or effectors proteins in a complex with LZAP were immunoprecipitated and subjected to LC-MS/MS. Members of the PPM family, PPM1B and PPM1A, were identified and the PPM1B-LZAP interaction was confirmed *in vivo*. Additional proteins, KIAA0776, DDRGK1 and UFM1, have since been described as LZAP binding proteins involved in regulation of LZAP protein level were also identified in the LC-MS/MS analysis. We noted that several proteins involved

in ufmylation were identified as LZAP associated proteins. KIAA0776 has recently been described as an E3-ligase in the ufmylation pathway. UFM1 is the small ubiquitin-like protein that is conjugated to proteins, and DDRGK1 is substrate of KIAA0776. Together these data suggest that LZAP may be regulated by this ubiquitin-like conjugation system or perhaps regulate the ufmylation pathway. To identify the domains of LZAP responsible for interaction with associated proteins, truncation mutants of LZAP were created. Both N-terminal and C-terminal non-overlapping regions of LZAP associate with RelA, p38 and PPM1B suggesting to us that LZAP may be forming homo-dimers or homo-oligomers. Co-immunoprecipitation using differentially tagged LZAP confirmed the existence of at least LZAP dimers. These preliminary data suggest that LZAP activity and protein level are regulated by phosphorylation through interaction with PPM family phosphatase and ubiquitination, and that in addition, LZAP may be modified or regulate the ufmylation pathway.

Introduction

The function, activity, and/or stability of many proteins are controlled by post-translational modification (PTM), by interaction with other proteins or by self-association of proteins to form dimers and higher-order oligomers.

Protein post-translational modification (PTM) increases the functional diversity of the proteome by the covalent addition of functional groups or proteins, proteolytic cleavage of regulatory subunits or degradation of entire proteins. These modifications include, amongst others, phosphorylation, glycosylation, ubiquitination, nitrosylation, methylation, acetylation, lipidation and proteolysis and influence almost all aspects of normal cell biology and pathogenesis. Post-translational modification can occur at any step in the "life cycle" of a protein and can dramatically alter a protein's activity, localization and stability (Thermo Scientific website/Overview of post translational modification). Many proteins are modified shortly after completion of translation to mediate proper protein folding or stability or to direct the nascent protein to distinct cellular compartments (e.g. nucleus, membrane). Other modifications occur after folding and localization are completed to activate or inactivate

catalytic activity or to otherwise influence biological activity. Phosphorylation of proteins by kinases at specific amino acid side chains, principally on serine, threonine or tyrosine residues, is a common method of catalytic activation or inactivation and the most important and well-studied PTM. Conversely, phosphatases hydrolyze the phosphate group to remove it from the protein acting as a counterbalance to kinases. Proteolytic cleavage of peptide bonds is a thermodynamically favorable reaction and therefore permanently removes peptide sequences or regulatory domains. Proteases comprise a family of enzymes that cleave peptide bonds and are critical for many normal cellular processes including: antigen processing, apoptosis, surface protein shedding and cell signaling. Proteins are also covalently linked to tags that target a protein for degradation or can direct subcellular localization. Ubiquitination is a common modification of this type. Ubiquitin is an 8-kDa polypeptide consisting of 76 amino acids that is appended to the NH₂ of lysine in target proteins via the C-terminal glycine of ubiquitin. Following an initial mono-ubiquitination event, a ubiquitin polymer can be created by linking ubiquitin to ubiquitin and creating poly-ubiquitinated proteins that are targeted for degradation by the 26S proteasome. Proteins can also be sequentially modified by processes such as post-translational cleavage and the addition of functional groups for production of mature and active proteins. For some proteins, phosphorylation and ubiquitination are tightly linked as illustrated by examples like IκBα¹⁷³, RelA¹⁷⁴ and GSK¹⁷⁵ in which phosphorylation within target proteins (phosphodegrons) is required to trigger ubiquitination and degradation. Consequently, characterization of PTMs, although challenging, provides invaluable insight into the cellular functions of proteins.

Protein-protein interactions are intrinsic to virtually every cellular process. Any listing of major research topics in biology—for example, DNA replication, DNA repair, transcription, translation, splicing, secretion, cell cycle control, signal transduction, and intermediary metabolism—is also a listing of processes in which protein complexes have been implicated as essential components¹⁷⁶. In addition to well-known examples of multi-subunit proteins, there are also a large number of transient protein-protein interactions, which in turn control a large number of cellular processes. All

modifications of proteins mentioned above necessarily involve such transient interactions. Transient protein-protein interactions are also involved in the recruitment and assembly of the transcription complex on specific promoters, the transport of proteins across membranes, the folding of native proteins catalyzed by chaperones, individual steps of the translation cycle, and the breakdown and re-formation of subcellular structures during the cell cycle (such as the cytoplasmic microtubules, the spindle apparatus, nuclear lamina, and the nuclear pore complex)¹⁷⁶. Thus, identification of binding partners can help advance understanding of protein activity and regulation. Co-immunoprecipitation coupled with liquid chromatography–mass spectrometry (LC-MS/MS) and provides a powerful tool for identification of large number of potential binding proteins.

The self-association of proteins to form dimers and higher-order oligomers is a common phenomenon contributing to numerous cellular processes. Dimerization and oligomerization confers structural and functional advantages to proteins, including improved stability, control of accessibility and specificity of active sites, and increased complexity. Oligomerization or dimerization expands the opportunities for regulation by providing combinatorial specificity, allostery, activation and inhibition. Recent structural and biophysical studies show that protein dimerization or oligomerization is a key factor in the regulation of proteins such as enzymes, ion channels, receptors and transcription factors contributing to increased enzyme activity by concentrating the active site, facilitation of local concentration of molecules, transmission of signals, and channeling of reagents (small molecules and ions) across membranes. In addition, self-association can help to minimize genome size, while maintaining the advantages of modular complex formation. However, inappropriate formation of oligomers can be associated with pathogenic states. Specific protein dimerization is integral to biological function, structure and control, and must be under substantial selection pressure to be maintained with such frequency throughout biology¹⁷⁷.

Upon initiation of this project, information related to regulation of LZAP including modification, enzymes responsible for potential modification (except for Cdk5¹⁰⁷), LZAP-associated proteins, and self-association status were not well described. With the emerging results indicating that LZAP has

tumor suppressor-like activity, regulates major cancer signaling pathways, is essential for early vertebrate development exploration of LZAP regulation under both physiological and pathological conditions is warranted. Here we present preliminary and hypothesis generating data exploring aspects of LZAP regulation.

Materials and Methods

Plasmid constructs and mutagenesis

His-LZAP was PCR from pCDNA3-LZAP and subcloned in to pCDNA3 vector. Truncation mutants of LZAP were as described in chapter 3. Single deletion mutations of LZAP were PCR from pCDNA3-Flag-LZAP wild type construct and mutations of LZAP containing multiple deletions were PCR from the single and double mutations. Primers use for deletion mutagenesis: LZAPD1 forward GTC AAC TAT GAG ATC CCC TCA GGG GCT GCC GAG ATG CGG GAG, LZAPD1 reverse CTC CCG CAT CTC GGC AGC CCC TGA GGG GAT CTC ATA GTT GAC, LZAPD2 forward CCA GAT GCC CTG ACA CTG CTT GAA ATC TTC TTA GCC CAG AGA GCA GTG, LZAPD2 reverse CAC TGC TCT CTG GGC TAA GAA GAT TTC AAG CAG TGT CAG GGC ATC TGG, LZAPD3 forward TCC CAG CTG CTG GCT TTG AAG AAA GAC ATC TCC AAG AGG TAC AGC GG, LZAPD3 reverse CC GCT GTA CCT CTT GGA GAT GTC TTT CTT CAA AGC CAG CAG CTG GGA.

Antibodies and reagents

Anti-His antibody was from Qiagen (#34698). Anti-HA antibody was from Santa Cruz (sc-7392). EZ view anti-Flag M2 affinity gel (F2426-5X1ML) and anti-c-Myc Agarose Affinity Gel (A7470) were purchased from Sigma-Aldrich.

in vivo ^{32}P orthophosphate labeling

24 hrs after transfection of His-LZAP or control vector, U2OS cells were washed and maintained in phosphate-free DMEM (Life Technologies #11971) supplied with 10% dialyzed FBS (Life Technologies #26400) for 24 hrs. After metabolically labeled with 100 $\mu\text{Ci}/\text{ml}$ [^{32}P] orthophosphate

(Perkin Elmer) for 6 hrs, supernatant from cell lysate in 0.5%NP-40 lysis buffer were incubated with anti-His or LZAP antibody. Immunoprecipitates were analyzed by SDS-PAGE and subsequent autoradiography using auto-radiography film.

Results

LZAP is phosphorylated and ubiquitinated

LZAP can be phosphorylated *in vitro* by Cdk5¹⁰⁷; however, Cdk5 expression is limited to cells of neural derivation and LZAP phosphorylation had not been observed *in vivo*. ³²[P] orthophosphate labeling of cells ectopically expressing His-tagged or un-tagged LZAP followed by immunoprecipitation with anti-His or anti-LZAP antibodies revealed that both His-tagged and un-tagged LZAP were phosphorylated *in vivo* (Fig. 4.1 A). Our findings that LZAP is a phosphoprotein that binds to PPM phosphatases coupled with the observation that alteration of Wip1 levels changes LZAP levels (Fig. 4.1C) led us do examine PPM phosphatase activity toward potential phosphorylation sites of LZAP. We also suspected that residues dephosphorylated by PPM phosphatases may indicate residues of LZAP that are phosphorylated *in vivo*. *In vitro* phosphatase assays using LZAP phospho-peptides (S91, T237 and S426) as substrate were performed. S426 was reported to be phosphorylated by cdk5 in the *in vitro* kinase assay¹⁰⁷ while S91 (S91Q92) and T237 (T237V238Y239) are consensus motifs, S/TQ or TXY, for Wip1 and PPM phosphatases^{141, 142}. Bacterially synthesized His-Wip1, GST-PPM1A and GST-PPM1B were incubated with LZAP-specific peptides All three phosphatases dephosphorylated pS91 and pT237 sites robustly while dephosphorylation of pS426, the *in vitro* cdk5 site, was not observed except by the control lambda phosphatase (Fig. 4.1 B).

Interestingly, we found that endogenous LZAP protein levels were decreased after siRNA knockdown of Wip1 (Fig. 4.1 C) suggesting that expression or stability of LZAP might be regulated by phosphorylation. Since phosphorylation is sometimes required as marker triggering ubiquitin

conjugation, LZAP ubiquitination status was measured by co-expression of Myc3-LZAP with HA-ubiquitin. After immunoprecipitation with anti-Myc antibody, ladder of ubiquitin conjugated LZAP was detected by anti-HA antibody (Fig. 4.1 C compare lanes 1 and 2). Consistent with decreased LZAP after depletion of Wip1 LZAP levels were increased with co-expression of Wip1 (Fig. 4.1 D compare lanes 5 and 6). It is possible that LZAP stability is increased upon Wip1 expression as indicated by decreased ubiquitination of LZAP when co-expressed with Wip1 (Fig. 4.1D compare lanes 2 and 3).

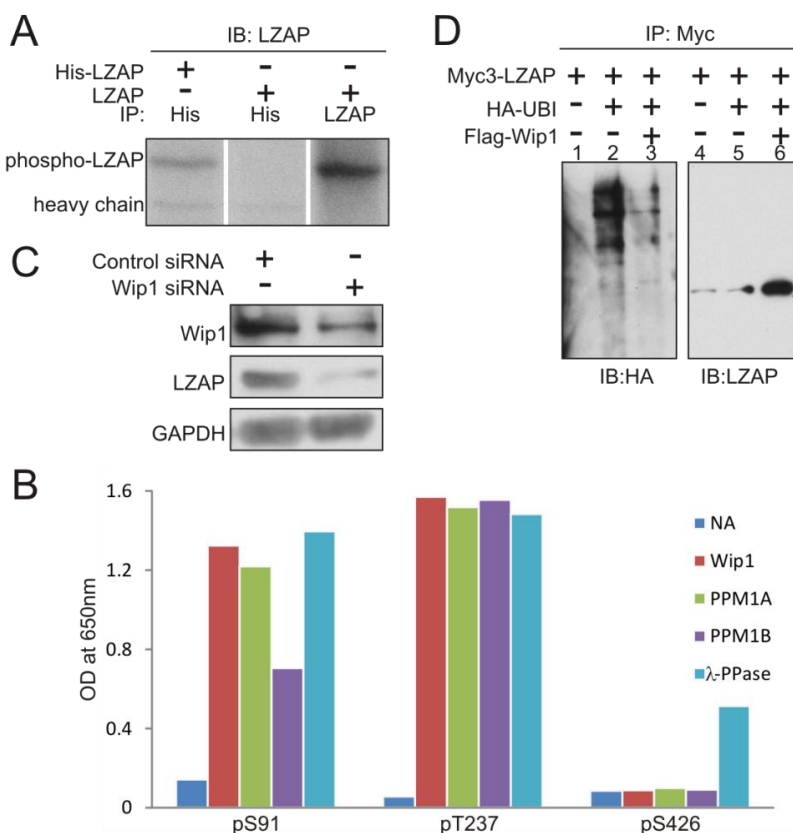


Fig. 4.1 LZAP phosphorylation and ubiquitination. (A) U2OS cells overexpressing His-tagged or untagged LZAP was phosphate starved overnight before incubation with 32 P] orthophosphate for 6 hr. After immunoprecipitation with His or LZAP antibody, samples were separated by SDS-PAGE and autoradiography performed. (B) LZAP-specific peptides with phosphorylation at residues corresponding to S91, T237 and S426 specific-phosphorylated LZAP peptides were incubated with recombinant His-Wip1, GST-PPM1A, or PPM1B in PP2C phosphatase buffer for 30 min. Free phosphate released into the buffer was measured by addition of malachite green and absorbance at 650nm. λ -phage phosphatase (λ -PPase) was used as positive control. (C) Cell lysate from U2OS cells with transient transfection of control or Wip1 siRNA was subjected to SDS-PAGE and Wip1, LZAP and GAPDH detected by immunoblotting. (D) Myc3-LZAP was co-expressed with or without HA-ubiquitin (HA-Ub) and Flag-Wip1 in U2OS cells treated with the proteasome inhibitor, MG132. LZAP immunoprecipitates were separated by SDS-PAGE and ubiquitin or LZAP detected by immunoblotting.

Identification of LZAP binding partners and LZAP binding domain mapping

To date, understanding of LZAP tumor suppressor pathways has been expanded by identification and understanding of the pathways and proteins LZAP regulates, but we still understand very little about pathways and proteins that LZAP regulates that are important in causing embryonic lethality associated with LZAP loss during early vertebrate development. To identify LZAP activities, we used an unbiased approach to identify additional LZAP binding proteins which might function as LZAP regulators or effector in cancer and/or normal development. Initially yeast two hybrid screening was performed on a human placenta library using full-length LZAP as bait (HybriGenics). However the pilot experiment showed that LZAP has a self-activation activity which prevented further screening. Therefore we turned to co-immunoprecipitation coupled with LC-MS/MS (Vanderbilt mass spectrometry research core lab). Flag-LZAP was ectopically expressed in HEK293T cells followed by immunoprecipitation using Flag-antibody conjugated beads. Immunoprecipitated proteins were eluted using 3x Flag peptide enzymatically digested then peptides analyzed by LC-MS/MS. More than 500 proteins and 1000 of their isoforms were identified by two or more peptides (Table 4.1) Putative LZAP binding proteins included: PPM1A and PPM1B, the two PPM family members and several enzymes related to PTM. A high portion of PPM1B protein sequence was covered (75%) and subsequent co-immunoprecipitation using Flag-PPM1B and Myc3-LZAP confirmed interaction between these proteins (Fig. 4.2 A lane 2). The interaction between nucleolin/C23 and LZAP was also recently confirmed using co-immunoprecipitation (data not shown). After our findings, other groups have reported that KIAA0776, DDRGK1 and UFM1 are LZAP-associated proteins¹¹⁸⁻¹²¹. Interestingly, these reports suggest that KIAA0776, DDRGK1 and UFM1 are involved in regulation of LZAP ubiquitination, stability and localization.

To identify domains of LZAP mediating its binding to LZAP-associated proteins, binding between LZAP truncation mutants and known binding partners (p38, RelA and PPM1B) was determined. As described in chapter 3 (Fig. 3.2), both N-terminal ($\alpha\alpha$ 112-358, M3) and C-terminal

(α 329-506, M7) of LZAP bound to p38. Similar results were observed from co-immunoprecipitation of selective LZAP mutants and PPM1B (Fig. 4.2 A) or RelA (Fig. 4.2 B and data not shown). PPM1B binds to LZAP N-terminal mutants M2 (α 1-303) and M3 (α 112-358) and C-terminal mutant M7 (α 329-506). RelA binds to the majority of LZAP truncations excluding a domain of LZAP occupying the mid portion of the protein (M4, α 201-358). The results of binding domains from our lab and the literature suggest that binding of LZAP to effectors or regulators is not straight forward (diagrammatically displayed, Fig. 4.3).

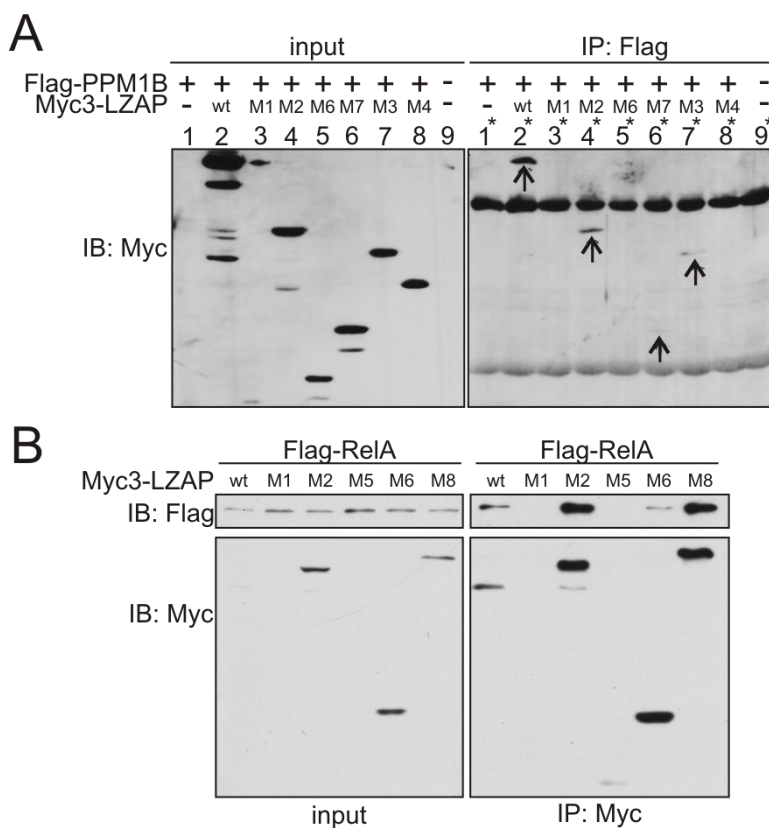


Fig. 4.2 Mapping of LZAP domains involved in binding to LZAP-associated proteins. **(A)** Flag-PPM1B was co-expressed with indicated Myc3-tagged full length or truncated LZAP in U2OS cells. Cell lysates were immunoprecipitated using anti-Flag M2 affinity gel and samples analyzed by SDS-PAGE and immunoblotting with Myc antibody. Arrows on the right panel indicate the bound LZAP truncations. **(B)** Flag-RelA was co-expressed with indicated Myc3-tagged full length or truncated LZAP or in U2OS cells. Cell lysate were immunoprecipitated using Myc antibody conjugated agarose beads. Samples were analyzed by SDS-PAGE and immunoblotting with anti-Flag and anti-Myc antibody.

Table 4.1 selective results from LZAP binding partner analysis. Proteins identified by others are yellow highlighted

| Gene Name | Coverage % | Description |
|-----------|------------|---|
| CDK5RAP3 | 93 | LZAP |
| UBC | 87 | Ubiquitin |
| KIAA0776 | 81 | UPF0555 protein |
| WDR77 | 79 | Methylosome protein 50, Androgen receptor cofactor p44 |
| PPM1B | 75 | Protein phosphatase 2C isoform beta. |
| MYCBP | 72 | C-Myc-binding protein |
| PRMT5 | 71 | Protein arginine N-methyltransferase 5 |
| UFM1 | 68 | Ubiquitin-fold modifier 1 |
| DDRGK1 | 61 | DDRGK domain-containing protein 1 |
| HSPA8 | 52 | Heat shock cognate 71 kDa protein |
| SPIN1 | 52 | Spindlin-1, Ovarian cancer-related protein |
| STK8 | 50 | Serine/threonine-protein kinase 38, NDR1 protein kinase |
| NMP1 | 44 | Nucleophosmin, Nucleolar phosphoprotein B23 |
| UFC1 | 44 | Ufm1-conjugating enzyme 1, Ubiquitin-fold modifier-conjugating enzyme 1 |
| EIF5A | 43 | Eukaryotic translation initiation factor 5A-1 |
| HUWE1 | 36 | E3 ubiquitin-protein ligase HUWE1, ARF-binding protein 1 |
| PPM1A | 33 | Protein phosphatase 1A, Protein phosphatase 2C isoform alpha |
| NCL | 30 | Nucleolin, Protein C23 |
| PPP1CA | 21 | Serine/threonine-protein phosphatase PP1-alpha catalytic subunit |
| MAP3K7 | 11 | Mitogen-activated protein kinase kinase kinase 7 |
| HDAC2 | 11 | Histone deacetylase 2 |

Table 4.2 Summary of LZAP truncations interaction with RelA or LZAP. The number of “+” indicates the signaling strength based on immunoblotting following co-immunoprecipitation, (-) indicates no detectable binding.

| Myc-LZAP | wt | M1 | M2 | M3 | M4 | M5 | M6 | M7 | M8 |
|-------------|-------------|-----|------|------|------|------|------|------|------|
| | Full length | 1- | 1- | 112- | 201- | 428- | 359- | 329- | 226- |
| aa residues | 111 | 303 | 358 | 358 | 506 | 506 | 506 | 506 | 506 |
| RelA | ++ | - | ++++ | +++ | - | NA | ++ | +++ | ++++ |
| LZAP | ++ | NA | +++ | ++ | + | NA | +++ | ++++ | +++ |

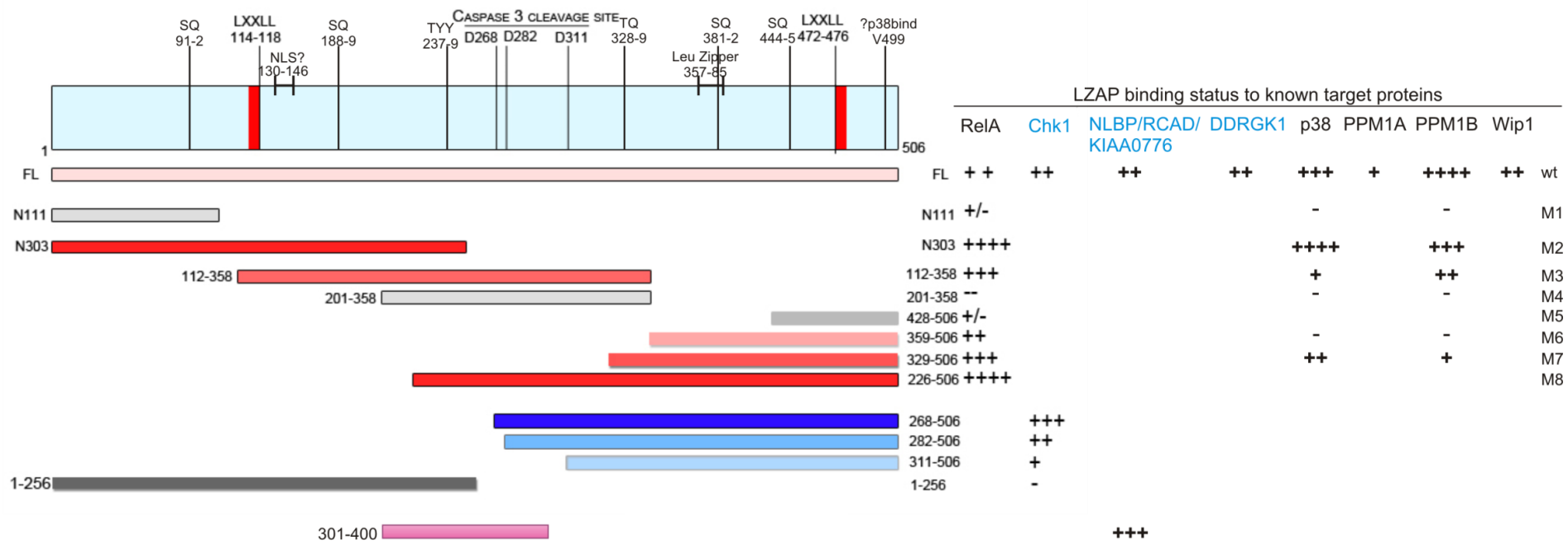


Fig. 4.3 LZAP motifs and binding of LZAP truncations to known LZAP associated proteins and diagram for LZAP protein motifs. The number of “+” indicates the signaling strength based on immunoblotting following co-immunoprecipitation, (–) indicates no detectable binding. Protein name in black indicates results of our studies, protein names in blue indicate results from the literature.

Binding domain mapping was complex with non-overlapping fragments of LZAP binding to multiple proteins suggesting two binding scenarios 1) both N-terminal and C-terminal LZAP contain motifs that directly bind p38, RelA and PPM1B, and/or 2) full length endogenous LZAP dimerizes with LZAP truncation mutants and bridges interaction between truncations and LZAP-associated proteins. LC/MALDI mass spectrometry suggested that some higher molecular weight bands following PAGE and silver staining of Flag-LZAP immunoprecipitation represent LZAP dimers¹¹⁹. To determine if LZAP self-associates, full-length Flag-LZAP was co-expressed with either full-length Myc3-LZAP or Myc3-LZAP truncation mutants in U2OS cells followed by immunoprecipitation using anti-Flag affinity gel. Full-length LZAP and the mutants M2 and M8 co-immunoprecipitated with LZAP respectively (Fig. 4.4 A, co-IP results of LZAP truncation mutants are summarized in Table 4.2). These results suggest that LZAP indeed can self-associate forming at least dimers. To determine the domain of LZAP mediating self-association, Flag-tagged C-terminal LZAP truncation M6 was co-expressed with Myc-M6 or Myc-tagged N-terminal LZAP truncation, M2. Immunoprecipitation of Flag-M6 revealed binding to M6 itself and N-terminal truncation mutant M2 (Fig. 4.4 B lanes 5 and 7). These experiments highlight the requirement for further experiments to distinguish if the interaction of truncation mutant association is direct or mediated by full-length LZAP that is expressed in all cells. In addition to testing truncation mutants of LZAP, a coiled coil domain predicted to be involved in protein-protein interaction was also deleted in LZAP and tested for binding activity. Coiled-coil motifs are characterized by two or more helices wound around one another. In some proteins (e.g. c-Jun), a two-stranded coiled coil is responsible for dimerization¹⁷⁸. Amino acids 129-152, and 452-488 in LZAP are regions likely to form coiled-coil motif (COILS¹³¹, score 95 of 100) and amino acids 346-361 is also predicted to form a coiled coil motif (score 50 of 100) (Fig. 4.4 C). These predicted regions are part of the N- and C- terminal truncation mutants which bind full length LZAP suggesting that they may be involved in dimerization. Flag-tagged deletion mutant Δ123, lacking all three coiled-coil domains, was co-

expressed with Myc3-LZAP. Interestingly, the deletion mutation still co-immunoprecipitated with LZAP with affinity based on band intensity similar to wild-type LZAP suggesting that either these domains are not necessary or that more residues and larger domain(s) are involved in LZAP self-association.

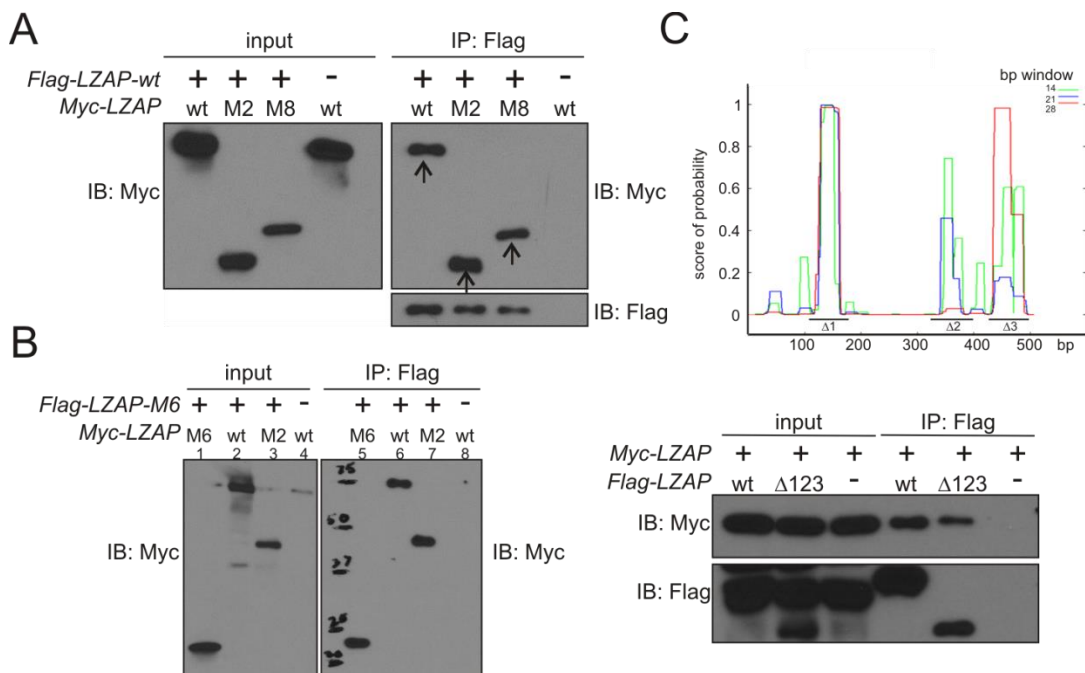


Fig. 4.4 Mapping of LZAP self-association domains **(A)** Flag-LZAP was co-expressed with indicated Myc3-tagged LZAP species, full length or truncations, in U2OS cells. Cell lysate were immunoprecipitated using anti-Flag M2 affinity gel and samples analyzed by SDS-PAGE and immunoblotting with Myc antibody. Arrows on the right panel indicate bound LZAP species. **(B)** Flag-LZAP M6 mutant was co-expressed with indicated Myc3-tagged LZAP species, full length or truncations, in U2OS cells. Binding was determined as described in (A). **(C)** Upper panel: diagram of analyses predicting the coiled-coil domains in LZAP. Lower panel: Myc3-LZAP was co-expressed with Flag-tagged LZAP species, full length or deletions, in U2OS cells. Binding was determined as described in (A).

Discussion

Since we reported that LZAP binds and activates the alternate reading frame protein p14^{ARF} in humans and activates p53⁸², LZAP's role in tumorigenesis has continued to emerge. We and others have described LZAP functions to regulate activities of ARF, p53, p38 MAPK¹¹⁷, NF-κB¹¹⁰, Wip1, Chk1 and Chk2^{113, 116}. Tumor suppressor qualities of LZAP were highlighted by our findings that LZAP is lost in 30% of head and neck squamous cell carcinomas (HNSCC)¹¹⁰. However, the mechanism(s) loss of LZAP expression in cancer remains unknown as does regulation of LZAP activity, stability or subcellular localization. The importance of LZAP biological functions calls for the studies to elucidate the mechanisms of LZAP regulation.

Here, we showed LZAP is phosphorylated and that LZAP binds PPM phosphatase Wip1, PPM1A and PPM1B and may itself be a substrate through PPM family members targeting amino acids S91 and T237. Peptide phosphatase assays suggest that PPM members cannot dephosphorylate the S426 residue of LZAP; however, S426 may still be a phosphorylated site of LZAP. Since LZAP may be targeted for dephosphorylation by Wip1 and phosphorylation can be associated with protein stability (e.g. IκBa¹⁷³, RelA¹⁷⁴ and GSK¹⁷⁵), we examined effects of Wip1 on LZAP expression levels. Interestingly, depletion of Wip1 was accompanied by a decrease of LZAP protein. In the absence of phospho-specific LZAP antibodies, we could not directly correlate LZAP phosphorylation status with stability, but we did explore if LZAP was ubiquitinated and if ubiquitination of LZAP was altered in the presence of Wip1 (Fig. 4.1 D). Remarkably, expression of Wip1 with LZAP was associated with increased LZAP protein levels, but decreased LZAP ubiquitination (Fig. 4.1 D). Interestingly, liquid chromatography and tandem mass spectrometry (LC-MS/MS) used for detection of LZAP-associated proteins identified several proteins involved in ubiquitination including ubiquitin and an E3 ubiquitin ligase. Perhaps just as interesting, several proteins including UFM1, UFC1 and KIAA0776 were also identified as LZAP associated proteins. These three proteins belong to a novel ubiquitin-like protein conjugating system, of which UFM1 is ubiquitin-like protein, UFC1

functions as the E2 enzyme¹²² and KIAA0776/UFL1 is recently identified as the E3 ufmylation ligase¹²³. While there is no data to suggest LZAP is modified by UFM1, it is interesting that another LZAP associated protein DDRGK1, is a substrate of this small protein conjugating system¹²³. Studies have confirmed that KIAA0776 binds LZAP and these two proteins form a complex with UFM1¹¹⁸ suggesting that LZAP may be a substrate for ufmylation or potentially regulate the E3 ligase KIAA0776. LZAP is reported as a stable protein that is not rapidly degraded in control cells (¹¹⁹ and our data not shown). Both Wip1 and KIAA0776 decrease LZAP ubiquitination^{120, 119} and KIAA0776 is an E3 ligase for the novel UFM1 conjugating system, it is possible that UFM1 and ubiquitin compete for the modification on LZAP and dephosphorylation of LZAP by Wip1 at specific residues favors ufmylation over ubiquitination.

Protein-protein interactions are essential, especially in the regulation of biochemical pathways and signaling cascades in the cells. With the increase in numbers of LZAP-associated proteins we sought to map critical binding domains to see if distinct functions for LZAP could be separated. Using truncations of LZAP, we found that both N- and C-terminal portions bind to p38 suggesting that independent regions in LZAP may bind p38; however, similar results found with two additional LZAP binding partners, RelA and PPM1B, suggested that LZAP self-association could also explain the propensity of non-overlapping regions of LZAP to bind a wide variety of proteins. This hypothesis was supported by findings that Myc3-LZAP co-immunoprecipitated with Flag-LAZP and that N- and C-terminal truncation mutants bound not only to full length LZAP but also other truncations. In an attempt to identify LZAP residues critical or required for self-association, 3 of 3 predicted coiled-coil domains were interrupted by deletion (129-152, 346-361 and 452-488, a total of 76 amino acid deletion). Unfortunately, co-immunoprecipitation experiments continued to display the binding of this triple-deletion mutant to full length LZAP suggesting additional or distinct residues in LZAP are required for self-association. Further, it is not clear if LZAP forms dimers or

higher-order oligomers or whether the activity of LZAP and the binding to other proteins depends on self-association.

In summary, we identified that LZAP is phosphorylated and ubiquitinated *in vivo* and that LZAP binds to PPM phosphatases Wip1 and PPM1B, as well as, to components of ubiquitin and UFM1 conjugation systems. Binding domain mapping revealed that LZAP is a self-association protein. All these primary findings raise questions and will lead to further study of the regulation of LZAP.

CHAPTER V

SUMMARY AND FUTURE DIRECTIONS

1. Summary

The objective of this work was to: 1) improve mechanistic understanding of LZAP activity through identification of binding partners and co-effectors of LZAP activity; 2) determine mechanism(s) through which LZAP is regulated. Known LZAP associated proteins, RelA and p38, were used as model LZAP target proteins for many studies dissecting LZAP activity. Findings presented in this dissertation demonstrate that: 1) PPM1A, a PPM family member, is a novel RelA phosphatase with tumor suppressor-like activity; 2) LZAP's ability to decrease target protein (e.g. RelA and p38) phosphorylation is at least partially dependent on PPM phosphatases (PPM1A and Wip1 respectively); 3) LZAP alters PPM activity, at least in some cases (e.g. p38) by enhancing the association of phosphatase and substrate; 4) LZAP is phosphorylated and ubiquitinated, 5) LZAP protein levels are altered by Wip1, suggesting that phosphorylation of LZAP may regulate its stability, 6) LZAP self-associates to form dimer or high-order oligomer with both N- and C-terminal regions of LZAP capable of self-association, and 7) LZAP has many potential binding partners some of which are unexplored, such as ubiquitination and ufmylation pathway components .

Dysregulation of the NF-κB pathway contributes to tumorigenesis in varied cancer types and is a driving force of prostate cancer metastasis. Previous studies in the Yarbrough lab revealed that LZAP is lost in 30% of head and neck squamous cell carcinomas (HNSCC) and those tumors with LZAP loss overexpress select RelA targets. The work here identified a new regulator of NF-κB, PPM1A, and provided evidence that PPM1A expression is decreased in human prostate cancer metastases. Excitingly, restoration of PPM1A expression inhibited NF-κB activity and growth of bony metastases after intravascular injection of prostate cancer cells. Thus, expression status of

LZAP and PPM1A may be used to identify tumors for therapies targeting NF-κB. In addition, since neither deletions of the PPM1A gene nor inactivating mutations of PPM1A have been described in cancer, enhancing expression or activity of PPM1A is potential therapeutic strategy that may inhibit bony metastasis or tumor growth.

2. Future directions

Our findings have provided insight into mechanisms of LZAP activity and LZAP regulation. In particular, regulation of PPM phosphatase activity toward substrates appears to be a central theme in LZAP activity; however, our findings have also raised exciting questions and generated a number of ideas yet to be explored.

2.1. Additional NF-κB target genes and NF-κB related proteins regulated by PPM1A

In this study, we used a NF-κB signaling pathway real time PCR array as the initial tool to identify genes regulated by PPM1A. This array profiles the expression of 84 genes related to NF-κB-mediated signaling transduction, of which about 30 genes are NF-κB responsive genes including cytokines and receptors. A large number of NF-κB regulated genes are not tested in this array indicating that PPM1A may regulate additional NF-κB target genes. An explorative study using RNAseq or microarray comparing gene expression between cells with or without PPM1A depletion will provide more candidate genes whose expression are regulated by PPM1A and may identify additional pathways impacted by PPM1A. Our data indicate that PPM1A decreases tumor cell invasion and prostate cancer cell bony metastasis, which at least partially depends on the inhibition of NF-κB pathway; therefore, a more extensive study identifying additional NF-κB genes regulated by PPM1A may find additional effectors of cancer cell invasion and metastasis.

The RANK/RANKL/OPG triad is one potential group of such genes. Osteoclastic bone resorption contributes to the establishment of tumors in the skeleton. It is now widely understood that the

molecular triad--receptor activator of NF- κ B ligand (RANKL), its receptor RANK, and the endogenous soluble RANKL inhibitor, osteoprotegerin (OPG)--play direct and essential roles in the formation, function, and survival of osteoclasts¹⁷⁹. Recently Jin *et al.* showed that the activation of NF- κ B signaling in prostate cancer cells increased the expression of the osteoclast inducing genes RANKL and PTHrP¹⁸⁰. It is unclear if NF- κ B is a direct transcriptional activator that increases expression of RANKL¹⁸⁰, but indirect effects of NF- κ B activation, namely TNF α and IL-1, stimulate RANKL expression in cells through activation of gp130 signal transducer following IL-1 stimulated expression of IL-6-type cytokines^{181, 182}. Although our data do not suggest that PPM1A alters TNF α or IL-1 expression, effects of PPM1A on RANKL, RANK or OPG expression should still be tested. PPM1A activity to inhibit metastases also suggest that its effects on parathyroid hormone-related protein (PTHrP), which induces both mRNA and protein expression of MCP-1 in human bone marrow endothelial cells and osteoblasts¹⁸³, should be explored.

Pathways and key proteins controlling epithelial-mesenchymal transition (EMT) are additional and interesting potential target of PPM1A. EMT is a complex stepwise phenomenon that occurs during embryonic development and tumor progression. EMT is characterized by the disruption of intercellular junctions, replacement of apical-basolateral polarity with front-to-back polarity and acquisition of migratory and invasive phenotypes¹⁸⁴. The loss of E-cadherin, a cell-cell adhesion molecule is the hallmark of EMT and E-cadherin is regulated by the transcriptional repressor, Snail. Absence of Snail results in embryonic lethality because of severe defects of gastrulation¹⁸⁵. Overexpression of Snail and its function in promoting tumor metastasis has been reported in breast cancer^{186, 187} and, more recently in prostate cancer¹⁸⁸. NF- κ B is one of the major regulators of Snail at both the translational and post-translational levels. NF- κ B has been shown to associate with the Snail1a promoter in zebrafish and directly activate Snail1a expression resulting in altered cell cycle during gastrulation¹⁸⁹. NF- κ B also binds the human snail promoter between -194 and -78 bp, leading to increased Snail transcription¹⁹⁰. Raf kinase inhibitor protein (RKIP), a metastatic

suppressor, was shown to inhibit NF- κ B activity, and conversely, Snail can repress the expression of RKIP. Therefore, there is a positive feedback circuitry between RKIP, NF- κ B and Snail, in which overexpression of Snail in tumors inhibits RKIP and induce EMT^{191,192}. Dysregulated NF- κ B/Snail/RKIP circuitry promotes tumor persistence and metastasis through activation of the epithelial to mesenchymal transition program¹⁹³. Since PPM1A inhibits NF- κ B transcription activity and decreases prostate cancer cell metastasis, it will be interesting to determine PPM1A activities can inhibit the NF- κ B /Snail pathway and EMT.

In this study, we showed PPM1A inhibited RelA phosphorylation *in vivo* independent of IKK α and IKK β , and PPM1A dephosphorylated RelA *in vitro* which suggest PPM1A is a RelA phosphatase *in vivo*. However, these data do not exclude the possibility that PPM1A might also regulate other upstream kinases (e.g. IKK ϵ) or proteins in NF- κ B activation to indirectly inhibit RelA phosphorylation. Recently, Hildebrand *et al.* reported that I κ B ζ , the atypical I κ B family member, is a key transcription regulator of MCP-1/CCL2¹³². I κ B ζ -deficient macrophages exhibited impaired secretion of MCP-1 when challenged with diverse inflammatory stimuli, such as LPS or peptidoglycan. Chromatin immunoprecipitation demonstrate that I κ B ζ is directly recruited to the proximal promoter region of the *Ccl2* gene and is required for transcription-enhancing histone H3 trimethylation at lysine-4. We showed that MCP-1 expression in cancer cells is inhibited by PPM1A, at least partially, through decreasing RelA binding to the *CCL2* promoter. Given the recent finding that I κ B ζ is critical for transcription of *Ccl2*, effects of PPM1A to regulate I κ B ζ , phosphorylation and downstream effects on MCP-1 expression should be explored. Moreover, it is not clear whether PPM1A regulates phosphorylation of other NF- κ B family members such as p50 and RelB. These possibilities could be explored using phospho-specific antibodies, kinase inhibitors and MEFs with knockout of gene(s) coding kinases.

2.2 Mechanisms of decreased PPM1A expression in prostate cancer and the role of PPM1A in other cancer types

Available public cancer datasets revealed that PPM1A mRNA expression was decreased approximately 2-fold in distant metastases of prostate tumors compared to primary prostate tumors without distant metastases (Fig. 2.8A). However, since the distant metastases and primary tumors were from different patients, it is not clear 1) whether the patients with distant metastasis had pre-existing lower PPM1A expression in their primary tumors vs. PPM1A expression decreasing during metastases, or 2) if there is heterogeneity of PPM1A expression in primary tumors and the metastases were derived from this subpopulation. Additionally, metastases usually in patients after primary cancer treatment; therefore, it is possible that the treatment selects for cells with decreased PPM1A expression. To efficiently answer these questions, a PPM1A antibody useful for IHC and tissue microarray is needed. A cohort study comparing PPM1A expression in samples from the same patient at different time points and disease stages (e.g. initial diagnostic biopsy, primary tumor without distant metastasis, primary tumor with lymph node metastasis and tumor from metastatic sites) will help to understand how and when PPM1A expression is altered in prostate cancer cells. Microarray/next generation sequencing can be used to determine PPM1A mRNA levels and tissue microarray using an anti-PPM1A antibody would determine PPM1A protein levels and expression patterns in tumor and adjacent tissues.

Interestingly, PPM1A expression is also decreased in breast cancer and colorectal cancers compared to normal tissue, suggesting that PPM1A loss may also be important in progression of these tumors (Oncomine, PPM1A gene, TCGA breast, TCGA colorectal and colorectal 2 data sets). To determine if PPM1A expression level is different based on the aggressiveness or subtypes of breast cancer or colorectal cancers, further analyses of the TCGA data could be helpful. The role of PPM1A in colorectal cancer has not been studied, but a single study, using xenograft of breast cancer MCF7 cells, revealed that PPM1A depletion increases MCF7 tumorigenic potential and tumor

growth¹⁴⁷ suggesting that loss or decreased PPM1A activity may increase aggressive behavior in breast cancer. While the molecular mechanisms of PPM1A's activity are not elucidated, dephosphorylation of RelA and inhibition of NF-κB activation could play a major role. IL-6 and MCP-1, two of the NF-κB targets inhibited by PPM1A, are also implicated in metastases in cancers of colon^{68,145}, and breast^{69, 71}. Experiments using cancer cells, as well as, metastatic mouse models are proposed to determine PPM1A's activity in breast or colorectal cancer progression and metastasis.

Little is known about the mechanism(s) regulating expression of PPM1A in cancer. Both genetic and epigenetic mechanisms may play a role and should be investigated. To date, neither loss of function mutations nor deletions mutation have been reported for PPM1A. Congruent with the lack of reported mutations and deletions, we have not found point mutations in the catalytic domain of PPM1A using TCGA data for head and neck squamous cell carcinoma, lung adenocarcinoma, breast cancer, and colorectal cancer. PPM1A promoter methylation and histone acetylation status could contribute to expression defects. Given the effect of PPM1A to decrease metastases in a prostate cancer intracardiac injection model, exploration into mechanisms that could restore PPM1A expression or activity in tumor may provide ideas for development of therapy.

2.3 LZAP as a potential regulator of PPM phosphatase activity toward LZAP-associated proteins

In chapter 3, we described that in cells with decreased PPM phosphatase expression (Wip1 or PPM1A) LZAP has diminished ability to inhibit target protein phosphorylation (p38 and RelA respectively). Conversely, PPM phosphatases have diminished activity to dephosphorylate targets in cells with depleted LZAP (Fig. 3.5 B and Fig.3.7 A and B). Together, these data suggest that LZAP and PPM phosphatases are, at least partially, dependent on each other to regulate target protein phosphorylation. Mechanistically, at least for p38, LZAP increases association of Wip1 with p38 potentially by directly bridging these proteins since LZAP binds both Wip1 and p38. Based on these data, the current working model is that LZAP facilitates protein dephosphorylation through

increasing the binding of phosphatase to substrate. This model is supported by the results of Wip1 and PPM1A *in vitro* phosphatase assays revealing that while LZAP increased PPM mediated dephosphorylation of full-length substrate, LZAP had no effect on dephosphorylation of peptide substrates which, due to the short sequence, probably lack the structure for LZAP to bind. Experiments with finer tuned concentration of each component in the reaction will be performed to test this working model.

Because we do not have LZAP mutants that lack binding ability toward PPM phosphatases or substrates, we have not been able to directly test the requirement of LZAP binding to increase dephosphorylation. LZAP self-association combined with the absence of cells lacking LZAP expression has increased the difficulty of binding domain mapping. Generation of a new conditional LZAP knockout mouse and experiments where mutant LZAP and binding proteins are created by IVT or in bacteria should help with these inquiries.

The interplay and role of LZAP in regulating RelA in the presence of PPM1A is slightly different compared to p38 in the presence of Wip1. Although we showed that: PPM1A is a RelA phosphatase, LZAP binds RelA and decreases RelA phosphorylation, and LZAP and PPM1A partially depend on one another to inhibit RelA phosphorylation, we did not observe RelA-PPM1A binding or LZAP-PPM1A binding in co-immunoprecipitation experiments; however, PPM1A was detected as an LZAP-associated protein by LC-MS/MS. LC-MS/MS may be more sensitive compared to antibody-based immunoblotting, which could explain why we saw PPM1A in the LZAP co-IP experiment by LC-MS/MS but not by SDS-PAGE and immunoblotting. To determine if the working model is a unifying mechanism for LZAP, we need to show more evidence of LZAP-PPM1A interaction and LZAP regulated PPM1A-RelA interaction, which may be transient interactions. A typical binding constant for a tight interaction (for example, antibody–antigen or protease–protease inhibitor) is 10^{-12} to 10^{-9} M, yielding a half-life of 12 min–19 h and facile isolation by co-purification. A typical binding constant for a transient interaction is 10^5 – 10^6 M, which yields a half-life of 0.1–1 s, which is a

typical half-life of an enzymatic reaction¹⁹⁴. These transit times hamper co-purification and co-crystallization and require other methods to detect protein-protein interaction. Cross-linking was used to identify RelA interaction with PP2A, another RelA phosphatase, since PP2A could not be detected by RelA immunoprecipitation in the absence of cross-linker⁴³. To better define the interaction of PPM1A with RelA, we will treat cells with cleavable or non-cleavable cross-linker then perform co-immunoprecipitation of RelA complexes and examine to determine if PPM1A and and/or LZAP can be detected. Recently, a PPM1A knockout mouse was created and reported by Yang *et al.*¹⁹⁵. PPM1A-/ null mouse embryonic fibroblast cells will be a useful tool to test the molecular mechanism of the dependency of LZAP on PPM1A. Without endogenous wild-type PPM1A, it is easier to determine the interaction between LZAP and PPM1A by ectopic expression of mutants of PPM1A. Soft agar assays will be used to determine transformation of wild-type and PPM1A-/ MEFs with or without siRNA knockdown or ectopic expression of LZAP and with oncogenic stimulation.. Human cancer cell lines with LZAP and PPM1A stable double knockdown by shRNA could also be used to test for xenograft tumor formation and growth as well as tumor cell metastasis following intravascular injection.

2.4 Regulation of LZAP expression, post-translational modification and stability

2.4.1 LZAP promoter regulation

Yarbrough lab found that LZAP is lost in 30% of head and neck squamous cell carcinomas (HNSCC) ¹¹⁰, but the mechanism(s) for the LZAP loss remains unknown. No genomic alteration (e.g. deletion mutation or point mutation) of LZAP has been identified including TCGA database searches, suggesting that epigenetic mechanism(s) are likely responsible for diminished expression of LZAP. Studies to determine LZAP promoter regulation including identification of transcription factors and co-factors responsible for LZAP gene transcription and promoter methylation may shed light on regulation of LZAP expression.

Interestingly, NF-κB and p53 binding sites were predicted in the *LZAP* gene promoter region (-20 kb to +10 kb relative to the transcription start site, SABioscience, Champion ChIP Transcription Factor Search Portal) (Fig. 5.1). We reported that LZAP regulates NF-κB¹¹⁰ and p53¹¹² activity. It is possible that both transcription factors have feedback regulation of LZAP expression so the dysregulation of NF-κB or p53 in cancer cells might not only be the results of LZAP loss but also function to further suppress LZAP expression. Chromatin immunoprecipitation (ChIP) assay will be the first step to determine if NF-κB or p53 binds to *LZAP* promoter region followed by cloning the predicted binding region(s) in the *LZAP* promoter to luciferase reporter construct to measure the effect of NF-κB or p53 on transcription. Histone acetylation status in this region will be evaluated by ChIP and HDAC inhibitors will be used to treat cancer cells to determine if it will increase LZAP expression.

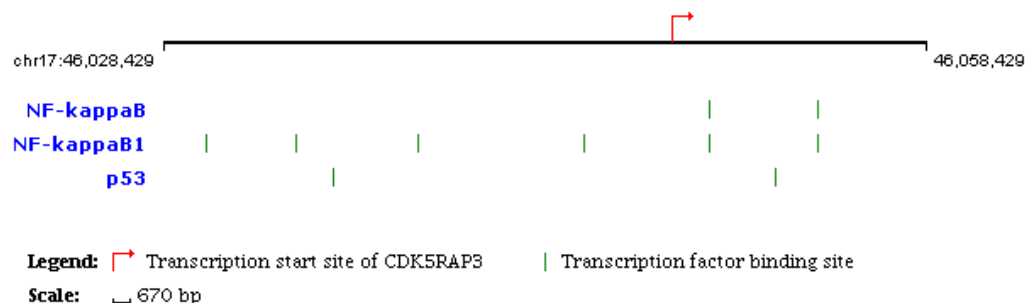


Fig. 5.1 Relevant transcription factor binding sites in LZAP gene promoter (predicted by SABiosciences' Text Mining Application and the UCSC Genome Browser)

DNA methylation, occurring at cytosines in CpG dinucleotides, is a potent mechanism of transcriptional repression. CpG islands are defined as DNA sequences that contain CpG dinucleotides at a frequency that is significantly higher than expected for a random distribution based on the base composition of the mammalian genome¹⁹⁶. Many tumor suppressor genes (TSGs) including p14^{ARF} and p16^{INK4A} have their promoter situated in a CpG island and are silenced by aberrant methylation in cancer, which appears to be a significant pathway for TSG inactivation in neoplasia¹⁹⁷. There are two predicted CpG islands located in -1.5kb to 0.5kb region of LZAP gene (predicted using MethPrimer). FaDu cells express the lowest level of LZAP protein among the 13 HNSCC cell lines tested. To determine if the CpG island in LZAP is methylated, bisulphite sequencing will be determined.

2.4.2 Phosphorylation sites in LZAP

Here, we showed that LZAP is a phosphoprotein and our data suggest that PPM phosphatase Wip1, PPM1A and PPM1B may dephosphorylate LZAP at amino acid residues S91 and T237. To explore the phosphorylation sites of LZAP *in vivo*, liquid chromatography and tandem mass spectrometry (LC-MS/MS) will be performed on immunoprecipitated Flag-tagged LZAP affinity purified after expression in 293T cells using Flag M2 gel (Sigma). We used this system to detect LZAP-associated proteins and have determined that more than 90% of LZAP is covered by MS data, including all conserved potential phosphorylated residues. Phosphorylation will be maximized by inhibition of phosphatases during the last 1 hour of cell growth using peroxovanadate (vanadate/H₂O₂ mixture) and calyculin A and/or through use of Wip1^{-/-} MEFs. Some phosphorylation sites (especially clusters of sites) can be very challenging to the LC-MS/MS method due to limitations in enzyme specificity and because of the potential for some phospho-groups to be especially labile in the gas phase (most often through beta elimination of T-phos and S-phos). As an alternative method, phosphorylation of 13 S, T or Y sites (Fig. 5.2), conservative or within SP/Q,

TXY motif, as well as sites identified in LC-MS/MS above will be assessed through site-directed mutagenesis (Tyr to Phe, Ser to Ala, and Thr to Ala) and 2D gel electrophoretic mapping of LZAP tryptic phospho-peptides. In case a single mutant does not inhibit phosphorylation, multiple simultaneous mutants will be made to identify critical sites of Ser, Thr, and Tyr phosphorylation. Phosphorylated residues will be identified by comparing wild-type and mutant LZAP tryptic phospho-peptide maps. Digestion of LZAP by trypsin should yield 26 peptides containing Ser/Thr/Tyr residues 8 of which contain the 9 highly conserved sites mentioned above. *In vivo* ^{32}P -phospho-labeling followed by immunoprecipitation, SDS-PAGE and autoradiography will be performed on an LZAP mutant containing all identified phosphorylation sites to verify results from LC-MS/MS and phospho-peptide mapping and to determine if all phospho-acceptor sites of LZAP have been identified. Data from mass spectrometry may identify phosphorylated sites that are not as evolutionarily conserved as those that are chosen for initial analyses. Likewise, mutational analyses using phospho-peptide mapping can determine which Ser, Thr, or Tyr residues in tryptic fragments are phospho-acceptor sites.



Fig. 5.2. Potential phosphorylation sites on LZAP. Human LZAP protein sequence was analyzed using NetPhos 2.0 and GPS 2.1 to identify potential phosphorylation sites. Evolutionarily conserved potential phospho-Thr (circle), Ser (square), and Tyr (triangle) are indicated above the line representation of LZAP. Potential kinases are listed above and potential Wip1 targets below target residues.

Sequence analyses of identified phosphorylation sites of LZAP will provide insight into kinases and phosphatases that may regulate LZAP phosphorylation. Once phosphorylation sites of LZAP are identified, phospho-specific LZAP antibodies can be created to those phospho-acceptor residues that alter LZAP activity. These antibodies will be critical for correlation of LZAP phosphorylation and activity.

Once phosphorylation sites of LZAP are identified and confirmed by mutagenesis, LZAP mutants targeting identified phosphorylated sites will be examined to determine consequences on LZAP half-life, subcellular localization, and association/activity toward RelA, Chk1/2, and p38 using techniques as described in chapter II-IV above. Mutants that alter LZAP stability or activity will provide insight into phosphorylation-dependent regulation of LZAP.

2.4.3 LZAP post-translational modification by ubiquitin or ubiquitin-like conjugating systems

LZAP is ubiquitinated and binds to components of an ubiquitin-like conjugating (ufmylation) system (UFM1, UFC1 and KIAA0776). Consistent with our data, Wu *et al.* showed LZAP was a stable protein that was protected from proteasome-mediated degradation unless KIAA0776 was depleted¹¹⁹. Since both ubiquitin and UFM1 are conjugated to lysine residues, it is possible that the two compete for the conjugating sites on LZAP. In this scenario, UFM1 conjugation would protect LZAP from ubiquitination-mediated proteasomal degradation. Experiments to measure the level of UFM1 conjugation on LZAP and the role of ufmylation in regulation of LZAP protein stability would be interesting, but to date studies examining physiological target(s) and biological functions of ufmylation remain largely undefined. Recently, components of the ufmylation system were shown to be transcriptionally up-regulated in HCT116 (colon cancer cell line), HepG2 (hepatocellular carcinoma cells) and MEFs by disturbance of the ER homeostasis and inhibition of vesicle trafficking¹⁹⁸ and similar results were reported in pancreatic cells¹¹⁸. Interestingly, LZAP was shown to be anchored to ER by KIAA0776, the E3 ligase of UFM1¹²¹ and another LZAP binding protein

C20orf116 /DDRGK1 was reported to be a target of ufmylation and to reside in the ER^{123,118}. KIAA0776 and LZAP have been implicated in ufmylation of endogenous Ufm1 targets and depletion of either KIAA0776 or LZAP resulted in unfolded protein response, an ER stress response activated in response to an accumulation of unfolded or misfolded proteins in the lumen of the endoplasmic reticulum suggesting that LZAP and KIAA0776 might be involved in normal ER function through regulation of ufmylation¹⁹⁸. Our data suggest that endogenous LZAP localizes preferentially in the nucleus and para-nuclear regions. It will be interesting to determine 1) if LZAP exerts different functions based on its subcellular localization, 2) if LZAP plays a similar role in ufmylation as it does in target protein phosphorylation by binding and introducing the substrate to the enzyme responsible for the specific post-translational modification, and 3) if the role of LZAP in normal ER functions makes LZAP indispensable in the early vertebrate embryonic development.

2.4.4 Additional post-translational modifications of LZAP

In addition to phosphorylation and ubiquitination, there are many types of PTM that can also regulate protein activity, stability and cellular localization . Specific antibodies are available for many known PTMs and sites; however, it is not practical or possible to localize unknown PTM sites by immunoblotting. Recent advances in mass spectrometry have increased the power of these techniques to identify protein post-translational modifications including: phosphorylation, acetylation, methylation and nitration. Recently, tyrosine nitration has been explored using electrospray ionization-tandem mass spectrometry using electron capture dissociation^{199, 200}. Non-biased identification of lysine acetylation²⁰¹, protein oxidation²⁰² and sumoylation²⁰³ can be efficiently performed using high performance liquid chromatography tandem MS analysis. An unbiased approach to determine modifications of LZAP following alterations in subcellular localization (as was seen with expression of Wip1, Fig. 3.6) or following cellular stress or following inhibition of the proteasome will provide further insight into mechanisms of LZAP regulation.

REFERENCES

1. Lammers T, Lavi S. Role of type 2C protein phosphatases in growth regulation and in cellular stress signaling. *Crit Rev Biochem Mol Biol.* 2007 Nov-Dec;42(6):437-61.
2. Chen LF, Greene WC. Shaping the nuclear action of NF-kappaB. *Nat Rev Mol Cell Biol.* 2004 May;5(5):392-401.
3. Sen R, Baltimore D. Multiple nuclear factors interact with the immunoglobulin enhancer sequences. *Cell.* 1986;46:705-16.
4. Baldwin AS. THE NF- B AND I B PROTEINS: New Discoveries and Insights. *Annual Review of Immunology.* 1996;14(1):649-81.
5. Baeuerle PA, Henkel T. Function and activation of NF-kappa B in the immune system. *Annu Rev Immunol.* 1994;12:141-79.
6. Siebenlist U, Franzoso G, Brown K. Structure, regulation and function of NF-kappa B. *Annu Rev Cell Biol.* 1994;10:405-55.
7. Ghosh S, May MJ, Kopp EB. NF-kappa B and Rel proteins: evolutionarily conserved mediators of immune responses. *Annu Rev Immunol.* 1998;16:225-60.
8. Karin M. How NF-kappaB is activated: the role of the IkappaB kinase (IKK) complex. *Oncogene.* 1999 Nov 22;18(49):6867-74.
9. Tergaonkar V. NFkappaB pathway: a good signaling paradigm and therapeutic target. *Int J Biochem Cell Biol.* 2006;38(10):1647-53.
10. Chen LF, Greene WC. Regulation of distinct biological activities of the NF-kappaB transcription factor complex by acetylation. *J Mol Med.* 2003 Sep;81(9):549-57.
11. Beg A, Ruben S, Scheinman R, Haskill S, Rosen C, Baldwin A, Jr. I kappa B interacts with the nuclear localization sequences of the subunits of NF-kappa B: a mechanism for cytoplasmic retention [published erratum appears in Genes Dev 1992 Dec;6(12B):2664-5]. *Genes Dev.* 1992 October 1, 1992;6(10):1899-913.

12. Vermeulen L, De Wilde G, Van Damme P, Vanden Berghe W, Haegeman G. Transcriptional activation of the NF-kappaB p65 subunit by mitogen- and stress-activated protein kinase-1 (MSK1). *EMBO J.* 2003 Mar 17;22(6):1313-24.
13. Viatour P, Merville MP, Bours V, Chariot A. Phosphorylation of NF-kappaB and IkappaB proteins: implications in cancer and inflammation. *Trends Biochem Sci.* 2005 Jan;30(1):43-52.
14. Perkins ND. Post-translational modifications regulating the activity and function of the nuclear factor kappa B pathway. *Oncogene.* 2006 Oct 30;25(51):6717-30.
15. Neumann M, Naumann M. Beyond IkappaBs: alternative regulation of NF-kappaB activity. *FASEB J.* 2007 Sep;21(11):2642-54.
16. Perkins ND. Regulation of NF-kappaB by atypical activators and tumour suppressors. *Biochem Soc Trans.* 2004 Dec;32(Pt 6):936-9.
17. Rocha S, Campbell K, Perkins ND. p53-and Mdm2-independent repression of NF- κ B transactivation by the ARF tumor suppressor. *Molecular Cell.* 2003;12:15-25.
18. Sakurai H, Chiba H, Miyoshi H, Sugita T, Toriumi W. IkappaB kinases phosphorylate NF-kappaB p65 subunit on serine 536 in the transactivation domain. *J Biol Chem.* 1999 Oct 22;274(43):30353-6.
19. Sakurai H, Suzuki S, Kawasaki N, Nakano H, Okazaki T, Chino A, et al. Tumor necrosis factor-alpha-induced IKK phosphorylation of NF-kappaB p65 on serine 536 is mediated through the TRAF2, TRAF5, and TAK1 signaling pathway. *J Biol Chem.* 2003 Sep 19;278(38):36916-23.
20. Bohuslav J, Chen LF, Kwon H, Mu Y, Greene WC. p53 induces NF-kappaB activation by an IkappaB kinase-independent mechanism involving phosphorylation of p65 by ribosomal S6 kinase 1. *J Biol Chem.* 2004 Jun 18;279(25):26115-25.
21. Sasaki CY, Barberi TJ, Ghosh P, Longo DL. Phosphorylation of RelA/p65 on serine 536 defines an I{kappa}B{alpha}-independent NF-{kappa}B pathway. *J Biol Chem.* 2005 Oct 14;280(41):34538-47.
22. Zhong H, Voll RE, Ghosh S. Phosphorylation of NF-kappa B p65 by PKA stimulates transcriptional activity by promoting a novel bivalent interaction with the coactivator CBP/p300. *Mol Cell.* 1998 Apr;1(5):661-71.
23. Zhong H, May MJ, Jimi E, Ghosh S. The phosphorylation status of nuclear NF-kappa B determines its association with CBP/p300 or HDAC-1. *Mol Cell.* 2002 Mar;9(3):625-36.

24. Chen LF, Williams SA, Mu Y, Nakano H, Duerr JM, Buckbinder L, et al. NF-kappaB RelA phosphorylation regulates RelA acetylation. *Mol Cell Biol*. 2005 Sep;25(18):7966-75.
25. Grivennikov SI, Karin M. Inflammation and oncogenesis: a vicious connection. *Curr Opin Genet Dev*. 2010 Feb;20(1):65-71.
26. Staudt LM. Oncogenic activation of NF-kappaB. *Cold Spring Harb Perspect Biol*. 2010 Jun;2(6):a000109.
27. Ruland J. Return to homeostasis: downregulation of NF-kappaB responses. *Nat Immunol*. 2011 Aug;12(8):709-14.
28. Hoffmann A, Levchenko A, Scott ML, Baltimore D. The IkappaB-NF-kappaB signaling module: temporal control and selective gene activation. *Science*. 2002 Nov 8;298(5596):1241-5.
29. Sun SC, Ganchi PA, Ballard DW, Greene WC. NF-kappa B controls expression of inhibitor I kappa B alpha: evidence for an inducible autoregulatory pathway. *Science*. 1993 Mar 26;259(5103):1912-5.
30. Le Bail O, Schmidt-Ullrich R, Israel A. Promoter analysis of the gene encoding the I kappa B-alpha/MAD3 inhibitor of NF-kappa B: positive regulation by members of the rel/NF-kappa B family. *EMBO J*. 1993 Dec 15;12(13):5043-9.
31. Kearns JD, Basak S, Werner SL, Huang CS, Hoffmann A. IkappaBepsilon provides negative feedback to control NF-kappaB oscillations, signaling dynamics, and inflammatory gene expression. *J Cell Biol*. 2006 Jun 5;173(5):659-64.
32. Arenzana-Seisdedos F, Thompson J, Rodriguez MS, Bachelerie F, Thomas D, Hay RT. Inducible nuclear expression of newly synthesized I kappa B alpha negatively regulates DNA-binding and transcriptional activities of NF-kappa B. *Mol Cell Biol*. 1995 May;15(5):2689-96.
33. Chen L, Fischle W, Verdin E, Greene WC. Duration of nuclear NF-kappaB action regulated by reversible acetylation. *Science*. 2001 Aug 31;293(5535):1653-7.
34. Liu B, Yang R, Wong KA, Getman C, Stein N, Teitel MA, et al. Negative regulation of NF-kappaB signaling by PIAS1. *Mol Cell Biol*. 2005 Feb;25(3):1113-23.
35. Lawrence T, Bebien M, Liu GY, Nizet V, Karin M. IKKalpha limits macrophage NF-kappaB activation and contributes to the resolution of inflammation. *Nature*. 2005 Apr 28;434(7037):1138-43.

36. Li Q, Lu Q, Bottero V, Estepa G, Morrison L, Mercurio F, et al. Enhanced NF-kappaB activation and cellular function in macrophages lacking IkappaB kinase 1 (IKK1). *Proc Natl Acad Sci U S A*. 2005 Aug 30;102(35):12425-30.
37. Natoli G, Chiocca S. Nuclear ubiquitin ligases, NF-kappaB degradation, and the control of inflammation. *Sci Signal*. 2008;1(1):pe1.
38. Tanaka T, Grusby MJ, Kaisho T. PDLIM2-mediated termination of transcription factor NF-kappaB activation by intranuclear sequestration and degradation of the p65 subunit. *Nat Immunol*. 2007 Jun;8(6):584-91.
39. Maine GN, Mao X, Komarck CM, Burstein E. COMMD1 promotes the ubiquitination of NF-kappaB subunits through a cullin-containing ubiquitin ligase. *EMBO J*. 2007 Jan 24;26(2):436-47.
40. Kinjyo I, Hanada T, Inagaki-Ohara K, Mori H, Aki D, Ohishi M, et al. SOCS1/JAB is a negative regulator of LPS-induced macrophage activation. *Immunity*. 2002 Nov;17(5):583-91.
41. Buss H, Dorrie A, Schmitz ML, Frank R, Livingstone M, Resch K, et al. Phosphorylation of serine 468 by GSK-3beta negatively regulates basal p65 NF-kappaB activity. *J Biol Chem*. 2004 Nov 26;279(48):49571-4.
42. Nelson DE, Ihekwaba AE, Elliott M, Johnson JR, Gibney CA, Foreman BE, et al. Oscillations in NF-kappaB signaling control the dynamics of gene expression. *Science*. 2004 Oct 22;306(5696):704-8.
43. Yang J, Fan GH, Wadzinski BE, Sakurai H, Richmond A. Protein phosphatase 2A interacts with and directly dephosphorylates RelA. *J Biol Chem*. 2001 Dec 21;276(51):47828-33.
44. Mumby M. PP2A: unveiling a reluctant tumor suppressor. *Cell*. 2007 Jul 13;130(1):21-4.
45. Sablina AA, Hahn WC. SV40 small T antigen and PP2A phosphatase in cell transformation. *Cancer Metastasis Rev*. 2008 Jun;27(2):137-46.
46. Schonthal AH. Role of serine/threonine protein phosphatase 2A in cancer. *Cancer Lett*. 2001 Sep 10;170(1):1-13.
47. Chew J, Biswas S, Shreeram S, Humaidi M, Wong ET, Dhillion MK, et al. WIP1 phosphatase is a negative regulator of NF-kappaB signalling. *Nat Cell Biol*. 2009 May;11(5):659-66.

48. Lowe JM, Cha H, Yang Q, Fornace AJ, Jr. Nuclear factor-kappaB (NF-kappaB) is a novel positive transcriptional regulator of the oncogenic Wip1 phosphatase. *J Biol Chem.* 2010 Feb 19;285(8):5249-57.
49. Sun W, Yu Y, Dotti G, Shen T, Tan X, Savoldo B, et al. PPM1A and PPM1B act as IKKbeta phosphatases to terminate TNFalpha-induced IKKbeta-NF-kappaB activation. *Cell Signal.* 2009 Jan;21(1):95-102.
50. Orlowski RZ, Baldwin J, Albert S. NF-[kappa]B as a therapeutic target in cancer. *Trends in Molecular Medicine.* 2002 2002/8/1;8(8):385-9.
51. Yamamoto Y, Gaynor RB. I[kappa]B kinases: key regulators of the NF-[kappa]B pathway. *Trends in Biochemical Sciences.* 2004 2004/2;29(2):72-9.
52. Rayet B, Gelinas C. Aberrant *rel/nfkB* genes and activity in human cancer. *Oncogene.* 1999;18:6938-47.
53. Baldwin AS. Control of oncogenesis and cancer therapy resistance by the transcription factor NF-{ {kappa} }B. *J Clin Invest.* 2001 February 1, 2001;107(3):241-6.
54. Arun P, Brown MS, Ehsanian R, Chen Z, Van Waes C. Nuclear NF-kappaB p65 phosphorylation at serine 276 by protein kinase A contributes to the malignant phenotype of head and neck cancer. *Clin Cancer Res.* 2009 Oct 1;15(19):5974-84.
55. Dong G, Loukinova E, Chen Z, Gangi L, Chanturita TI, Liu ET, et al. Molecular Profiling of Transformed and Metastatic Murine Squamous Carcinoma Cells by Differential Display and cDNA Microarray Reveals Altered Expression of Multiple Genes Related to Growth, Apoptosis, Angiogenesis, and the NF-{ {kappa} }B Signal Pathway. *Cancer Res.* 2001 June 1, 2001;61(12):4797-808.
56. Finco TS, Westwick JK, Norris JL, Beg AA, Der CJ, Baldwin Jr. AS. Oncogenic Ha-Ras-induced Signaling Activates NF-kappa B Transcriptional Activity, Which Is Required for Cellular Transformation. *J Biol Chem.* 1997 September 26, 1997;272(39):24113-6.
57. Arsura M, Mercurio F, Oliver AL, Thorgeirsson SS, Sonenshein GE. Role of the Ikappa B Kinase Complex in Oncogenic Ras- and Raf-Mediated Transformation of Rat Liver Epithelial Cells. *Mol Cell Biol.* 2000 August 1, 2000;20(15):5381-91.
58. Lin A, Karin M. NF-[kappa]B in cancer: a marked target. *Seminars in Cancer Biology.* 2003 2003/4;13(2):107-14.

59. Romieu-Mourez R, Kim DW, Shin SM, Demicco EG, Landesman-Bollag E, Seldin DC, et al. Mouse Mammary Tumor Virus c-rel Transgenic Mice Develop Mammary Tumors. *Mol Cell Biol*. 2003 August 15, 2003;23(16):5738-54.
60. Duffey DC, Chen Z, Dong G, Ondrey FG, Wolf JS, Brown K, et al. Expression of a Dominant-Negative Mutant Inhibitor- $\{\kappa\}\alpha\beta$ of Nuclear Factor- $\{\kappa\}\beta$ in Human Head and Neck Squamous Cell Carcinoma Inhibits Survival, Proinflammatory Cytokine Expression, and Tumor Growth in Vivo. *Cancer Res*. 1999 July 1, 1999;59(14):3468-74.
61. Jemal A, Siegel R, Ward E, Murray T, Xu J, Thun MJ. Cancer statistics, 2007. *CA Cancer J Clin*. 2007 Jan-Feb;57(1):43-66.
62. Nelson WG, De Marzo AM, Isaacs WB. Prostate cancer. *N Engl J Med*. 2003 Jul 24;349(4):366-81.
63. Min J, Zaslavsky A, Fedele G, McLaughlin SK, Reczek EE, De Raedt T, et al. An oncogene-tumor suppressor cascade drives metastatic prostate cancer by coordinately activating Ras and nuclear factor-kappaB. *Nat Med*. 2010 Mar;16(3):286-94.
64. Setlur SR, Royce TE, Sboner A, Mosquera JM, Demichelis F, Hofer MD, et al. Integrative microarray analysis of pathways dysregulated in metastatic prostate cancer. *Cancer Res*. 2007 Nov 1;67(21):10296-303.
65. Zhang J, Patel L, Pienta KJ. Targeting chemokine (C-C motif) ligand 2 (CCL2) as an example of translation of cancer molecular biology to the clinic. *Prog Mol Biol Transl Sci*. 2010;95:31-53.
66. Craig MJ, Loberg RD. CCL2 (Monocyte Chemoattractant Protein-1) in cancer bone metastases. *Cancer Metastasis Rev*. 2006 Dec;25(4):611-9.
67. Azevedo A, Cunha V, Teixeira AL, Medeiros R. IL-6/IL-6R as a potential key signaling pathway in prostate cancer development. *World J Clin Oncol*. 2011 Dec 10;2(12):384-96.
68. Wolf MJ, Hoos A, Bauer J, Boettcher S, Knust M, Weber A, et al. Endothelial CCR2 Signaling Induced by Colon Carcinoma Cells Enables Extravasation via the JAK2-Stat5 and p38MAPK Pathway. *Cancer Cell*. 2012 Jul 10;22(1):91-105.
69. Sosnowski DM, Krishnan V, Kraemer WJ, Dunn-Lewis C, Mastro AM. Changes in Cytokines of the Bone Microenvironment during Breast Cancer Metastasis. *Int J Breast Cancer*. 2012;2012:160265.

70. Roca H, Varsos ZS, Sud S, Craig MJ, Ying C, Pienta KJ. CCL2 and interleukin-6 promote survival of human CD11b⁺ peripheral blood mononuclear cells and induce M2-type macrophage polarization. *J Biol Chem*. 2009 Dec 4;284(49):34342-54.
71. Qian BZ, Li J, Zhang H, Kitamura T, Zhang J, Campion LR, et al. CCL2 recruits inflammatory monocytes to facilitate breast-tumour metastasis. *Nature*. 2011 Jul 14;475(7355):222-5.
72. Coward J, Kulbe H, Chakravarty P, Leader D, Vassileva V, Leinster DA, et al. Interleukin-6 as a therapeutic target in human ovarian cancer. *Clin Cancer Res*. 2011 Sep 15;17(18):6083-96.
73. Dorff TB, Goldman B, Pinski JK, Mack PC, Lara PN, Jr., Van Veldhuizen PJ, Jr., et al. Clinical and correlative results of SWOG S0354: a phase II trial of CNTO328 (siltuximab), a monoclonal antibody against interleukin-6, in chemotherapy-pretreated patients with castration-resistant prostate cancer. *Clin Cancer Res*. 2010 Jun 1;16(11):3028-34.
74. Lu G, Wang Y. Functional diversity of mammalian type 2C protein phosphatase isoforms: new tales from an old family. *Clin Exp Pharmacol Physiol*. 2008 Feb;35(2):107-12.
75. Aburai N, Yoshida M, Ohnishi M, Kimura K. Sanguinarine as a potent and specific inhibitor of protein phosphatase 2C in vitro and induces apoptosis via phosphorylation of p38 in HL60 cells. *Biosci Biotechnol Biochem*. 2010;74(3):548-52.
76. Barford D, Das AK, Egloff MP. The structure and mechanism of protein phosphatases: insights into catalysis and regulation. *Annu Rev Biophys Biomol Struct*. 1998;27:133-64.
77. Moorhead GB, Trinkle-Mulcahy L, Ulke-Lemee A. Emerging roles of nuclear protein phosphatases. *Nat Rev Mol Cell Biol*. 2007 Mar;8(3):234-44.
78. Barford D. Molecular mechanisms of the protein serine/threonine phosphatases. *Trends Biochem Sci*. 1996 Nov;21(11):407-12.
79. Mann DJ, Campbell DG, McGowan CH, Cohen PT. Mammalian protein serine/threonine phosphatase 2C: cDNA cloning and comparative analysis of amino acid sequences. *Biochim Biophys Acta*. 1992 Feb 28;1130(1):100-4.
80. Das AK, Helps NR, Cohen PT, Barford D. Crystal structure of the protein serine/threonine phosphatase 2C at 2.0 Å resolution. *EMBO J*. 1996 Dec 16;15(24):6798-809.
81. Lifschitz-Mercer B, Sheinin Y, Ben-Meir D, Bramante-Schreiber L, Leider-Trejo L, Karby S, et al. Protein phosphatase 2Calpha expression in normal human tissues: an immunohistochemical study. *Histochem Cell Biol*. 2001 Jul;116(1):31-9.

82. Lin X, Duan X, Liang YY, Su Y, Wrighton KH, Long J, et al. PPM1A functions as a Smad phosphatase to terminate TGFbeta signaling. *Cell*. 2006 Jun 2;125(5):915-28.
83. Shohat M, Ben-Meir D, Lavi S. Protein phosphatase magnesium dependent 1A (PPM1A) plays a role in the differentiation and survival processes of nerve cells. *PLoS One*. 2012;7(2):e32438.
84. Cobb MH, Goldsmith EJ. How MAP kinases are regulated. *J Biol Chem*. 1995 Jun 23;270(25):14843-6.
85. Waskiewicz AJ, Cooper JA. Mitogen and stress response pathways: MAP kinase cascades and phosphatase regulation in mammals and yeast. *Curr Opin Cell Biol*. 1995 Dec;7(6):798-805.
86. Li R, Gong Z, Pan C, Xie DD, Tang JY, Cui M, et al. Metal-dependent protein phosphatase 1A functions as an extracellular signal-regulated kinase phosphatase. *FEBS J*. 2013 Apr 6.
87. Ofek P, Ben-Meir D, Kariv-Inbal Z, Oren M, Lavi S. Cell cycle regulation and p53 activation by protein phosphatase 2C alpha. *J Biol Chem*. 2003 Apr 18;278(16):14299-305.
88. Kim JS, Rho B, Lee TH, Lee JM, Kim SJ, Park JH. The interaction of hepatitis B virus X protein and protein phosphatase type 2 Calpha and its effect on IL-6. *Biochem Biophys Res Commun*. 2006 Dec 8;351(1):253-8.
89. Zhang B, Zhou Z, Lin H, Lv X, Fu J, Lin P, et al. Protein phosphatase 1A (PPM1A) is involved in human cytotrophoblast cell invasion and migration. *Histochem Cell Biol*. 2009 Aug;132(2):169-79.
90. Chida T, Ando M, Matsuki T, Masu Y, Nagaura Y, Takano-Yamamoto T, et al. N-myristoylation is essential for protein phosphatases PPM1A and PPM1B to dephosphorylate their physiological substrates in cells. *Biochem J*. 2012 Oct 22.
91. Kusuda K, Kobayashi T, Ikeda S, Ohnishi M, Chida N, Yanagawa Y, et al. Mutational analysis of the domain structure of mouse protein phosphatase 2Cbeta. *Biochem J*. 1998 May 15;332 (Pt 1):243-50.
92. Fiscella M, Zhang H, Fan S, Sakaguchi K, Shen S, Mercer WE, et al. Wip1, a novel human protein phosphatase that is induced in response to ionizing radiation in a p53-dependent manner. *Proc Natl Acad Sci U S A*. 1997 Jun 10;94(12):6048-53.
93. Tong Y, Quirion R, Shen SH. Cloning and characterization of a novel mammalian PP2C isozyme. *J Biol Chem*. 1998 Dec 25;273(52):35282-90.

94. Takekawa M, Adachi M, Nakahata A, Nakayama I, Itoh F, Tsukuda H, et al. p53-inducible wip1 phosphatase mediates a negative feedback regulation of p38 MAPK-p53 signaling in response to UV radiation. *EMBO J.* 2000 Dec 1;19(23):6517-26.
95. Tarulli GA, De Silva D, Ho V, Kunasegaran K, Ghosh K, Tan BC, et al. Hormone-sensing cells require Wip1 for paracrine stimulation in normal and premalignant mammary epithelium. *Breast Cancer Res.* 2013 Jan 31;15(1):R10.
96. Lu X, Nannenga B, Donehower LA. PPM1D dephosphorylates Chk1 and p53 and abrogates cell cycle checkpoints. *Genes Dev.* 2005 May 15;19(10):1162-74.
97. Sluss HK, Armata H, Gallant J, Jones SN. Phosphorylation of serine 18 regulates distinct p53 functions in mice. *Mol Cell Biol.* 2004 Feb;24(3):976-84.
98. Shieh SY, Ikeda M, Taya Y, Prives C. DNA damage-induced phosphorylation of p53 alleviates inhibition by MDM2. *Cell.* 1997 Oct 31;91(3):325-34.
99. Lu X, Ma O, Nguyen TA, Jones SN, Oren M, Donehower LA. The Wip1 Phosphatase acts as a gatekeeper in the p53-Mdm2 autoregulatory loop. *Cancer Cell.* 2007 Oct;12(4):342-54.
100. Shreeram S, Demidov ON, Hee WK, Yamaguchi H, Onishi N, Kek C, et al. Wip1 phosphatase modulates ATM-dependent signaling pathways. *Mol Cell.* 2006 Sep 1;23(5):757-64.
101. Kastan MB, Lim DS. The many substrates and functions of ATM. *Nat Rev Mol Cell Biol.* 2000 Dec;1(3):179-86.
102. Fujimoto H, Onishi N, Kato N, Takekawa M, Xu XZ, Kosugi A, et al. Regulation of the antioncogenic Chk2 kinase by the oncogenic Wip1 phosphatase. *Cell Death Differ.* 2006 Jul;13(7):1170-80.
103. Oliva-Trastoy M, Berthonaud V, Chevalier A, Ducrot C, Marsolier-Kergoat MC, Mann C, et al. The Wip1 phosphatase (PPM1D) antagonizes activation of the Chk2 tumour suppressor kinase. *Oncogene.* 2007 Mar 1;26(10):1449-58.
104. Kallioniemi A, Kallioniemi OP, Piper J, Tanner M, Stokke T, Chen L, et al. Detection and mapping of amplified DNA sequences in breast cancer by comparative genomic hybridization. *Proc Natl Acad Sci U S A.* 1994 Mar 15;91(6):2156-60.
105. Ried T, Petersen I, Holtgreve-Grez H, Speicher MR, Schrock E, du Manoir S, et al. Mapping of multiple DNA gains and losses in primary small cell lung carcinomas by comparative genomic hybridization. *Cancer Res.* 1994 Apr 1;54(7):1801-6.

106. Wong N, Lai P, Lee SW, Fan S, Pang E, Liew CT, et al. Assessment of genetic changes in hepatocellular carcinoma by comparative genomic hybridization analysis: relationship to disease stage, tumor size, and cirrhosis. *Am J Pathol*. 1999 Jan;154(1):37-43.
107. Ching YP, Qi Z, Wang JH. Cloning of three novel neuronal Cdk5 activator binding proteins. *Gene*. 2000 Jan 25;242(1-2):285-94.
108. Plevin MJ, Mills MM, Ikura M. The LxxLL motif: a multifunctional binding sequence in transcriptional regulation. *Trends Biochem Sci*. 2005 Feb;30(2):66-9.
109. Pike AC, Brzozowski AM, Hubbard RE. A structural biologist's view of the oestrogen receptor. *J Steroid Biochem Mol Biol*. 2000 Nov 30;74(5):261-8.
110. Wang J, An H, Mayo MW, Baldwin AS, Yarbrough WG. LZAP, a putative tumor suppressor, selectively inhibits NF-kappaB. *Cancer Cell*. 2007;12(3):239-51.
111. Liu D, Wang WD, Melville DB, Cha YI, Yin Z, Issaeva N, et al. Tumor suppressor Lzap regulates cell cycle progression, doming, and zebrafish epiboly. *Dev Dyn*. 2011 Jun;240(6):1613-25.
112. Wang J, He X, Luo Y, Yarbrough WG. A novel ARF-binding protein (LZAP) alters ARF regulation of HDM2. *Biochemical Journal*. 2006;393(Pt 2):489-501.
113. Jiang H, Wu J, He C, Yang W, Li H. Tumor suppressor protein C53 antagonizes checkpoint kinases to promote cyclin-dependent kinase 1 activation. *Cell Res*. 2009 Apr;19(4):458-68.
114. Bulavin DV, Amundson SA, Fornace AJ. p38 and Chk1 kinases: different conductors for the G(2)/M checkpoint symphony. *Curr Opin Genet Dev*. 2002 Feb;12(1):92-7.
115. Graves PR, Yu L, Schwarz JK, Gales J, Sausville EA, O'Connor PM, et al. The Chk1 protein kinase and the Cdc25C regulatory pathways are targets of the anticancer agent UCN-01. *J Biol Chem*. 2000 Feb 25;275(8):5600-5.
116. Jiang H, Luo S, Li H. Cdk5 activator-binding protein C53 regulates apoptosis induced by genotoxic stress via modulating the G2/M DNA damage checkpoint. *J Biol Chem*. 2005 May 27;280(21):20651-9.
117. An H, Lu X, Liu D, Yarbrough WG. LZAP inhibits p38 MAPK (p38) phosphorylation and activity by facilitating p38 association with the wild-type p53 induced phosphatase 1 (WIP1). *PLoS One*. 2011;6(1):e16427.

118. Lemaire K, Moura RF, Granvik M, Igoillo-Esteve M, Hohmeier HE, Hendrickx N, et al. Ubiquitin fold modifier 1 (UFM1) and its target UFBP1 protect pancreatic beta cells from ER stress-induced apoptosis. *PLoS One*. 2011;6(4):e18517.
119. Wu J, Lei G, Mei M, Tang Y, Li H. A novel C53/LZAP-interacting protein regulates stability of C53/LZAP and DDRGK domain-containing Protein 1 (DDRGK1) and modulates NF-kappaB signaling. *J Biol Chem*. 2010 May 14;285(20):15126-36.
120. Kwon J, Cho HJ, Han SH, No JG, Kwon JY, Kim H. A novel LZAP-binding protein, NLBP, inhibits cell invasion. *J Biol Chem*. 2010 Apr 16;285(16):12232-40.
121. Shiwaku H, Yoshimura N, Tamura T, Sone M, Ogishima S, Watase K, et al. Suppression of the novel ER protein Maxer by mutant ataxin-1 in Bergman glia contributes to non-cell-autonomous toxicity. *EMBO J*. 2010 Jul 21;29(14):2446-60.
122. Komatsu M, Chiba T, Tatsumi K, Iemura S, Tanida I, Okazaki N, et al. A novel protein-conjugating system for Ufm1, a ubiquitin-fold modifier. *EMBO J*. 2004 May 5;23(9):1977-86.
123. Tatsumi K, Sou YS, Tada N, Nakamura E, Iemura S, Natsume T, et al. A novel type of E3 ligase for the Ufm1 conjugation system. *J Biol Chem*. 2010 Feb 19;285(8):5417-27.
124. Cao Y, Karin M. NF-kappaB in mammary gland development and breast cancer. *J Mammary Gland Biol Neoplasia*. 2003 Apr;8(2):215-23.
125. Wu JT, Kral JG. The NF-kappaB/IkappaB signaling system: a molecular target in breast cancer therapy. *J Surg Res*. 2005 Jan;123(1):158-69.
126. Chen L-F, Green WC. Shaping the nuclear action of NF- κ B. *Nature Reviews Molecular Cell Biology*. 2004;5:392-401.
127. Abdelmohsen K, Pullmann R, Jr., Lal A, Kim HH, Galban S, Yang X, et al. Phosphorylation of HuR by Chk2 regulates SIRT1 expression. *Mol Cell*. 2007 Feb 23;25(4):543-57.
128. Lu Y, Cai Z, Galson DL, Xiao G, Liu Y, George DE, et al. Monocyte chemotactic protein-1 (MCP-1) acts as a paracrine and autocrine factor for prostate cancer growth and invasion. *Prostate*. 2006 Sep 1;66(12):1311-8.
129. Drake JM, Gabriel CL, Henry MD. Assessing tumor growth and distribution in a model of prostate cancer metastasis using bioluminescence imaging. *Clin Exp Metastasis*. 2005;22(8):674-84.

130. Jin R, Sterling JA, Edwards JR, Degriff DJ, Lee C, Park SI, et al. Activation of NF-kappa B Signaling Promotes Growth of Prostate Cancer Cells in Bone. *PLoS One*. 2013;8(4):e60983.
131. Lupas A, Van Dyke M, Stock J. Predicting coiled coils from protein sequences. *Science*. 1991 May 24;252(5009):1162-4.
132. Hildebrand DG, Alexander E, Horber S, Lehle S, Obermayer K, Munck NA, et al. IkappaBzeta is a transcriptional key regulator of CCL2/MCP-1. *Journal of immunology*. [Research Support, Non-U.S. Gov't]. 2013 May 1;190(9):4812-20.
133. Wang CY, Mayo MW, Baldwin AS, Jr. TNF- and cancer therapy-induced apoptosis: potentiation by inhibition of NF-kappaB. *Science*. 1996 Nov 1;274(5288):784-7.
134. Zhang J, Patel L, Pienta KJ. CC chemokine ligand 2 (CCL2) promotes prostate cancer tumorigenesis and metastasis. *Cytokine Growth Factor Rev*. 2010 Feb;21(1):41-8.
135. Chandran UR, Ma C, Dhir R, Bisceglia M, Lyons-Weiler M, Liang W, et al. Gene expression profiles of prostate cancer reveal involvement of multiple molecular pathways in the metastatic process. *BMC Cancer*. 2007;7:64.
136. Yu YP, Landsittel D, Jing L, Nelson J, Ren B, Liu L, et al. Gene expression alterations in prostate cancer predicting tumor aggression and preceding development of malignancy. *J Clin Oncol*. 2004 Jul 15;22(14):2790-9.
137. Wu TT, Sikes RA, Cui Q, Thalmann GN, Kao C, Murphy CF, et al. Establishing human prostate cancer cell xenografts in bone: induction of osteoblastic reaction by prostate-specific antigen-producing tumors in athymic and SCID/bg mice using LNCaP and lineage-derived metastatic sublines. *Int J Cancer*. 1998 Sep 11;77(6):887-94.
138. Ghosh S, Karin M. Missing pieces in the NF-kappaB puzzle. *Cell*. 2002 Apr;109 Suppl:S81-96.
139. Gardam S, Beyaert R. The kinase NIK as a therapeutic target in multiple myeloma. *Expert Opin Ther Targets*. 2011 Feb;15(2):207-18.
140. Chaturvedi MM, Sung B, Yadav VR, Kannappan R, Aggarwal BB. NF-kappaB addiction and its role in cancer: 'one size does not fit all'. *Oncogene*. 2011 Apr 7;30(14):1615-30.
141. Yamaguchi H, Durell SR, Chatterjee DK, Anderson CW, Appella E. The Wip1 phosphatase PPM1D dephosphorylates SQ/TQ motifs in checkpoint substrates phosphorylated by PI3K-like kinases. *Biochemistry*. 2007 Nov 6;46(44):12594-603.

142. Yamaguchi H, Minopoli G, Demidov ON, Chatterjee DK, Anderson CW, Durell SR, et al. Substrate specificity of the human protein phosphatase 2Cdelta, Wip1. *Biochemistry*. 2005 Apr 12;44(14):5285-94.
143. Browning DD, Pan ZK, Prossnitz ER, Ye RD. Cell type- and developmental stage-specific activation of NF-kappaB by fMet-Leu-Phe in myeloid cells. *J Biol Chem*. 1997 Mar 21;272(12):7995-8001.
144. Smale ST. Hierarchies of NF-kappaB target-gene regulation. *Nat Immunol*. 2011 Aug;12(8):689-94.
145. Mueller L, Seggern LV, Schumacher J, Goumas F, Wilms C, Braun F, et al. TNF-alpha similarly induces IL-6 and MCP-1 in fibroblasts from colorectal liver metastases and normal liver fibroblasts. *Biochem Biophys Res Commun*. 2010 Jun 2.
146. Zollo M, Di Dato V, Spano D, De Martino D, Liguori L, Marino N, et al. Targeting monocyte chemotactic protein-1 synthesis with bindarit induces tumor regression in prostate and breast cancer animal models. *Clin Exp Metastasis*. 2012 Apr 7.
147. Lammers T, Peschke P, Ehemann V, Debus J, Slobodin B, Lavi S, et al. Role of PP2Calpha in cell growth, in radio- and chemosensitivity, and in tumorigenicity. *Mol Cancer*. 2007;6:65.
148. Obenauer JC, Cantley LC, Yaffe MB. Scansite 2.0: Proteome-wide prediction of cell signaling interactions using short sequence motifs. *Nucleic Acids Res*. 2003 Jul 1;31(13):3635-41.
149. Wagner EF, Nebreda AR. Signal integration by JNK and p38 MAPK pathways in cancer development. *Nat Rev Cancer*. 2009 Aug;9(8):537-49.
150. Cuenda A, Rousseau S. p38 MAP-kinases pathway regulation, function and role in human diseases. *Biochim Biophys Acta*. 2007 Aug;1773(8):1358-75.
151. Zarubin T, Han J. Activation and signaling of the p38 MAP kinase pathway. *Cell Res*. 2005 Jan;15(1):11-8.
152. Thornton TM, Rincon M. Non-classical p38 map kinase functions: cell cycle checkpoints and survival. *Int J Biol Sci*. 2009;5(1):44-51.
153. Bulavin DV, Fornace AJ, Jr. p38 MAP kinase's emerging role as a tumor suppressor. *Adv Cancer Res*. 2004;92:95-118.

154. Ghatan S, Larner S, Kinoshita Y, Hetman M, Patel L, Xia Z, et al. p38 MAP kinase mediates bax translocation in nitric oxide-induced apoptosis in neurons. *J Cell Biol.* 2000 Jul 24;150(2):335-47.
155. Ishikawa Y, Kusaka E, Enokido Y, Ikeuchi T, Hatanaka H. Regulation of Bax translocation through phosphorylation at Ser-70 of Bcl-2 by MAP kinase in NO-induced neuronal apoptosis. *Mol Cell Neurosci.* 2003 Oct;24(2):451-9.
156. Esteva FJ, Sahin AA, Smith TL, Yang Y, Pusztai L, Nahta R, et al. Prognostic significance of phosphorylated P38 mitogen-activated protein kinase and HER-2 expression in lymph node-positive breast carcinoma. *Cancer.* 2004 Feb 1;100(3):499-506.
157. Junntila MR, Ala-Aho R, Jokilehto T, Peltonen J, Kallajoki M, Grenman R, et al. p38alpha and p38delta mitogen-activated protein kinase isoforms regulate invasion and growth of head and neck squamous carcinoma cells. *Oncogene.* 2007 Aug 9;26(36):5267-79.
158. Greenberg AK, Basu S, Hu J, Yie TA, Tchou-Wong KM, Rom WN, et al. Selective p38 activation in human non-small cell lung cancer. *Am J Respir Cell Mol Biol.* 2002 May;26(5):558-64.
159. Pomerance M, Quillard J, Chantoux F, Young J, Blondeau JP. High-level expression, activation, and subcellular localization of p38-MAP kinase in thyroid neoplasms. *J Pathol.* 2006 Jul;209(3):298-306.
160. Bulavin DV, Saito S, Hollander MC, Sakaguchi K, Anderson CW, Appella E, et al. Phosphorylation of human p53 by p38 kinase coordinates N-terminal phosphorylation and apoptosis in response to UV radiation. *EMBO J.* 1999 Dec 1;18(23):6845-54.
161. Lu X, Bocangel D, Nannenga B, Yamaguchi H, Appella E, Donehower LA. The p53-induced oncogenic phosphatase PPM1D interacts with uracil DNA glycosylase and suppresses base excision repair. *Mol Cell.* 2004 Aug 27;15(4):621-34.
162. Zhang Y, Xiong Y, Yarbrough WG. ARF promotes MDM2 degradation and stabilizes p53: ARF-INK4a locus deletion impairs both the Rb and p53 tumor suppression pathways. *Cell.* 1998 Mar 20;92(6):725-34.
163. Yarbrough WG, Bessho M, Zanation A, Bisi JE, Xiong Y. Human tumor suppressor ARF impedes S-phase progression independent of p53. *Cancer Res.* 2002 Feb 15;62(4):1171-7.
164. Zhang Y, Xiong Y. Mutations in human ARF exon 2 disrupt its nucleolar localization and impair its ability to block nuclear export of MDM2 and p53. *Mol Cell.* 1999 May;3(5):579-91.

165. Corti O, Hampe C, Koutnikova H, Darios F, Jacquier S, Prigent A, et al. The p38 subunit of the aminoacyl-tRNA synthetase complex is a Parkin substrate: linking protein biosynthesis and neurodegeneration. *Hum Mol Genet*. 2003 Jun 15;12(12):1427-37.
166. Spaziani A, Alisi A, Sanna D, Balsano C. Role of p38 MAPK and RNA-dependent protein kinase (PKR) in hepatitis C virus core-dependent nuclear delocalization of cyclin B1. *J Biol Chem*. 2006 Apr 21;281(16):10983-9.
167. Lavoie JN, L'Allemand G, Brunet A, Muller R, Pouyssegur J. Cyclin D1 expression is regulated positively by the p42/p44MAPK and negatively by the p38/HOGMAPK pathway. *J Biol Chem*. 1996 Aug 23;271(34):20608-16.
168. Raingeaud J, Whitmarsh AJ, Barrett T, Derijard B, Davis RJ. MKK3- and MKK6-regulated gene expression is mediated by the p38 mitogen-activated protein kinase signal transduction pathway. *Mol Cell Biol*. 1996 Mar;16(3):1247-55.
169. Raingeaud J, Gupta S, Rogers JS, Dickens M, Han J, Ulevitch RJ, et al. Pro-inflammatory cytokines and environmental stress cause p38 mitogen-activated protein kinase activation by dual phosphorylation on tyrosine and threonine. *J Biol Chem*. 1995 Mar 31;270(13):7420-6.
170. Fu J, Yang Z, Wei J, Han J, Gu J. Nuclear protein NP60 regulates p38 MAPK activity. *J Cell Sci*. 2006 Jan 1;119(Pt 1):115-23.
171. Bulavin DV, Phillips C, Nannenga B, Timofeev O, Donehower LA, Anderson CW, et al. Inactivation of the Wip1 phosphatase inhibits mammary tumorigenesis through p38 MAPK-mediated activation of the p16(Ink4a)-p19(Arf) pathway. *Nat Genet*. 2004 Apr;36(4):343-50.
172. Xia Y, Ongusaha P, Lee SW, Liou YC. Loss of Wip1 sensitizes cells to stress- and DNA damage-induced apoptosis. *J Biol Chem*. 2009 Jun 26;284(26):17428-37.
173. Chen Z, Hagler J, Palombella VJ, Melandri F, Scherer D, Ballard D, et al. Signal-induced site-specific phosphorylation targets I kappa B alpha to the ubiquitin-proteasome pathway. *Genes Dev*. 1995 Jul 1;9(13):1586-97.
174. Geng H, Wittwer T, Dittrich-Breiholz O, Kracht M, Schmitz ML. Phosphorylation of NF-kappaB p65 at Ser468 controls its COMMD1-dependent ubiquitination and target gene-specific proteasomal elimination. *EMBO Rep*. 2009 Apr;10(4):381-6.
175. Aragon E, Goerner N, Zaromytidou AI, Xi Q, Escobedo A, Massague J, et al. A Smad action turnover switch operated by WW domain readers of a phosphoserine code. *Genes Dev*. 2011 Jun 15;25(12):1275-88.

176. Phizicky EM, Fields S. Protein-protein interactions: methods for detection and analysis. *Microbiol Rev*. 1995 Mar;59(1):94-123.
177. Marianayagam NJ, Sunde M, Matthews JM. The power of two: protein dimerization in biology. *Trends Biochem Sci*. 2004 Nov;29(11):618-25.
178. Glover JN, Harrison SC. Crystal structure of the heterodimeric bZIP transcription factor c-Fos-c-Jun bound to DNA. *Nature*. 1995 Jan 19;373(6511):257-61.
179. Dougall WC, Chaisson M. The RANK/RANKL/OPG triad in cancer-induced bone diseases. *Cancer Metastasis Rev*. 2006 Dec;25(4):541-9.
180. O'Brien CA. Control of RANKL gene expression. *Bone*. 2010 Apr;46(4):911-9.
181. O'Brien CA, Gubrij I, Lin SC, Saylors RL, Manolagas SC. STAT3 activation in stromal/osteoblastic cells is required for induction of the receptor activator of NF-kappaB ligand and stimulation of osteoclastogenesis by gp130-utilizing cytokines or interleukin-1 but not 1,25-dihydroxyvitamin D3 or parathyroid hormone. *J Biol Chem*. 1999 Jul 2;274(27):19301-8.
182. Wei S, Kitaura H, Zhou P, Ross FP, Teitelbaum SL. IL-1 mediates TNF-induced osteoclastogenesis. *J Clin Invest*. 2005 Feb;115(2):282-90.
183. Lu Y, Xiao G, Galson DL, Nishio Y, Mizokami A, Keller ET, et al. PTHrP-induced MCP-1 production by human bone marrow endothelial cells and osteoblasts promotes osteoclast differentiation and prostate cancer cell proliferation and invasion in vitro. *Int J Cancer*. 2007 Aug 15;121(4):724-33.
184. Wu Y, Zhou BP. TNF-alpha/NF-kappaB/Snail pathway in cancer cell migration and invasion. *Br J Cancer*. 2010 Feb 16;102(4):639-44.
185. Carver EA, Jiang R, Lan Y, Oram KF, Gridley T. The mouse snail gene encodes a key regulator of the epithelial-mesenchymal transition. *Mol Cell Biol*. 2001 Dec;21(23):8184-8.
186. Martin TA, Goyal A, Watkins G, Jiang WG. Expression of the transcription factors snail, slug, and twist and their clinical significance in human breast cancer. *Ann Surg Oncol*. 2005 Jun;12(6):488-96.
187. Parker BS, Argani P, Cook BP, Liangfeng H, Chartrand SD, Zhang M, et al. Alterations in vascular gene expression in invasive breast carcinoma. *Cancer Res*. 2004 Nov 1;64(21):7857-66.

188. Smith BN, Odero-Marah VA. The role of Snail in prostate cancer. *Cell Adh Migr.* 2012 Sep-Oct;6(5):433-41.
189. Liu X, Huang S, Ma J, Li C, Zhang Y, Luo L. NF-kappaB and Snail1a coordinate the cell cycle with gastrulation. *J Cell Biol.* 2009 Mar 23;184(6):805-15.
190. Barbera MJ, Puig I, Dominguez D, Julien-Grille S, Guaita-Esteruelas S, Peiro S, et al. Regulation of Snail transcription during epithelial to mesenchymal transition of tumor cells. *Oncogene.* 2004 Sep 23;23(44):7345-54.
191. Katsman A, Umezawa K, Bonavida B. Chemosensitization and immunosensitization of resistant cancer cells to apoptosis and inhibition of metastasis by the specific NF-kappaB inhibitor DHMEQ. *Curr Pharm Des.* 2009;15(7):792-808.
192. Wu K, Bonavida B. The activated NF-kappaB-Snail-RKIP circuitry in cancer regulates both the metastatic cascade and resistance to apoptosis by cytotoxic drugs. *Crit Rev Immunol.* 2009;29(3):241-54.
193. Bonavida B, Baritaki S. The novel role of Yin Yang 1 in the regulation of epithelial to mesenchymal transition in cancer via the dysregulated NF-kappaB/Snail/YY1/RKIP/PTEN Circuitry. *Crit Rev Oncog.* 2011;16(3-4):211-26.
194. Rudolph J. Inhibiting transient protein-protein interactions: lessons from the Cdc25 protein tyrosine phosphatases. *Nat Rev Cancer.* 2007 Mar;7(3):202-11.
195. Yang X, Teng Y, Hou N, Fan X, Cheng X, Li J, et al. Delayed re-epithelialization in Ppm1a gene-deficient mice is mediated by enhanced activation of Smad2. *J Biol Chem.* 2011 Dec 9;286(49):42267-73.
196. Suzuki MM, Bird A. DNA methylation landscapes: provocative insights from epigenomics. *Nat Rev Genet.* 2008 Jun;9(6):465-76.
197. Martin V, Jorgensen HF, Chaubert AS, Berger J, Barr H, Shaw P, et al. MBD2-mediated transcriptional repression of the p14ARF tumor suppressor gene in human colon cancer cells. *Pathobiology.* 2008;75(5):281-7.
198. Zhang Y, Zhang M, Wu J, Lei G, Li H. Transcriptional regulation of the Ufm1 conjugation system in response to disturbance of the endoplasmic reticulum homeostasis and inhibition of vesicle trafficking. *PLoS One.* 2012;7(11):e48587.

199. Jones AW, Mikhailov VA, Iniesta J, Cooper HJ. Electron capture dissociation mass spectrometry of tyrosine nitrated peptides. *J Am Soc Mass Spectrom*. [Research Support, Non-U.S. Gov't]. 2010 Feb;21(2):268-77.
200. Guo J, Prokai L. Conversion of 3-nitrotyrosine to 3-aminotyrosine residues facilitates mapping of tyrosine nitration in proteins by electrospray ionization-tandem mass spectrometry using electron capture dissociation. *J Mass Spectrom*. [Research Support, N.I.H., Extramural Research Support, Non-U.S. Gov't]. 2012 Dec;47(12):1601-11.
201. Cong X, Held JM, DeGiacomo F, Bonner A, Chen JM, Schilling B, et al. Mass spectrometric identification of novel lysine acetylation sites in huntingtin. *Molecular & cellular proteomics : MCP*. [Research Support, N.I.H., Extramural]. 2011 Oct;10(10):M111 009829.
202. Spickett CM, Pitt AR. Protein oxidation: role in signalling and detection by mass spectrometry. *Amino Acids*. [Review]. 2012 Jan;42(1):5-21.
203. Osula O, Swatkoski S, Cotter RJ. Identification of protein SUMOylation sites by mass spectrometry using combined microwave-assisted aspartic acid cleavage and tryptic digestion. *J Mass Spectrom*. [Research Support, N.I.H., Extramural]. 2012 May;47(5):644-54.